Fluorescent Lamp Characterisation

and the Design of an

Optimal Battery Powered Ballast

Stirling Vaughan Marais

2 April 2013

Submitted in fulfilment of the academic requirements for the Master of Science degree at University of Natal.

Abstract

Many electronic ballasts fail in service due to a failure, on behalf of the designer, to fully understand the dynamics of fluorescent lamps. This is mainly due to a shortage of detailed lamp specifications relevant to electronic inverters and a lack of electronic ballast design "Cookbooks".

This work describes the operation of 9 W compact fluorescent lamps with built in starters and presents an optimal battery powered ballast. The operation and performance of 9 W compact fluorescent lamps, from both reputable manufacturers and "No Name Brands", is investigated. Tests conducted include arc discharge performance using both ac and dc, from which the static V/I characteristics and equivalent plasma resistances are computed. The electrical and thermal properties of the electrodes together with the lamp starting voltage requirements are investigated. The performance of the glow starters is thoroughly analysed in terms of glow discharge threshold, dynamic resistance and high frequency response.

A review of current commercial electronic ballasts is presented together with an analysis of merits and shortfalls of each design. A novel, single ended, class C inverter is described which relies on secondary capacitance for energy conversion and not solely on inductive energy. The result is a high efficiency, low cost design which provides a near symmetrical lamp current waveform. A power conversion efficiency of 85% is achieved at an output power of 8 W, whilst the transistor dissipates less than 300 mW. It will be shown that it is possible, at a small cost penalty, to increase efficiency further and to eliminate transistor switching losses.

Dedication

To my wife, Isabel.

Preface

This whole thesis, with exception to that indicated in the text, is the candidate's own work and has not been submitted in part, or in whole, at any other University.

The research was conducted at home under the supervision of Dr Paul Bouwer.

The candidate has been involved for many years in the design of consumer electronic equipment and has always been intrigued at the vast performance spread of commercially available fluorescent lamp inverters in particular. This is due to either cost constraints or poor design, or both. The design problems are aggravated when compact fluorescent lamps with internal starters are used because of the extra load presented by these components. The candidate has now chosen to research the operating requirements of fluorescent lamps so that the nature of the load is fully understood, and to design an optimal battery powered ballast.

Acknowledgements

To UEC Projects (Pty) Ltd: Thank you for your moral and financial support. Thanks to Johan Joubert and Ismail Randeree for supporting my research in spite of its content not being directly related to my work R&D activities. In thanking you I can say that this exercise has greatly increased my working knowledge in the fields of switch mode power supplies and transient analysis, and has therefore improved my design and analysis capabilities.

To Isabel and children Tracy and Haydn: Without your support and understanding this work would not have been possible. The last few years have certainly not been as much fun for you as it has been for me.

To Dr Paul Bouwer: Thank you for tireless assistance and direction, particularly during thesis preparation.

To RML Lighting: Thanks to Ricky for supplying me with inverters, fluorescent lamps and luminaires. You remained a key link with industry and provided important information regarding current trends and preferences.

To SANCI: Thank you for your financial support. Thanks also to Robert Henderson for his support and interest in my research.

Table of Contents

List of Symbols

A_e	effective core area [m^2]
A_l	magnetic path length [m]
B_{max}	maximum flux density [T]
B_{opp}	operating flux density [T]
c	velocity [ms^{-1}]
C	capacitance [F]
C_b	ballast capacitance [F]
C_{sec}	secondary capacitance [F]
E	energy [J]
Ec	capacitive energy [J]
E_{sw}	energy dissipated in the switching element [J]
f_n	natural frequency of oscillation [Hz]
f_s	switching frequency [Hz]
h	Plank's constant [Js]
i	instantaneous current [A]
i_{peak}	peak current [A]
i_{load}	load current [A]
I_{pk}	peak current [A]
I_{pri}	primary current [A]
I_{sec}	secondary current [A]
l_e	effective magnetic path length [m]
L_{pri}	primary inductance [H]
L_{sec}	secondary inductance [H]
M	mutual inductance [H]
N_{pri}	number of primary turns

N_{sec}	number of secondary turns
P_{arc}	power dissipated during arc discharge [W]
P_{device}	power dissipated in the switching device [W]
P_{ign}	ignition power [W]
P_{lamp}	power dissipated in the lamp [W]
P_o	output power [W]
R_{load}	resistance of the load [Ω]
t_{on}	conduction time [s]
$T_{ambient}$	ambient temperature [^{o}C]
T_{device}	device temperature [^{o}C]
T_s	switching period [s]
V_{arc}	peak arc discharge voltage [V]
Vcc	supply voltage [V]
V_{ign}	peak ignition voltage [V]
V_{lamp}	peak lamp voltage [V]
V_{load}	load voltage [V]
V_{sat}	switch saturation voltage [V]
ζ	damping factor
η	efficiency
$\Theta_{j\text{-}a}$	junction to ambient thermal resistance [KW^{-1}]
λ	wavelength [m]
ρ	resistivity [Ωm]
τ	time constant [s]
υ	frequency of light [Hz]
ω_n	natural radian frequency [$rads^{-1}$]

List of Abbreviations

BJT	Bipolar Junction Transistor
BF	Ballast Factor
CF	Crest Factor
ESR	Equivalent Series Resistance
EMI	Electromagnetic Interference
GAT	Glow to Arc Transition
SMPS	Switch Mode Power Supplies

1 Introduction

1.1 Background

The applications suitable for battery powered fluorescent lighting are growing due to advances in lamp and battery design. Compact fluorescent lamps facilitate smaller luminaire design than their linear counterparts, and sealed lead acid batteries provide a longer service life than nickel cadmium batteries. Due to these advances it is now feasible to, for example, provide reliable battery powered lighting that is charged by solar cells, and fluorescent lamps are replacing incandescent lamps in many portable lighting applications. The demand for battery powered fluorescent lighting in the traditional fields, such as emergency lighting, is also increasing. The manufacture of battery powered ballasts is therefore potentially lucrative. The development of electronic ballasts is, however, a major problem in the industry.

The problem lies with understanding the complex dynamics of the fluorescent lamp. No simple mathematical expression can describe the lamp's characteristics during an arc discharge at all frequencies, and the author is not aware of any attempt to mathematically describe the starting characteristics. Due to the vastly different requirements during starting and arc discharge, circuit efficiency is usually compromised unless circuit complexity is increased. The circuit complexity is, however, limited by manufacturing price as the market is fiercely competitive.

Electronic ballast development is further hampered by a lack of relevant published lamp performance parameters. This is possible due to the following reasons:

- The vast majority of fluorescent lamp applications are simple mains installations and so there is no great demand for detailed specifications.
- The publication of detailed specifications may leave reputable lamp manufacturers open to piracy.
- The starting requirement, in particular, is affected by a myriad of conditions including starting pulse width, amplitude and frequency, humidity, ambient temperature and the proximity of conductive surfaces to the lamp[1]. It is therefore not feasible to detail specifications which would satisfy all applications.

The above factors have resulted in old designs, such as the single transistor oscillator[1,5,34], to still be manufactured in vast numbers in spite of it causing premature lamp ageing due to its poor current waveform. The demand for the design of higher performance, competitively priced, ballasts is therefore high.

1.2 Compact Fluorescent Lamps

Compact fluorescent lamps are replacing the traditional linear fluorescent lamps in both emergency and portable lighting applications due to their small external dimensions. This translates into smaller external luminaire dimensions and therefore lower manufacturing cost, and increased portability. Widespread usage is reducing unit manufacturing cost of compact lamps to price levels where they are now competitive with their linear counterparts.

The compact fluorescent lamps are generally available in 7 W, 9 W, 18 W and 26 W versions. The 9 W lamp was chosen because it is presently the most popular for emergency and portable lighting applications. Emergency lighting using higher wattage lamps seems to have limited appeal, perhaps due to reduced battery life. Compact fluorescent lamps are generally available with or without an internal starter. The version with the internal starter,

the PL-S 9 W (Philips designation), was chosen because:

- It is generally cheaper than the starterless version due to consumer demand.
- It lends itself for use in maintained emergency lighting applications as less wiring is required.
- It presents the greater challenge to start due to the additional load of the starter components, *i.e.* the glow starter and suppression capacitor.

1.3 Thesis Overview

Chapter 2 presents a review of fluorescent lamp theory. The aim of this chapter is to describe the dynamics of fluorescent lamps by examining the atomic physics of the discharge process, by detailing parameters affecting performance and by reviewing mathematical models of the discharge.

The lamp components, static V/I characteristics and starting dynamics are described and characteristics are related to design criteria. A review of parameters affecting performance such as lamp current frequency, current amplitude, ambient temperature, and current form is also included. Particular emphasis is placed on current frequency effects as gains in luminous efficacy are achievable at high frequencies[1,7,8]. Methods of assisting starting are also described. The mechanisms responsible for electrode damage are analysed because poor ballast design is usually manifested in rapid blackening of the tube ends, which results in premature lamp ageing. Both simple and complex mathematical models of the discharge are discussed and a simple circuit model is presented. The circuit model accuracy is verified in Chapters 4 and 7.

The performance of a sample of six lamps, and their starter components, is examined in

Chapter 3. Light output is measured at various input powers, for both 50 Hz and dc, by using an integrating sphere. The 50 Hz tests are included to provide comparisons of luminous efficacy. The results indicate that reliable operation at 50 Hz is only possible with lamp powers above 4 W without external cathode heating, and that total luminous flux at rated power may vary by as much as 40% between lamps. The dc tests are included to demonstrate the advantages of having no periodic arc extinction. The dc tests also reveal a minimal increase in luminous efficacy above that obtained at 50 Hz. Data from the dc tests is used to plot the V/I characteristics and equivalent plasma resistance of the lamps. The equivalent plasma resistance curve is particularly useful during ballast design.

In order to optimise lamp starting conditions the typical electrode thermal delay and steady state temperature for various heater currents is measured. The results reveal a non-linear increase in thermal delay at low heater currents and that the electrode temperature plot flattens at high heater currents. The heater currents at which an electrode transverse discharge is maintained is also revealed. The starting dc voltage requirement for various heater currents indicates a more predictable starting performance at high heater currents.

Measurements are performed on the glow starters at dc, 50 Hz and high frequencies. The 50 Hz measurements reveal both the glow discharge threshold and dynamic resistance, and minimum power required for glow starter switching. The dc performance tests reveal the mechanism responsible for polarity sensitive starting performance with dc ballasts. The tests also reveal an increase in dynamic resistance with decreasing switch contact separation, a phenomenon which may be exploited when using electronic ballasts. An investigation into the effects of the suppression capacitor value upon glow switch closure times contains a warning to the designers of dc type ballasts.

A review of local and international standards for ballast design and an analysis of present commercial ballasts is presented in Chapter 4. The aim of this chapter is to develop a guideline for ballast design based on market requirements and technical considerations. It is not enough for a design to satisfy technical requirements alone, market success can only

be achieved through circuit elegance. For this reason no complex circuits are reviewed. The performance of popular circuits supplied by the industry is measured and appraised. A theoretical appraisal of published designs is also included.

A description, in the complex frequency domain, of the function of the new ballast is given in Chapter 5. It is shown that it is possible to affect switching under zero current conditions by relying both on capacitive stored energy, instead of inductive energy, for power conversion in a single ended inverter, and by relying on circuit initial conditions. The advantages over conventional flyback inverter techniques include increased efficiency, rapid energy conversion and inherent switch overvoltage protection. Class C operation provides near sinusoidal lamp current through secondary circuit resonance.

A full component dependency analysis and design procedure is given in Chapter 6. Equations are developed from first principles as conventional flyback inverter theory does not apply. The design procedure includes the magnetic circuit design and the selection of a ferrite transformer. Component selection criteria are also detailed and a sample circuit is designed.

The performance of the new inverter, with both a resistive load and a fluorescent lamp, is measured in Chapter 7. The sample circuit achieved a power conversion efficiency of 85% whilst the switching device loss only accounts for a mere 23% of the total circuit losses. An analysis of circuit losses indicates that power conversion efficiencies exceeding 90% are possible. The power conversion technique facilitates circuit optimisation for arc discharge conditions without impairing starting performance. Starting performance was reliable with all lamps at -12°C whilst providing an acceptable starting scenario. The high frequency operation yielded an average 16% improvement in luminous efficacy over that obtained at 50 Hz.

The lamp current consists of complete cycles of decaying sinusoids and although the lamp current crest factor may exceed 1.7, the bandwidth of distortion components lies beyond

that which can cause premature lamp failure. The manufacturing cost of the new ballast is competitive with that of the single transistor inverter.

1.4 Summary and Claims

Industry interest in the fluorescent lamp characterisation is reflected in a request by the South African Council on Illumination (SANCI) for publication in their proceedings. A copy of the paper is included at the back of this thesis. The author believes that the energy conversion technique has never before been used in the electronic ballasts and now holds a provisional patent on the process (S.A. Provisional Patent Number 95/7324).

Originality is claimed for the following aspects of the material presented in this thesis:

- The development of a simple circuit model for a 9 W compact fluorescent lamp with a built in starter which accurately simulates the lamp and starter components during an arc discharge, and the analysis of the internal glow starter dynamics during starting.
- The use of an energy conversion technique which minimises switching losses and facilitates rapid energy conversion.

2 Fluorescent Lamp Theory

2.1 Typical Mains Operation

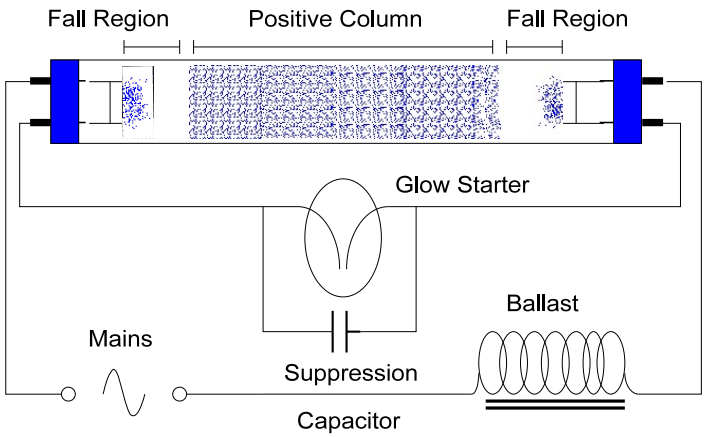

Figure 2.1: Typical mains connection of a fluorescent lamp.

Normal mains operation shall be used to describe fluorescent lamp operation in a typical circuit, such as that in Figure 2.1 above. When mains is first applied to the circuit no current flows through the lamp, because there are few charge carriers present in the gas and the mains voltage is too low to initiate ionisation. Mains voltage is, however, sufficient to initiate a glow discharge in the starter. The heat generated by this discharge heats the bimetal switch in the starter, which then bends closed. As the bimetal switch closes, the glow discharge inside the starter extinguishes and current, of the order of 200 mA, flows through the lamp electrodes. The electrode current, limited by the ballast, causes the electrodes to heat up and emit thermionically. When the bimetal switch cools sufficiently

to reopen, the full supply voltage is then presented across the lamp and the starter. If the starter opened when the alternating current flowing through the ballast was near to its minimum, then the lamp would not ignite and the glow starter would close again, repeating the cycle.

If the starter contacts opened when the ballast current was near its maximum then the ballast, a large inductor, would provide a large voltage transient across the lamp. This voltage transient, coupled with the effects of the electrodes emitting thermionically, would be sufficient to initiate an arc discharge in the lamp. The electrodes now continue to emit thermionically due to bombardment of mercury ions during the cathode phase, electron energy during the anode phase and the passage of lamp current.

The passage of electrons down the tube, accelerated by the electric field, causes excitation and ionisation of mercury vapour atoms. Some excited atoms return to the ground state and, in the process, emit a photon of light in the ultra violet region. The phosphor coating inside the tube then converts the incident ultra violet radiation into visible light.

Cumulative ionisation of mercury atoms in the discharge produces a runaway current or negative resistance characteristic. The discharge is stabilised by the fact that the combined characteristics of both the lamp and the ballast is positive.

During an arc discharge the lamp voltage is approximately 100 V, which is insufficient to initiate a glow discharge in the starter. The suppression capacitor is included to limit electromagnetic interference caused by glow starter switching and to increase the time that the glow starter remains closed.

2.2 Lamp Components

2.2.1 The Gas

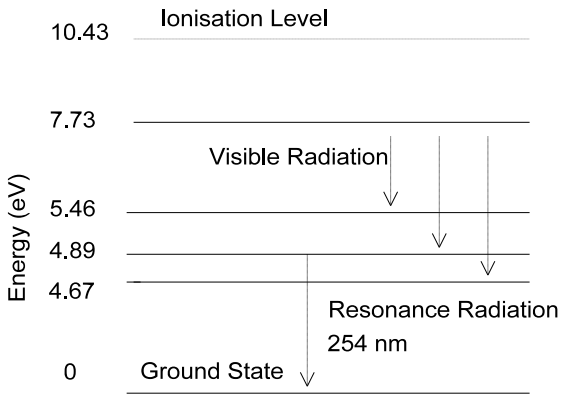

Figure 2.2: Energy level diagram for mercury[1].

The fluorescent lamp is filled with a rare gas, usually argon, and a small quantity of mercury. At room temperature the mercury vapour pressure is very low and attains the correct pressure when the lamp wall is at approximately 40°C. The task of the mercury vapour is to develop a plasma and emit electromagnetic radiation.

During an arc discharge, electrons, emitted by the cathode, accelerate towards the anode under the influence of the applied electric field. During their journey the electrons collide, some 10^9 times per second, with mercury vapour atoms. Elastic collisions, excitation or ionisation occurs. After an elastic collision the incident electron will be thrown off its original course after imparting a negligible amount of energy to the atom, which is some 370 000 times heavier than an electron. The sheer quantity of elastic collisions per unit time does, however, increase the average velocity of the gas. The temperature of the gas

rises and stabilises once thermal dissipation through the wall of the tube into the surrounding air equals energy acquired. The elastic collisions result in the impinging electron continuing on its journey towards the anode.

The inelastic collisions result in the impinging electron imparting energy to the atom. This may take the form of exciting the atom to a higher energy level or ionising the atom. Excitation entails elevating the outer electron to remote discrete orbits. The atom will remain in an excited state for about 10^{-8} s before spontaneously returning to the ground state and, in the process, emit a photon of light with a wavelength proportional to the level transition. The frequency of radiation emitted is directly proportional to the energy change ΔE

$$\Delta E = \frac{hc}{\lambda} \quad [J] \ , \tag{2.1}$$

where h is Planck's constant, c is the velocity of light and λ is the wavelength of the emitted radiation. The lowest energy level to the ground state gives rise to resonant radiation and, as this energy level requires the least excitation energy, returns the best radiation efficiency. Resonant lines of mercury lie at 185 and 254 nm, both in the ultraviolet region, the latter being the stronger. The discrete energy levels are responsible for the spectral character of fluorescent light. As the colliding electron's energies are not discrete, the energy imparted to Hg atoms is covered by a certain distribution. The art of fluorescent tube design is therefore to control the kinetic energies of electrons thus ensuring efficient production of radiation. To achieve this, a buffer gas is added which limits the electron mean free paths by providing increased opportunities for resonant excitation. The buffer gas has higher energy levels than mercury so as not to waste energy by providing unwanted radiation.

An atom in the excited state may collide with an electron and become ionised. Its electron would then move on to excite and ionise other atoms whilst the ion would be attracted towards the cathode. This cumulative process, termed cumulative ionisation, is responsible

for the negative resistance characteristic of fluorescent lamps.

An atom may also be excited to a metastable state where it may remain for up to 100 ms if further undisturbed[1]. Whilst in these metastable states, 6^3P_0 and 6^3P_2, the atom cannot decay to the ground state by radiation, they therefore act as energy buffers[8]. Whilst in this state the atom may collide with another electron and pass into a higher energy level (cumulative excitation) or become ionised (cumulative ionisation).

The metastable state is very important to gaseous discharges as it ensures a continuous supply of electrons in the discharge, replacing those lost to recombination at the wall of the tube. Without the combined effects of metastable states and the plasma relaxation time, operation at mains frequencies would not be feasible.

The mercury vapour pressure is determined by the coldest spot on the tube. Mercury vapour atoms are thus in short supply during lamp starting and attain the optimum density for efficient radiation production when the tube wall is approximately 40°C. If the vapour pressure is too low then there are insufficient collisions between free electrons and Hg atoms resulting in poor luminous efficiency. If the vapour pressure is too high then there is an increasing risk of self absorbtion. Self absorption or radiation imprisonment occurs when radiation is absorbed by other atoms in the ground state, which may re-radiate at the same wavelength, or pass to higher energy levels. The ventilation of luminaires is therefore an important consideration especially in those units designed to be water tight. The combination of ballast and lamp dissipation may well cause elevated lamp temperatures and hence lower lumen efficiency. The cold spots of 9 W compact fluorescent lamps are the corners at the end of the glass envelope[2,8,9]. The performance of the lamp therefore varies according to mounting position.

2.2.2 The Electrodes

The electrodes consist of a coiled coil or a triple coil tungsten filament. Tungsten is used because other metals evaporate too quickly, causing blackening at the tube ends. The filament is coated with one or more of the alkaline earth oxides which promote thermionic emission. The coiled coil or triple coil construction facilitates adhesion of the oxide coating and the close coupled geometry makes heating easier. The oxide is relatively soft and is consumed during lamp operation through evaporation and sputtering. Sputtering occurs if ions arrive at the electrode with sufficient kinetic energy as to dislodge pieces of the oxide coating. Care is taken to manufacture the electrodes to close tolerances to preserve waveform symmetry and hence luminous ripple.

The principle tasks of the electrode are to transfer current to the gas in the cathode phase, and to transfer current from the gas in the anode phase. The design of the electrode is governed mainly by its function during the cathode phase because electrons easily enter a metal where they release energy, but cannot so easily gain energy to leave it. The minimum energy required to produce electron emission in a material is termed the thermionic work function of that material, whose units are electron volts (eV). The oxide coating has a low thermionic work function, but is relatively soft. Oxide deterioration is accelerated by excessive ion bombardment or excessive heating.

During starting the electrodes must be heated to reduce sputtering and to assist starting. The heating current is specified for the PL 9W lamp as between 153 and 240 mA[9,10]. The ideal starting temperature of the electrodes is about 800ºC[2].

During an arc discharge the energy required to sustain thermionic emission comes from the passage of discharge current, or joule heating, ion bombardment during the cathode phase and by electron bombardment during the anode phase. The cathode fall increases with reducing lamp current in order to maintain thermionic emission, resulting in increased ion bombardment and hence sputtering.

During the cathode phase the electrode must supply electrons to the gas discharge. This process, electron emission, is essential in maintaining an arc discharge. The energy imparted by ions striking the cathode may be sufficient to liberate an electron. The liberated electron would then accelerate towards the anode and enter the positive column. The alighting ion would recombine and form a mercury atom. The recombination process may result in a photon of light being emitted. The frequency of the light emitted is not covered by a discrete spectrum but is covered by a recombination continuum due to the distribution of recombination energies[6].

When the cathode is heated an abundant supply of electrons forms on the surface in the surrounding medium. The applied electric field then accelerates these electrons towards the anode. During an arc discharge an electric field exists in the space adjoining the cathode. This field or cathode fall adjusts itself automatically to both provide ions with sufficient kinetic energy to maintain electron emission in the cathode and to provide emitted electrons with sufficient energy to enter the plasma and cause ionisation. It is therefore desirable for the cathode to have a low thermionic work function in order to reduce the cathode fall and improve lamp efficiency. The thickness of the cathode fall is in the order of one mean free path length of the electrons.

During an arc discharge, emission and collection of electrons does not take place uniformly over the whole surface of the electrode. A small bright spot in the filament appears at the place where the density of the emission current during the cathode phase is much greater than elsewhere. During the life of the lamp this hot spot usually shifts as emitter material is consumed[3].

During the cathode phase a negative space charge forms in front of the electrode at the beginning and end of every half cycle, unless the current is a square wave. This periodic space charge is a source of radio frequency noise called the re-ignition-extinction noise at frequencies in the region of 500 kHz[3].

During the anode phase electrons enter the metal and lose kinetic energy. This energy corresponds to the thermionic work function of the electrode, and is dissipated in the form of heat. The anode fall voltage is of the order of the ionisation potential of the gas, because electrons must be accelerated to an energy high enough to supply ion current for the positive column[11]. In practice the anode fall is small and does not vary significantly, however, a reduction in the anode fall and hence an improvement in efficiency is possible by operating the lamp at higher frequencies[1,4,6,7].

A negative space charge forms in front of the anode periodically, because the electrodes continue emitting thermionically after every voltage reversal. The anode phase results in more heat being supplied to the electrodes than the cathode phase, because electron current is responsible for more than 99% of the lamp current[3]. During the anode phase the majority of the electrons arrive at the supply connected end of the filament[3], the other end being connected to the starter.

Radio interference is caused by anode oscillations when the active part of the electrode during the anode phase is too small to accumulate sufficient electrons. The anode potential then rises above that of the plasma. The effect is to accelerate additional electrons causing additional ionisation of gas atoms. The anode potential then drops after the anode has accumulated sufficient electrons. This cycle generates radio frequency noise[3].

2.2.3 The Phosphor Coating

The task of the phosphor is to convert incident ultra-violet radiation emitted by mercury atoms into radiation in the visible spectrum. This process[1,4], fluorescence, occurs in solids when there is simultaneous excitation and emission of radiation. In phosphors, irradiation at the correct wavelength leads to excitation of its atoms and subsequent radiation emission. The emitted radiation being at a longer wavelength than the absorbed radiation, thereby complying with Stokes Law. This phenomenon produces two different spectra, *viz.* absorption and emission spectra.

The energy distribution of the emitted radiation is independent of that which is absorbed. This enables the designers of fluorescent lamps to use a mixture of phosphors which transform spectral resonance energy into a quasi continuous spectrum of visible frequencies, albeit with varying efficiencies. The trade off for better colour rendering is therefore efficiency. These effects are also readily apparent by the poor colour rendering of lamps of obscure origin. Their phosphors do not contain the desired mix due to financial and perhaps technological constraints.

The phosphor is white, to facilitate transmission of visible radiation, but is black to 254 nm, therefore incident ultraviolet rays are readily absorbed. Another property of fluorescent lamp phosphors is phosphorescence. This is the phenomenon whereby the phosphor continues to emit light after the excitation has ended. This is important to reduce luminous ripple during mains operation (50→60 Hz) by providing emission during periodic current zeroes. The afterglow of fluorescent lamps is of the order of 10 ms[1]. The afterglow of the phosphor should therefore not be confused with the relaxation time of the plasma when measuring lamp performance.

The phosphor manages to convert approximately half the incident energy into visible energy. Although phosphors attain quantum efficiencies of 80%, *i.e.* almost every incident quantum of ultraviolet light is converted to a quantum of visible light, the fact that the

emitted radiation has a longer wavelength results a loss of energy[1]. As

$$E = h\nu \quad [J] \ . \tag{2.2}$$

The energy (E) is inversely proportional to wavelength (λ) and, as the centre wavelength of emitted visible light is approximately double the wavelength of the incident ultra-violet radiation, half the energy will be lost in the form of heat.

2.2.4 The Starter Assembly

The starter assembly in compact fluorescent lamps consists of a glow starter and a suppression capacitor. For normal mains operation the task of the starter is to initiate discharge by first pre-heating the electrodes and then interrupting the current through the ballast which, in turn, provides a striking voltage transient. The starter consists of a bimetal switch housed in a glass envelope containing a mixture of rare gases and a small amount of radioactive material[1,2,4]. Radioactive material is added to assist the ionisation process.

Mains voltage is sufficient to initiate a glow discharge between the switch contacts. The contacts have a high work function and do not emit thermionically under normal operating conditions. Glow starters therefore operate in the abnormal glow discharge region, where their resistance is positive. Heat generated by the discharge causes the bimetal switch to bend and close. The switch consists of at least one bimetal member which bends when heated, owing to different coefficients of expansion of two metals in the member. When the switch contacts close, the glow discharge extinguishes and the bimetal member cools. The short circuit provides short circuit current or pre-heating current through the lamp electrodes.

The resistivity of the glow discharge is a function of electrode, or switch contact, proximity. The glow discharge consists of *inter alia* a negative glow, Faraday dark spaces and the positive column. As the contacts close both the Faraday dark spaces and the

negative glow length are unaffected whilst the positive column shrinks. The minimum separation is about twice the dark space thickness. At a separation of less than this, the dark space distorts and the discharge extinguishes[12]. This indicates that there may be a reduction in glow starter current just prior to, and just after, contact closure.

The glow discharge threshold voltage is chosen between the limits of minimum supply voltage and maximum lamp voltage[2]. The glow starter presents a zener like action, *i.e.* no current flows until a certain voltage threshold is exceeded. Thereafter, the heat necessary to bend the bimetal element is supplied by dissipation in the cathode fall. The slope of the V/I characteristic during the abnormal glow discharge represents the dynamic resistance of the discharge. As the bimetal member has a finite thermal time constant, the time required to bend closed depends upon the energy dissipated in the cathode fall. Also, as the bimetal member will experience heat loss there will be a certain minimum glow dissipation which will effect element deflection, and therefore switch closure. The period which the contacts remain closed, *i.e.* the closure time, is selected between the limits of onset of lamp electrode thermionic emission and excessive electrode heating.

As the contacts open, the short circuit current is interrupted which may result in the ballast developing a back emf. The ballast energy content depends upon when in the current cycle the interruption occurred. This back emf, combined with the effects of electrode heating, initiates an arc discharge in the lamp. The glow starter discharge causes a certain loss of power at the moment of opening and the suppression capacitor limits the bandwidth of the opening voltage transient. These combined effects hamper the starting of compact fluorescent lamps with internal starters when using electronic ballasts. The suppression capacitor usually has a value between 0.006 and 0.02 μF which suppresses the radio interference, which may be caused by the fluorescent lamp[1,2]. Meyer *et al*[2] states that "The capacitor...enhances the operation of the glow switch by keeping its bi-metal parts longer together ....". At this stage it is unclear what mechanism is responsible for this phenomenon.

2.3 Major Regions of the Discharge

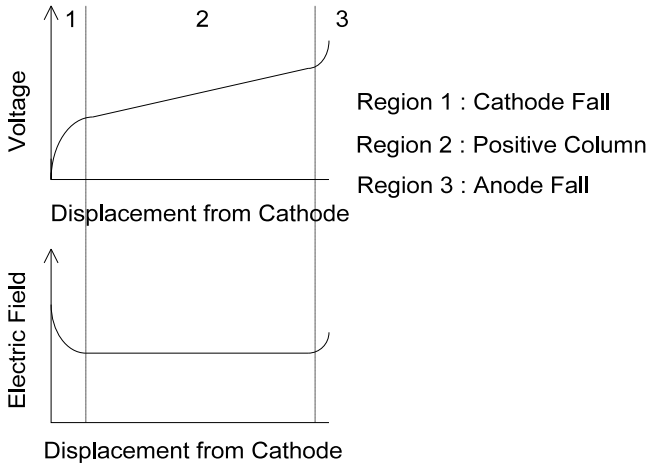

Figure 2.3: Variation in electric field strength and voltage along the length of the tube[1].

Figure 2.3 shows the variation of both electric field and voltage along the length of the tube. The cathode and anode fall areas emit little radiation and are present only to match the dynamic requirements of the positive column to the emission, and absorbtion capabilities of the electrodes. The large region of charge neutrality between the fall areas is called the positive column. This region of uniform potential gradient is responsible for the generation of most of the electromagnetic radiation. It consists of a mixture of gas atoms, excited gas atoms, ions and electrons all moving largely at random[1,6]. The concentrations of electrons and ions are equal and much lower than the concentrations of uncharged particles. Space charges are found only in the layers near the electrodes.

As the quantity of free electrons and ions per unit volume in the positive column is equal, it is therefore a region of charge neutrality or plasma. However, the degree of ionisation of the plasma decreases from the centre towards the tube wall. Radial gradients are therefore present in concentrations of particals and also in temperature[6]. These gradients

cause diffusion currents to and from the centre and also set up a heat flow towards the tube wall. Ions and electrons move radially towards the tube wall where they recombine. Recombination of ions and electrons takes place mainly at the wall of the tube[4,6]. This neutral charge drift or ambipolar diffusion is responsible for considerable loss of energy. Radiation may also be emitted as a result of this recombination, the spectrum of which is covered by a continuum[6].

The effective temperatures of the gas or electrons is related to their particle velocities by[12]

$$\frac{1}{2}m\overline{c^2} = \frac{3}{2}kT\ , \qquad \textbf{(2.3)}$$

where m is the mass of the mercury atom or electron, $\overline{c^2}$ is its mean square velocity, k is Boltzman's constant and T is the temperature. The ions and atoms form a gas at a temperature only slightly above the surroundings of the tube, typically 10 to 30°C above ambient[4]. The electrons require much more energy to cause ionisation and typically have energies corresponding to electron temperatures from 10 000 K to 20 000 K[4,7]. This additional energy is derived from their acceleration by the electric field. The electrons are mainly responsible for charge transport as the ions move more slowly. The ions are responsible for only 0.1 to 1% of the total current[4]. Electron and gas temperatures converge with increasing current density, attaining parity in high pressure discharges[4].

The metastable states of mercury atoms can also play an important part during the re-ignition of maintained[5] light fittings. It is advantageous to apply emergency supply to the lamp spontaneously, before gas ions recombine and excited atoms return from metastable states. This negates the complex process of re-ignition. If the changeover process is delayed then ignition will be more difficult than with a cold lamp due to the high gas pressure.

A buffer gas, usually argon, is added to control the mobility of the electrons thereby

reducing losses to the wall of the tube by ambipolar diffusion and increasing the chances of collisions with mercury atoms. It is desirable to keep the mercury vapour pressure low in order to reduce the chances of radiation self absorbtion, or radiation imprisonment. However, if no buffer gas is used then the average unimpeded path of the electrons emitted from the cathode is too large and most electrons would fly into the wall of the tube or into the anode. Collisions between electrons and mercury atoms would also result in large energy transfers and thus excitation to higher, less efficient, levels.

The presence of the buffer gas improves starting by ionising mercury atoms due to the Penning effect[1,2,4,6,12]. The Penning effect occurs if the level of the metastable state of the main gas, in this case argon, is higher than the ionisation potential of the mercury vapour. Collisions between argon atoms in the metastable state and neutral mercury atoms can result in the mercury atom being ionised. Argon is chosen because its metastable potential is 11.5 V whilst the ionisation potential of mercury is 10.4 V.

Inert gases must be used because they will not react with the metal filling or other components inside the lamp. Argon is most frequently used due to its high atomic weight thereby limiting energy transfers during elastic collisions. Since the energy levels of the nobel gases are higher than that of mercury, they are rarely excited, besides, their resonant radiation lies far in the ultra violet region. The buffer gas also protects the phosphor coating from mercury ions.

The dynamic equilibrium between ions and electrons is maintained through ionisation and recombination. Electron oscillations can result through disturbances to this equilibrium, but due to their high mobility these oscillations occur at high frequencies and therefore have no visual effect. However, due to their low mobility, ion disturbances can result in oscillations from zero to a few megahertz. Ion disturbances or striations can be seen as slow moving or even stationary regions of higher optical emission intensity[12,13].

When power is removed from the lamp the mercury ions recombine and as the lamp cools

the mercury liquifies.

2.4 Static V/I Characteristics

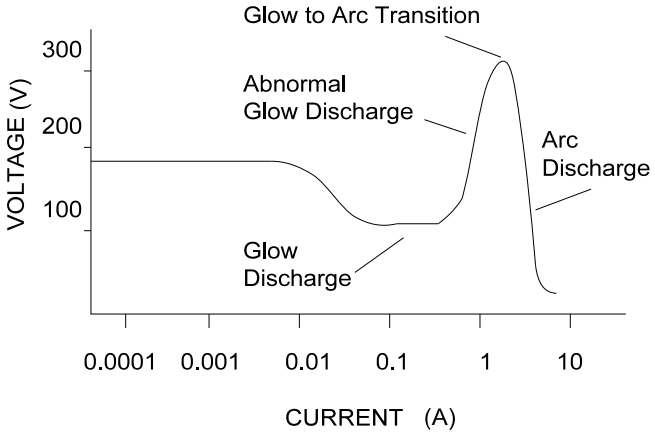

Figure 2.4: Typical static characteristics of a fluorescent lamp when driven from a constant current source[4].

Figure 2.4, on the following page, shows the general V/I characteristics of low pressure fluorescent lamps without cathode heating[1,4]. This curve was derived by using a variable current source, essential during the constant and negative voltage characteristic regions.

2.4.1 Glow Discharge

At room temperature a few electrons are present in the tube, liberated by cosmic radiation or may be left from the previous discharge. As the electric field intensity inside the tube increases, a point is reached where the electrons gain sufficient kinetic energy to ionise gas atoms. The liberated electrons, on average, drift

towards the anode and in the process may excite or ionise other atoms. When the ions alight on the cathode they attract an electron and are thereby neutralised, and the energy they release may liberate another electron. The probability of a further electron being liberated is low, *viz.* 1 in 100. In this low current region the cathode is not wholly covered by alighting ions so that the current density on the cathode remains constant, and hence the cathode fall is constant.

This phenomenon is readily visible as a voltage is increased across a glow starter. A blueish glow forms on some parts of the cathode, *i.e.* the cathode glow[12], and quickly envelops the entire cathode as the voltage is increased further.

The cathode fall for glow discharges is of the order of 100 V. This potential is required to provide impinging ions with sufficient kinetic energy to liberate electrons from the cathode. The anode fall potential is negligible at low currents.

2.4.2 Abnormal Glow Discharge

When the cathode becomes completely covered by alighting ions, a further increase in current results in an increase in voltage as the current density at the cathode must now increase. This results in a positive resistance characteristic. The increasing current density raises the temperature of the cathode because more ions are alighting. The cathode fall adjusts itself automatically so that the electron emission sustains cumulative ionisation and hence ion production. Glow Starters operate in this region, the dissipated power being used to heat their bimetal switches.

With further increases in current the cathode temperature rises to a point where electrons in the cathode attain sufficient energy to leave the attraction of their atoms and escape into the surrounding medium. A glow to arc transition has thus occurred as thermionic emission is initiated.

2.4.3 Glow to Arc Transition

The glow to arc transition (GAT) is dependant upon the number of ions in the vicinity of the cathode and the accelerating potential. The number of ions is dependant upon the mercury vapour pressure which is dependant upon ambient temperature. It follows that the GAT point varies with lamp temperature, an important consideration when operating the fluorescent lamp at low powers.

A lamp biased near to the GAT on the negative resistance arc discharge region could revert to an abnormal glow discharge under cold ambient temperature conditions.

2.4.4 Arc Discharge

An arc discharge is initiated as current increases beyond the GAT point. The essential characteristic of an arc discharge being that the cathode emits thermionically[1] although, strictly speaking, the differentiation should be made on the basis of electron and gas temperature differential[11]. In a glow discharge the mean unimpeded electron path is low resulting in high electron temperatures and low gas temperatures whilst in an arc discharge the mean path and hence electron temperatures are lower.

In fluorescent lamps the transition is, however, a cathode related phenomenon. The cathode fall potential during an arc discharge is approximately 10 V, this being the required potential to both provide alighting ions with sufficient kinetic energy so that cathode thermionic emission is maintained, and to provide emitted electrons with sufficient kinetic energy to enter the plasma and cause ionisation.

Electrons emitted from the cathode are accelerated towards the anode by the electric field.

In the process they may produce cumulative ionisation. Cumulative ionisation, as the name suggests, results in a runaway effect and hence a negative characteristic. Provided with a low impedance supply, this cumulative effect would ultimately result is the lamp exploding, and so the lamp must be biased at a desired operating point.

At low frequencies the discharge follows the current variations and therefore the instantaneous lamp voltage can be read off the static V/I characteristic.[1,4,11]. It follows that the linearity of the region about the operating point markedly influences lamp voltage distortion at low frequencies. If dc is used then the lamp model during arc discharge is simply a negative resistance. The value being the average slope of the V/I characteristic around the intended operating point.

2.5 Lamp Ignition

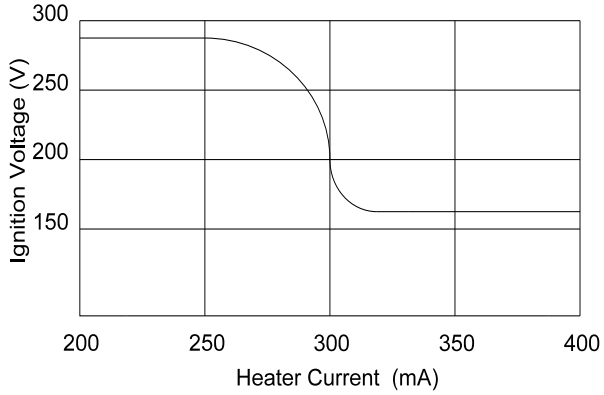

Figure 2.5: Typical relationship between required ignition voltage and electrode preheating current[1].

The lamp ignition, or starting, dynamics deserves close inspection because it is usually easy to maintain an arc discharge with an electronic ballast, but difficult to initiate one. With compact fluorescent lamps containing internal starters the pre-heating cycle involves periodic short circuits caused by starter switch closure, during which pre-heating current must be supplied to the electrodes. This is followed by high impedance conditions, during which a high starting voltage must be applied. The two operating conditions present two very different loads to the electronic ballast, which must not suffer any ill effects even after extended starting attempts due to the presence of an old lamp or lack of one at all.

A mains ballast may typically store 0.1 J, if the glow starter opened whilst the ballast current was near its maximum. This energy is available to develop a high voltage, high energy transient to overcome the load presented by the starter, suppression capacitor, *etc*., and initiate lamp ignition. The electronic ballast, however, usually has no comparable inductive energy storage capability to provide ignition voltages.

A typical emission curve[1] is shown in Figure 2.5 on the previous page. This shows the relationship between electrode pre-heating current and required striking potential. The lamp used by Elenbaas[1] for this test had a conductive stripe along the length of the tube, connected to the ignition voltage. The reason for the stripe was to reduce the required ignition voltage.

The graph can be described as having two well defined regions, either insufficient or sufficient heater current. The transition between the two regions occurs over a heater current span of only 50 mA. This electrode only begins to emit thermionically above 250 mA.

Little reduction in ignition voltage is gained above 300 mA. This is because the electron emission is limited by the space charge which forms around the electrode[12]. Coulomb repulsion by electrons in the space charge ensures that the emission curve does not intercept the x axis. An electric field is required to draw electrons away from the electrode to reduce the space charge there.

Excessive pre-heating current will result in unnecessary emitter evaporation and reduced lamp life or, in the extreme case, filament rupture. The waveform shape or frequency of the heater current is not important as long as the rms current falls within the specified limits.

The ignition process can be divided into three phases, glow starter activation, electrode heating phase and an ignition phase. With mains operation these phases may be repeated to attain lamp ignition.

2.6 Parameters Affecting Performance

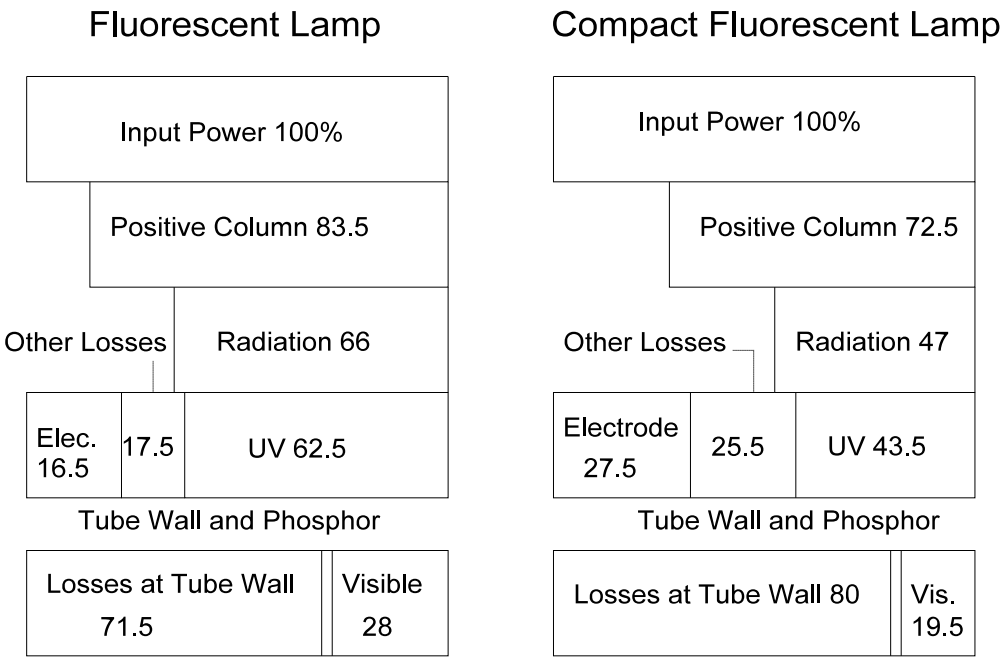

Figure 2.6: Power conversion losses for both linear and compact fluorescent lamps[1,2].

Figure 2.6 shows the energy balance in fluorescent lamps[1,2]. The conversion efficiency of input electrical power into visible radiation in low pressure fluorescent lamps, although better than their incandescent counterparts, is only about 28%. With compact fluorescent lamps the figure is worse at 19.5%. Losses are incurred in the electrodes, the gas and the phosphor. Electrode losses are incurred in maintaining thermionic emission. The excess energy is carried away by conduction, convection and radiation. Gas losses take the form of power required to maintain the level of ionisation to counteract the effects of ambipolar diffusion and losses due to self absorption. Phosphor losses are due to the quantum efficiency of wavelength conversion.

2.6.1 Current Frequency

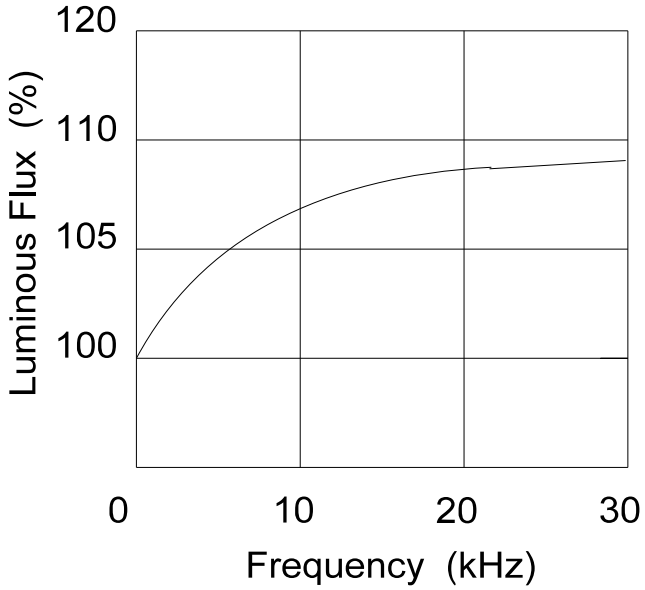

Figure 2.7: Luminous flux relative to 50 Hz plotted against lamp current frequency[2].

Due to the complex dynamics of electrode thermal delay and relaxation times of the plasma and electron gas, the lamp performance varies considerably with supply frequency.

At low frequencies, as in mains operation, the lamp periodically extinguishes and then re-ignites at every current zero. This re-ignition voltage requirement is far lower than that of a cold lamp, because the plasma remains for up to 10 ms[6] after the lamp has extinguished and the electrodes are already at operating temperature. As the lamp re-ignites the process of cumulative ionisation follows the lamp current fluctuations resulting in a non-linear voltage-current characteristic. The periodic re-ignition reduces efficiency and the waveform consequent distortion is a source of electromagnetic interference.

As the supply frequency increases the ionisation state can no longer follow the rapid changes in lamp current and the plasma density becomes constant, resulting in a constant effective resistance throughout the cycle[1]. A further advantage is that no periodic re-ignition is required. As the frequency increases the electrode falls also decrease resulting in increases in efficiency[1,7,8]. The use of direct current has a similar effect on efficiency as high supply frequency because the plasma density remains constant.

The mechanism responsible for plasma relaxation is ambipolar diffusion. This is the process whereby electrons and ions travel to the wall of the tube, where they recombine. Polman *et al*[7] cites representative values for ambipolar diffusion (T_a) of 1 ms and electron temperature relaxation time (T_e) of 5 μs. As the plasma relaxation time is less than 10 ms, at mains frequencies both the plasma density and the electron temperature are modulated by the instantaneous current variations[6]. There are, however, frequencies where the current variations are followed by the electron temperature (T_e) but not by the whole plasma[6,7].

Polman *et al*[7] conducted an experiment by modulating a dc discharge. When the modulation period was greater than both plasma and electron temperature relaxation times, the result was a slowly varying dc discharge with hardly any variation in electron temperature. This is because only slight changes in electron temperature cause current variations due to the exponential relationship between electron temperature and the ionisation rate. When the modulation period ($2\pi/\omega$) was much less than both periods then the discharge was too slow to follow the variation, and the electron temperature adjusted to a level corresponding to the average current. When the modulation period was in the region $T_a \leq 2\pi/\omega \leq T_e$ the modulated discharge current caused a modulation in electron temperature with no modulation in plasma concentration, as expected. However, as the modulation coefficient was increased above 0.5 the concentration of excited atoms increased, contrary to expectations. The result was that there were relatively more electrons of high energy than there would be in a dc discharge with the same average electron energy. This clearly caused an increase in populations of electrons at high energy levels,

resulting in an increase in 436 nm emission. As this emission is visible, blueish light, no phosphor conversion is necessary and so efficiency is improved. These effects occur when a rapid increase in field strength caused a rapid rise in electron temperature, as in pulsed discharges.

The highest efficiencies are achieved at frequencies of 100 kHz[7,17], although an upper frequency limit of 50 kHz is recommended due to increasing electromagnetic interference generated by the lamp[2].

Capacitive coupling between the lamp and luminaire requires consideration at high frequencies. Although capacitive coupling assists lamp ignition, efficiency is adversely affected during an arc discharge. Hammer[21] cautions that the capacitive coupling could result in substantial current flowing if the separation distance is less than 3 mm. His data, using 2.5 m long T12 lamps, revealed that 12 mm was adequate for reliable starting at 25 kHz. His measurements also revealed that a 30% increase in lumen efficiency over mains operation is achievable at 25 kHz. Hammer also observed that there were no significant shift in chromacity co-ordinates when the lamps were dimmed with high frequency operation.

Elenbaas[1] captured oscillograms of lamp voltage at various frequencies. The waveforms are nearly sinusoidal at 8 kHz. He states that "... for lamps of 1 or 1.5 inch diameter, the form of both current and voltage is nearly sinusoidal at 400 Hz and higher". This observation will impact on the model selected for the 9 W compact fluorescent lamp.

2.6.2 Current Amplitude

Increases in current above the rated value will be accompanied by a decrease in efficiency. The increase in lamp dissipation raises mercury vapour pressure resulting in an increased probability of self absorbtion of the resonant radiation, *i.e.* radiation imprisonment. This is a process whereby photons emitted by mercury atom relaxation are absorbed by other atoms, the receptor atom may already be excited and may pass into a higher energy level, or become ionised. Self absorption reduces efficiency because at each absorbtion and re-emission there is a finite possibility that the energy is released in a non-radiative process[1,2,8].

Efficiency also decreases as current decreases below the rated value because the same power is required to maintain thermionic emission[19]. Also, decreased lamp dissipation will result in a lower vapour pressure and therefore longer mean free electron paths. The electrons may therefore attain higher impact velocities resulting in higher, less efficient, energy levels being excited at the expense of resonant levels[1,2].

Work done by Kalinowsky[25] revealed a 5% reduction in efficiency for a 20% decrease in lamp power below the rated value. These tests were conducted on 36 compact fluorescent lamps at 60 Hz. This data suggests that efficient operation is still possible below the rated operating power.

At low frequencies, up to approximately 500 Hz, the discharge follows the instantaneous current variations. Since efficiency decreases with increasing current density the highest efficiency will occur with direct current and the lowest will occur with high instantaneous currents[1]. It follows that efficiency decreases, at low current frequencies, as the current peak factor increases above unity.

2.6.3 Ambient Temperature

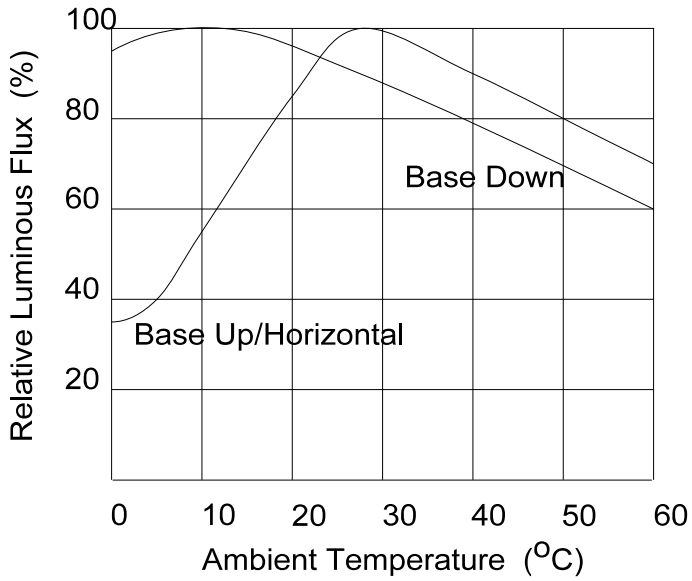

Figure 2.8: Performance of 9 W compact fluorescent lamps versus temperature and attitude[9].

Low ambient temperatures will cause a lower mercury vapour pressures resulting in a lower probability of collisions, longer mean free paths an hence increased likelihood of excitation to higher, less efficient, energy levels. Operation at higher ambient temperatures leads to higher mercury vapour pressure and hence increased self absorbtion. The number of elastic collisions rises resulting in an increase of gas temperature. Mercury vapour pressure is determined by the temperature of the lamp cold spot. The mounting position of the lamp and luminaire ventilation therefore affects efficiency. Osram[9] specifies base up at ambient temperatures between 30 and 65°C for most efficient operation for their compact fluorescent lamps.

Hammer[26] found that there is a 3% improvement in efficiency with new generation compact fluorescent lamps when operated at 50ºC instead of at the reference rating of 25ºC. This is perhaps due to the realisation that the lamps will probably be used in small compact luminaires with poor ventilation. At light outputs of less than 50% of the rated value, Hammer found a negligible change in light output between ambient temperatures of 15 and 50ºC[21]. These tests were conducted on T10 lamps at 25 kHz.

2.7 Parameters Affecting Ignition

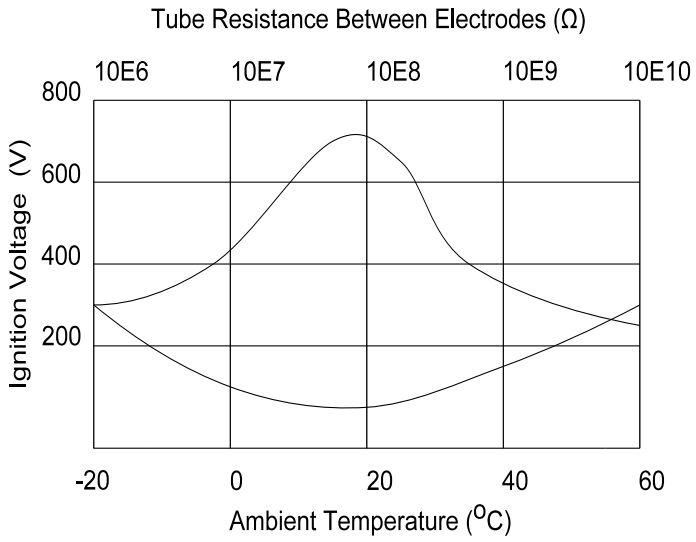

Figure 2.9: Required ignition voltage versus ambient temperature (lower curve) and tube resistance (upper curve)[1].

The required ignition voltage is determined by the abundance of free electrons and ions, so it follows that any method of increasing the electron and ion supply would aid ignition. A transverse discharge is one such method. This is an arc discharge initiated between the

filament leads at high heater currents.

Another method to assist ignition is to provide an adjacent field[1,4,5,15]. The capacitive coupling between this nearby field and the lamp will initiate a glow discharge inside the lamp if the potential difference is high enough. The glow discharge provides charged particles which then assist ignition. An adjacent earthing strip has a similar effect. The proximity of conductive surfaces to the lamp will affect ignition performance if there is a return path, via earth connections or electronics, to the electrodes.

Required ignition potential is related to the external resistance of the tube[1,5]. Figure 2.9 shows the relationship between required ignition potential and external tube resistance. Ignition is therefore assisted by extremes of tube resistance. Ambient humidity and condensation therefore play an important part in ignition performance.

Gas temperature also affects starting performance. At low temperatures the mercury vapour pressure is low and there is a lower probability of production of ions through mercury ionisation, and so ignition becomes more difficult. At high temperatures the vapour pressure rises and the average unimpeded path shortens. The electrons therefore lose energy by undergoing elastic collisions and fewer are able to acquire sufficient velocity to cause ionisation, and so ignition also becomes more difficult. Hammer[15] conducted experiments with 40 W biaxial lamps with starting aids at various ambient temperatures using a 60 Hz supply. He found that the starting voltage requirement was 470 - 570 $V_{pk\text{-}pk}$ greater at the extreme temperatures of 0 and 60 °C, than that required at an ambient temperature of 25°C. The upper temperature starting requirement is of particular interest in the design of maintained emergency lighting systems because emergency ignition may be initiated with a hot lamp.

2.8 Lamp Life

Lamp life is determined mainly by the electrodes. During normal operation the oxide coating on the electrodes is consumed due to sputtering and evaporation. Positive ions do not impinge uniformly along the length of the electrode during arc discharge because the resistance of the electrode dictates that the connected end is always at a higher potential than the end connected to the starter. The discharge hot spot shifts very slowly from the connected end of the electrode to the opposite end as the emitter coating is consumed[1,3]. The starting voltage requirement also rises as the emitter material becomes exhausted.

Starting cycles have the most detrimental effect upon the electrodes due to sputtering caused by the starting voltage surge. A continuously burning lamp will last 2.5 times the rated life, where the rated life refers to operation with the lamp switched every 2 hours[4].

If an attempt is made to start the lamp without preheating the electrodes then high striking voltages are required. This is because it is necessary to first produce positive ions and then accelerate these ions towards the cathode with sufficient kinetic energy so that the bombardment of the ions on the cathode produces enough heat to begin electron emission. This has a severe negative effect upon lamp life as the high voltage provides the ions with large kinetic energies and they strike the cathode with force sufficient to dislodge pieces of emitter material. These pieces of emitter material are deposited at the tube ends. Sputtered pieces of emitter material are clearly visible at the ends of old lamps. If half the starts are by cold cathode then life is reduced by about 30%[2]. Preheating is therefore essential in order to prolong lamp life.

Thermionic emission is sustained during an arc discharge by the passage of lamp current, ion bombardment during the cathode phase and electron bombardment during the anode phase. Evaporation is therefore directly proportional to electrode temperature and so it follows that operation at elevated lamp currents will increase evaporation accordingly[2].

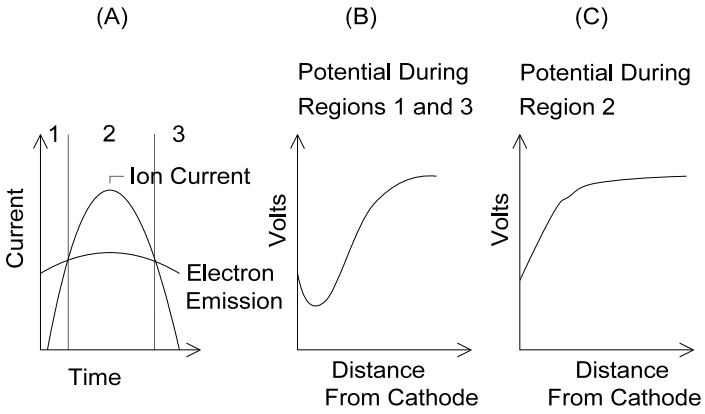

Figure 2.10: Variation of instantaneous cathode near field voltage during a current half cycle[3].

Figure 2.10 shows the effects of electrode thermal delay during one half cycle when the electrode acts as a cathode[3]. Graph (A) shows instantaneous electron emission and ion currents. Note that due to thermal delay during periods 1 and 3 the electron emission is greater than that required for the discharge current and a negative space charge forms at the cathode, see graph (B).

During period 2 the discharge requires more electrons than the cathode can readily supply. The negative space charge disappears and a positive electric field takes its place causing an increase in electron emission from the cathode. During this period the positive ions take a greater part in the discharge current. Due to the disappearance of the negative space charge the positive ions arrive at the cathode with more kinetic energy and higher electrode bombardment results. It follows that the form of the current has an effect on electrode life.

The ratio of peak current to rms current is termed the peak or crest factor (CF). The maximum crest factor has been set at 1.7, by international agreement, in order to avoid undue shortening of the lamp life[1,2,21]. A crest factor of 1.7 reduces lamp life by some 30%

at mains frequencies[2]. Given that the peak of a pure sinusoidal waveform is 1.4 times the rms value, the peak lamp current must be controlled within tight limits.

At high frequency it may be possible to have elevated crest factor currents, without a significant reduction in lamp life, due to the following hypothesis. As the mercury ions have a much greater inertia than electrons, they will acquire less and less kinetic energy as the frequency increases[12]. Therefore, during the disappearance of the negative space charge, *i.e.* during current peaks, sputtering will decrease with increasing frequency as the ions will alight on the electrodes with less energy. An indication of the ion mobility is given by the upper frequency limit, a few megahertz[12], of ion oscillations. Ion bombardment would therefore be insignificant above this frequency limit.

As mercury ions strike the cathode they recombine to form atoms. It follows that the use of direct current results in migration of mercury towards the cathode end of the lamp. This process is known as electrophoresis[1]. The result is that mercury resonant radiation reduces at the anode end due to a lack of mercury atoms. This part of the lamp then emits less light, resulting in reduced efficiency. Periodic lamp reversal is therefore necessary. Electrophoresis can be counteracted by operating the lamp at elevated ambient temperatures, greater than 50°C, by using unventilated luminaires[1].

As the electrode emitter material is consumed by evaporation, the lamp life is prolonged if the current is reduced within limits[2]. This may counteract other design trade offs in the design of maintained light fittings as these lamps need not operate at rated power. However, if the lamp is operated at 25% light output then considerably higher than rated heater voltage is required otherwise lamp life will be severely reduced, perhaps by as much as 50%, due to sputtering[2].

The glow current, *i.e.* the initial current which flows before ignition, should be limited to 10→15 mA peak in order to reduce sputtering[20]. If follows that the electrodes should be adequately heated before the starting lamp voltage is applied. The electrodes should be

heated for at least 500 ms before the starting voltage is applied[21].

2.9 Models of the Discharge

The discharge process contains many variables and so accurate modelling is difficult. Variables include ambient temperature, mercury vapour pressure, plasma and electron temperature relaxation times. Due to its complex dynamics accurate models of the lamp are still the subject of considerable interest. It is, however, important that some model of the lamp is developed to facilitate ballast design.

2.9.1 DC Model

The model for dc currents is a negative resistance. The value of which is the operating point on the static V/I characteristic. If flyback dc-dc converters are used then the lamp model is simply a resistor, because this type of converter is essentially a constant current source. The value of the resistor can be computed from the V/I characteristic by obtaining the lamp voltage which corresponds to the converter short circuit current. A stable arc discharge is therefore assured in spite of the negative resistance characteristic of the lamp.

2.9.2 Low Frequency Model

The model of the lamp for mains voltages will not be covered here. At frequencies between 200 and 800 Hz the ionisation follows the lamp current so the instantaneous lamp voltage (v) could be characterised by[18]

$$v = \frac{1+b.i.L/H}{1+b.i} \quad [V] \tag{2.4}$$

where i is the instantaneous lamp current, b is a scaling factor. L and H are the valley and

peak voltages respectively.

A more accurate and complex model is presented by Laskowski[23]. This model is based on the principle of energy conservation. Explicit functional relationships between the arc temperature and lamp radiation, and heat conduction and arc conductivity are modelled by expressions with six constants. The values of the constants are obtained from a few measurements and a least squares fitting procedure. Electrical energy supplied to the lamp is accounted for through the summation of all the energy processes at every point in time. Input power is simple resistive heating whilst output power is removed as radiation and heat conduction. These few energy processes account for 95% of the energy in a real lamp system.

Expressions have been derived for the input power to the lamp, total radiated energy, power conducted from the arc to the tube wall, arc resistance and temperature of the arc column. For the sake of brevity the equations are not listed. The feedback nature of the lamp and the interdependencies of the lamp subsystems require that the basic power process subsystems be linked by a feedback network. Laskowski states that the model is accurate for frequencies between dc and 30 kHz. For frequencies above 1 kHz accuracy is only good for sinusoids. For this reason and due to the model complexity, the author believes that this model would not be suitable for use in high frequency inverter design.

2.9.3 High Frequency Model

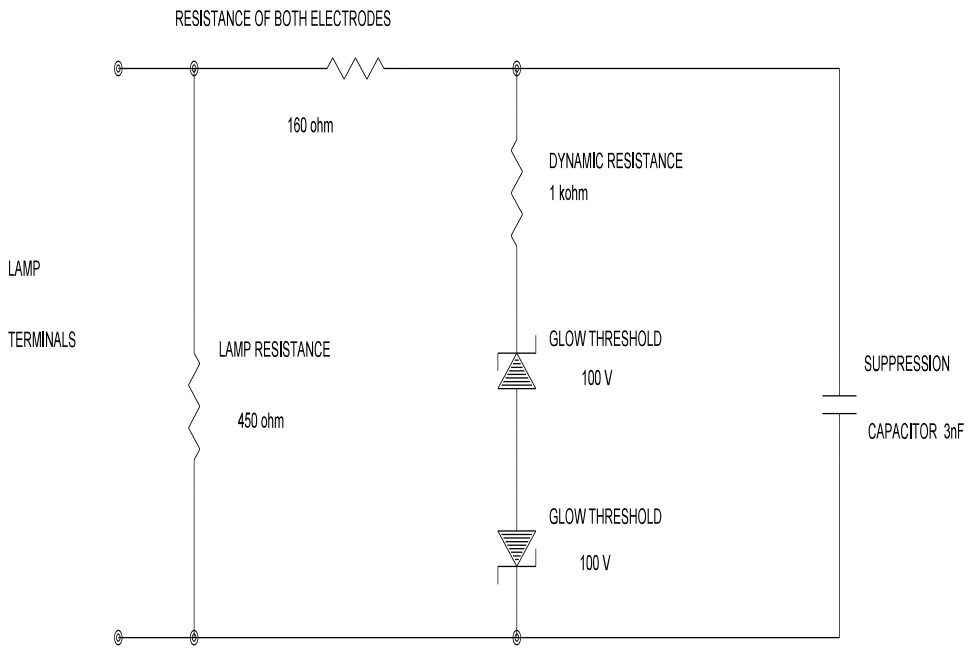

Figure 2.11: The proposed model of a fluorescent lamp, glow starter and suppression capacitor at high frequencies based on the author's measurements. The equivalent lamp resistor is only valid for a lamp powers of 7→8 W.

It is clear that the model must be chosen to suit the selected operating conditions. At low frequencies the lamp operation is complicated by periodic re-ignition[1,16], but as the frequency increases the lamp resistivity becomes constant for any given lamp power. There is evidence that lamp voltages are nearly sinusoidal at 8 kHz[1]. There is also evidence that the plasma resistivity changes dramatically between 10 and 100 kHz with pulse discharges[7,17]. This suggests that if the lamp current contains any transient components then the model is further complicated.

If an operating frequency above 20 kHz is used then the lamp may be modelled as a simple resistor provided that the lamp is powered by a current source[22]. In most emergency lighting applications, energy conversion will be accomplished by means of flyback inverters where the energy available for conversion is fixed. In these cases the value of the lamp equivalent resistor can be obtained by selecting an operating point on the static V/I characteristic. This model, however, can only be used for arc discharge conditions. The electrodes resistances can be modelled as a single resistor in series with the glow starter, see Figure 2.11, as the connected ends of the electrodes are at higher potentials than the other ends, *i.e.* the glow starter end. However, it is accepted that this equivalent resistance varies according to the hot spot position and age of the lamp. The glow starter can be modelled as two back to back zener diodes in series with a resistor. The value of the resistor is equal to the dynamic resistance of the glow discharge.

2.10 Summary

During starting the resistivity of the lamp is very high and can be neglected. The ballast ignition performance can therefore be assessed by using the load of the glow starter and suppression capacitor. The exact starting voltage requirements can only be determined by experimentation as the ignition dynamics are too dependant on environmental conditions, such as humidity, temperature, *etc.*, for accurate modelling to be successful. Ballast development must include exhaustive testing to confirm ignition reliability.

The use of dc lamp current is not recommended because it reduces lamp life through electrophoresis. Electrophoresis can be counteracted by either operating the lamp at high ambient temperatures greater than 50^{o}C or regular lamp reversal[1]. Lamp reversal incurs the penalty of extra cost of a change over relay or the reliance on physical lamp reversal.

3 Lamp Performance Measurements

3.1 General

The aim was to characterise the lamps and thereby optimise operation and ignition. Comprehensive performance figures are not readily available from lamp manufacturers, perhaps to curb imitation.

The primary function of a battery operated luminaire is to produce light and inverter efficiency alone does not guarantee system efficiency as the lumen efficiency varies with current form, frequency and amplitude. Other influencing factors include electrode dissipation and starting aid current during arc discharge.

Two lamps each from three different manufacturers were tested. The manufacturers were Philips, Osram and `No Name Brand'. The latter were used to investigate whether any other characteristics would be distinguishable from reputable products besides lumen maintenance and colour rendering. All the lamps were first aged for 100 hours to obtain more representative results[15,21,26].

All tests were conducted with the lamps in a horizontal position. The total light output was measured by situating the lamp in an integrating sphere with an aperture to accommodate a cosine corrected illuminance meter[39,40]. Absolute measurements of luminous flux are beyond the scope of this work, rather, relative values of light output are of interest.

The starter components were removed from the lamps and tested separately.

3.2 Manufacturer's Specifications

The following tables are specifications for 9 W compact fluorescent lamps. The Philips measurements were conducted at an ambient temperature of 35°C, with a supply of 220 V 50 Hz. The lamps were mounted in a horizontal position. The Osram measurement were conducted at an ambient temperature of 25°C, with the same supply, but with the lamps in a the base up position.

50 Hz Operation	Philips	Osram
Current	170 mA	170 mA
Voltage	60 V	60 V
Wattage	8.7 W	8.7 W
Luminous Flux	600 lm	600 lm
Luminous Efficacy	69 lmW^{-1}	69 lmW^{-1}
Preheat Current	153-240 mA	153-240 mA
Ignition Time	≈ 2 s	≈ 1.5 s
Equivalent Electrode Resistance	160 Ω	160 Ω

High Frequency Operation	Philips	Osram
Current	-	170 mA
Voltage	-	48 V
Wattage	-	8.2 W

3.3 50 Hz Performance

The aim was to gain some insight into performance spread between manufacturers and to obtain a reference of total light output.

3.3.1 Test Method

The lamps were connected via a ballast to a variable mains supply. The characteristic square voltage waveform facilitated rms measurement, but the current waveform is rich in harmonics[16]. An rms to dc voltage converter was constructed[32] to obtain a more accurate rms measurement of the current. Although the measurements of both rms voltage and current may have been accurate, the computation of input power was subject to error due to the estimates of phase lag, as the current waveform is appreciably distorted. The phase lag also increases with decreasing input power as re-ignition is progressively delayed. The measurement of current phase lag at rated power was approximated from the manufacturers operating specifications. Lamp current and voltage are quoted as 170 mA and 60 V respectively whilst the rated power is 8.7 W. The `current lag' is therefore 32º. It is understood that this simplistic approximation of input power which assumes that the waveforms are pure sinusoids is subject to error especially with poor waveform symmetry, but the results yielded good correlation with the dc measurements.

Full voltage was applied to achieve ignition. Measurements were conducted after a 10 minute warm up period to allow the mercury pressure, and hence luminous flux, to stabilise. Lamp voltage, current and light output were then monitored as the supply voltage was decreased. Visual anomalies were noted as well as the point at which the lamps extinguished. The tests were conducted at an ambient temperature of 25ºC.

3.3.2 Test Results

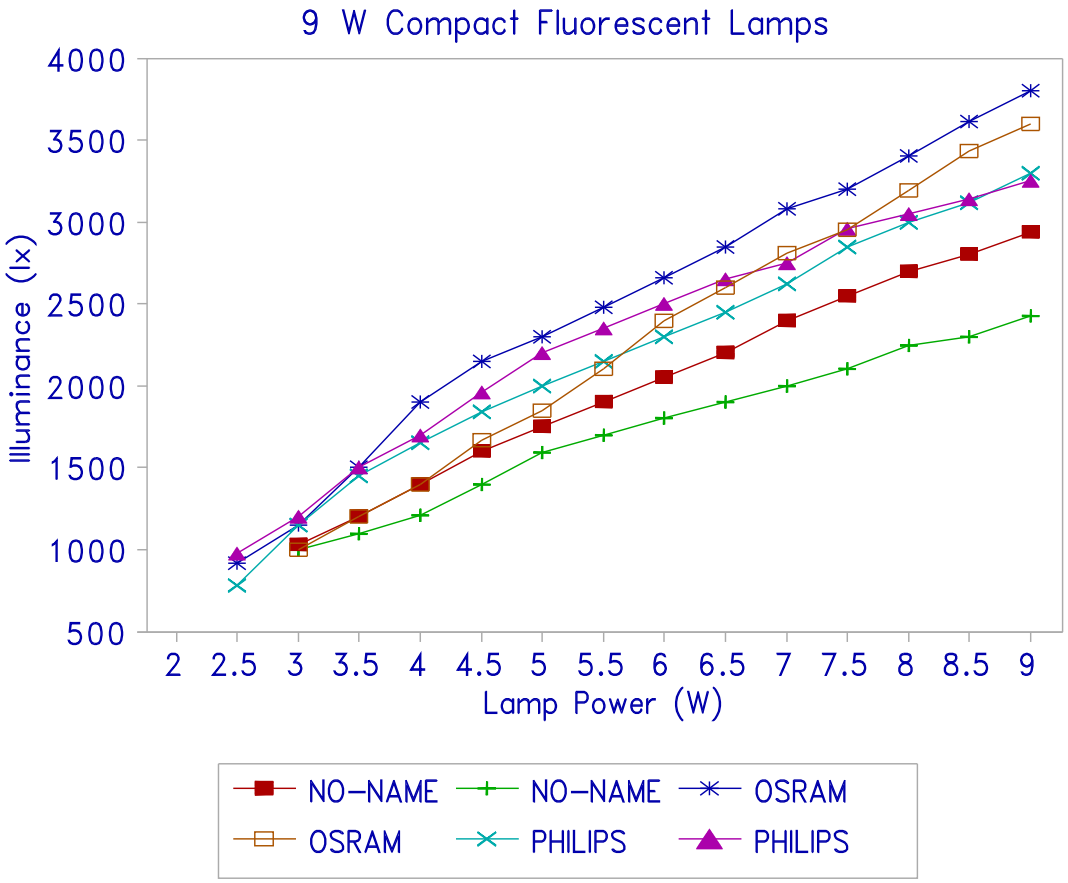

Figure 3.1: Measured relative 50 Hz performance of various brand name lamps. No external heating was provided.

From Figure 3.1 both "No Name Brand" lamps were less efficient than the lamps made by either Osram or Philips besides having poorer colour rendering. Although no measurements of spectral luminance were conducted it was visually apparent that less energy was emitted in the longer wavelength regions as red colours were poorly rendered. It was also evident that below 3 W operation became unreliable due to either insufficient available restriking voltage at every current reversal or insufficient electrode dissipation. Lamp extinction is indicated on the graph by the lowest power registered for each lamp. At low powers the lamp voltage could also exceed the glow discharge threshold on some lamps, which could result in glow starter operation and hence lamp extinction.

The luminous efficacy between the best and worse lamps was approximately 40% at rated power. The difference in luminous efficacy between the Osram and Philips lamps was possibly because the Philips lamps are optimised for operation at an ambient temperature of 35°C, whereas the tests were conducted at 25°C. Ion instabilities, or striations, were noticed with both "No Name Brand" lamps at low lamp currents. No instabilities were observed on either the Philips or Osram lamps. This may indicate that lower quality lamps are more prone to arc discharge instability then lamps from reputable manufacturers.

3.4 DC Performance

The dc performance of the lamp is similar to the performance at high frequency as there is no periodic arc extinction[1]. The aim of the tests was to gain some insight into improving the lumen efficacy by using dc or a high frequency supply.

3.4.1 Test Method

The output from a variable mains supply was full wave rectified and smoothed. The resulting dc supply was then connected to the lamp via a ballast resistor. Full voltage was applied to achieve ignition. Measurements were conducted after a 10 minute warm up period, in order to allow the mercury pressure to stabilise. Lamp voltage, current and light output were then monitored as the supply voltage was decreased. Visual anomalies were noted, as well as the point at which the lamps extinguished.

3.4.2 Test Results

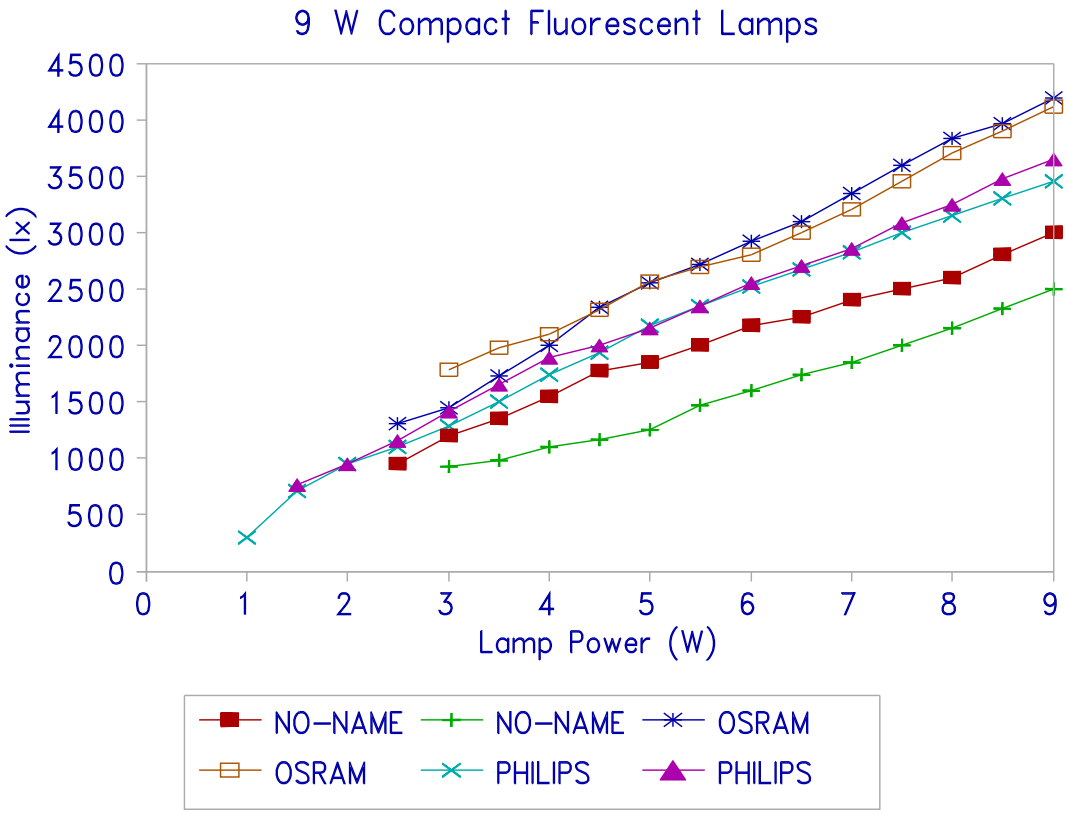

Figure 3.2: Measured relative dc performance of various brand name lamps. No external electrode heating was provided.

Note that, in Figure 3.2, both Philips lamps were able to sustain an arc discharge below 2.5 W. The elongation of the cathode fall at low powers was clearly visible, this being necessary to maintain thermionic emission from the electrodes. For this reason operation at reduced powers must be accompanied by increased heater current otherwise excessive ion bombardment will occur. Reliable operation with all lamps, however, was only possible above 3 W. This situation could be significantly improved by providing additional electrode heating.

As with 50 Hz ac operation, the "No Name Brand" lamps returned the lowest lumen efficacy and the poorest colour rendering.

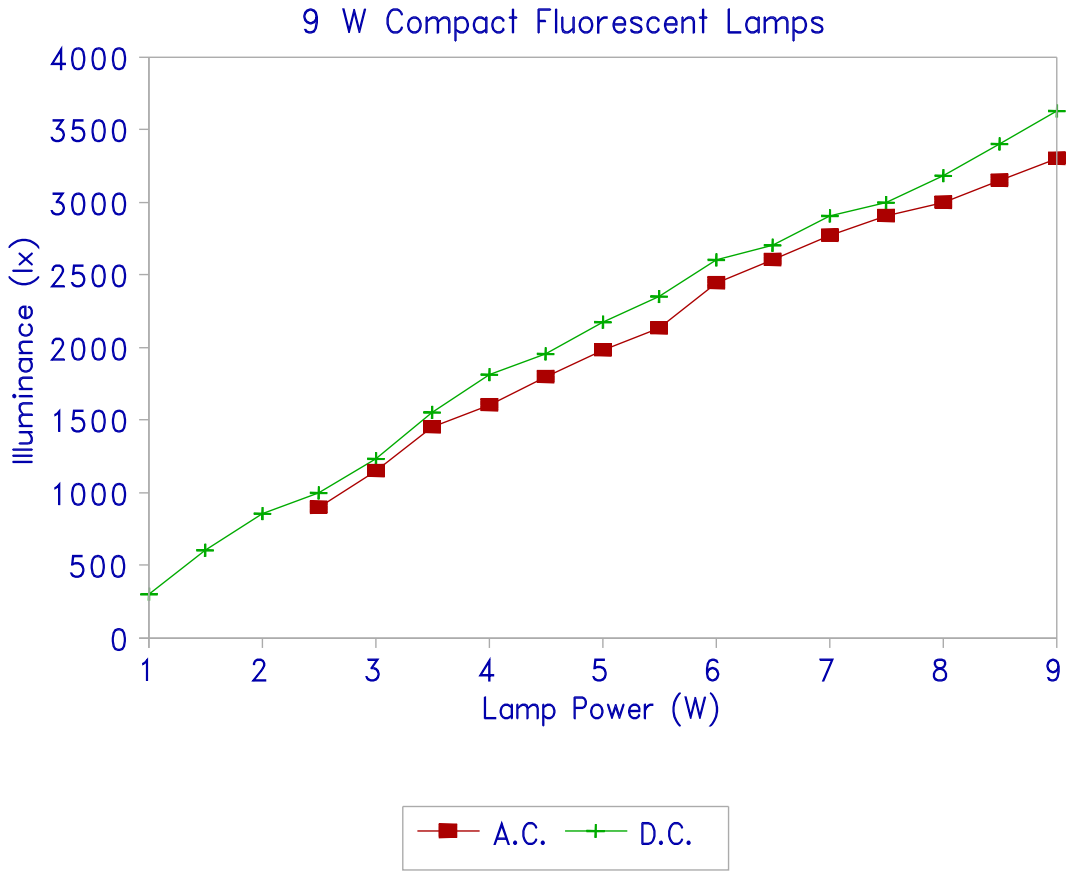

Figure 3.3: Comparison between average 50 Hz and dc performance measurements.

Figure 3.3 shows a comparison between the average 50 Hz and dc performances. The graph indicates that improvements in luminous efficacy from 4 to 16% are possible when using a dc lamp supply. Similar improvements in efficacy should be possible at high frequency, as the ionisation rate is also constant. Osram specify their lamp rated power as 8.7 W at 50 Hz and 8.2 W at 40 kHz, presumably for the same light output. This 6% improvement in luminous efficacy correlates well with the results obtained in these tests,

justifying the measurements techniques used.

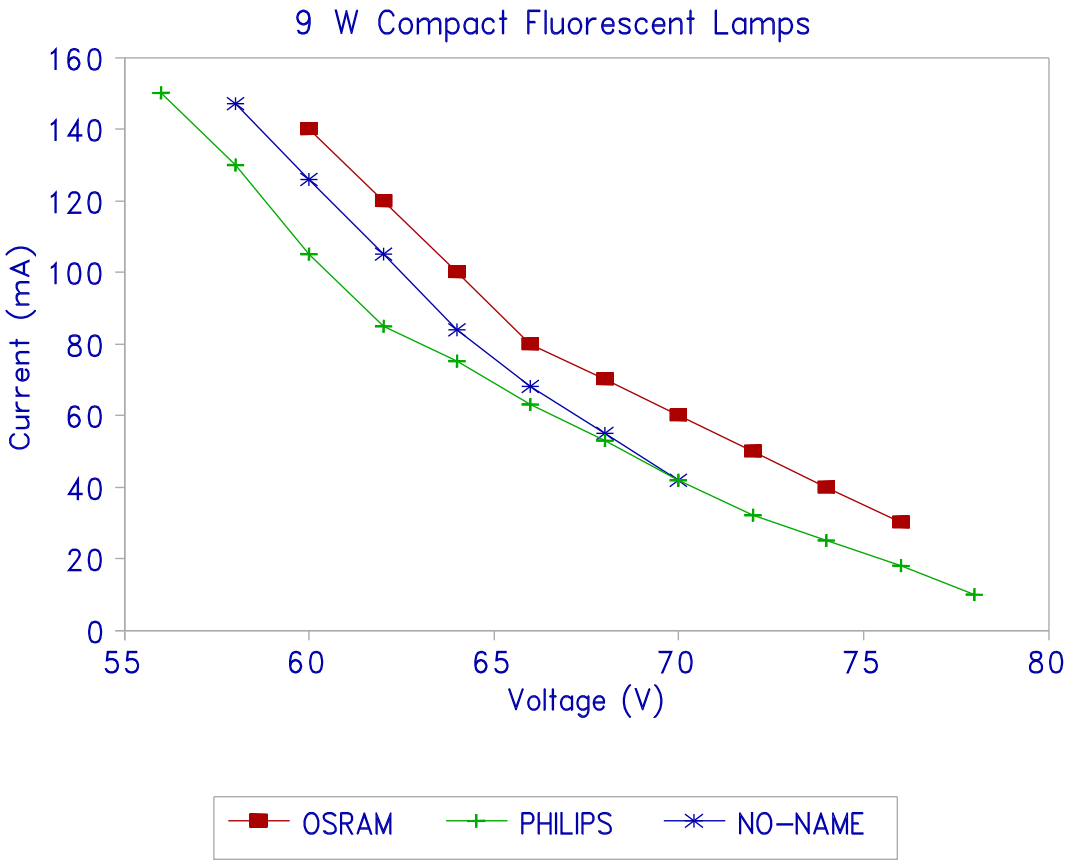

Figure 3.4: Measured comparison of the average static V/I characteristics.

Figure 3.4 shows the negative resistance characteristic of all six lamps using dc. The dynamic resistance varies with lamp current. The average value is approximately -150 Ω. This negative resistance is significant for slowly varying lamp currents as it will cause significant distortion of the lamp voltage. It is also significant when the lamp supply impedance is low as current runaway will result if a ballast is not used. If the current period is less than the plasma recombination time of 1 ms, then the plasma resistance can be determined for each value of lamp current.

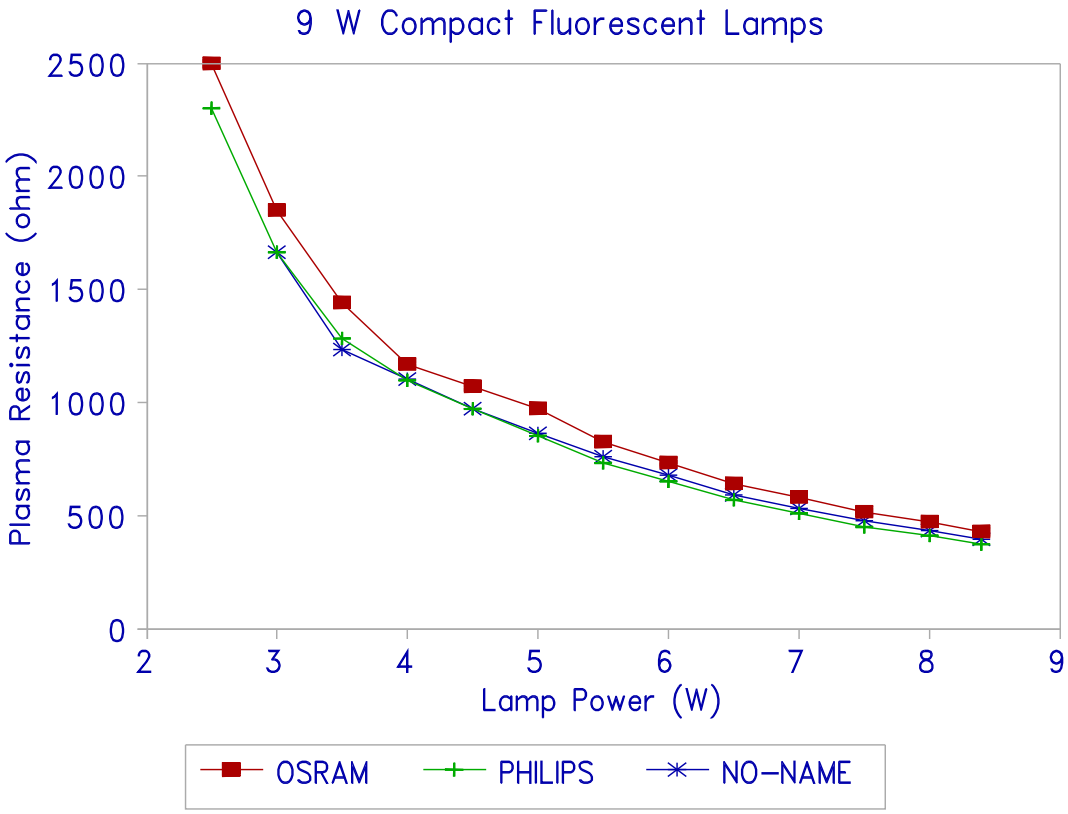

Figure 3.5: Calculated dc lamp input power plotted against the effective plasma resistance for dc or high frequency operation.

The graph above was constructed from the same data as the previous graphs. Note the good correlation between the lamp plasma resistances at higher powers. This indicates that the performance criteria for lamp manufacturers is mainly based on electrical considerations and that relative luminous power is of secondary importance.

This graph is useful during ballast design because it indicates values of equivalent resistance which may be used to substitute the lamp, especially if the ballast output can be modelled as a constant current source.

3.5 The Electrodes

The thermal properties of the electrodes were investigated in order to optimise starting conditions. Of particular interest was the thermal delay of the electrodes and how this figure varies with heater current. During the heating phase, with the starter switch closed, it is reasonable to assume that the output of the electronic ballast will be current limited regardless of the topology chosen. For this reason the test was conducted by driving the electrodes via a constant current source. The compliance of the current source was high in order to prevent current variations during electrode resistance changes.

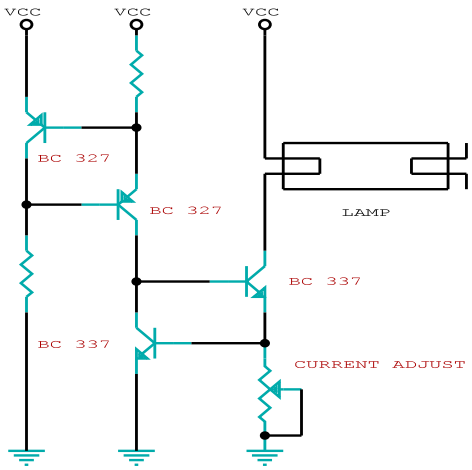

Figure 3.6: The high compliance constant current source used for electrode thermal delay measurements.

3.5.1 Test Method

Various currents were passed through each electrode. No connections were made to the unused electrode during testing. The electrode voltage and other visual effects were noted.

3.5.2 Test Results

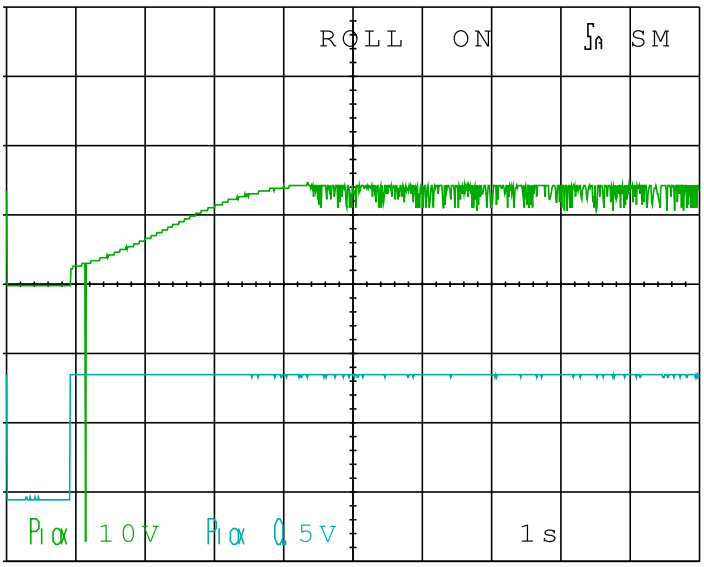

Figure 3.7: A typical thermal delay of an electrode. In this case the electrode voltage was measured when current was 170 mA.

Figure 3.7 shows a typical electrode heating characteristic. The upper trace shows the voltage across the electrode and the lower trace shows the voltage across a 5.5 Ω series resistor. Note the electrode voltage waveform oscillations occurring approximately three seconds after the application of the electrode current. This is due to a transverse discharge which developed between the two pins of the electrode. This particular electrode current, 170 mA, is the threshold for the formation of a transverse discharge. This discharge is clearly visible as a bright glow surrounding the electrode.

The electrical characteristics of all the electrodes tested were within 10%, probably because this is one of the easiest of the lamp characteristics for manufacturers to copy successfully.

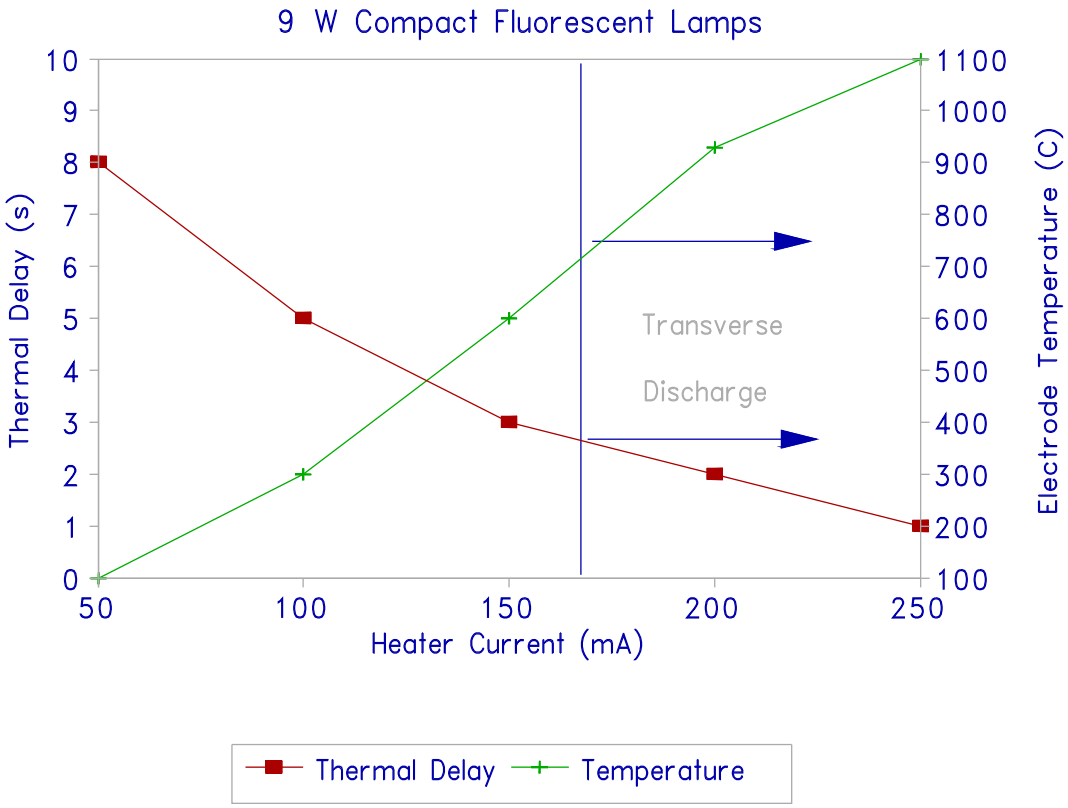

Figure 3.8: Measured electrode thermal delay and calculated temperature at various heater currents.

The electrode temperatures shown in Figure 3.8 assume uniform heating[5]. The filament temperature was calculated by measuring the resistance of the filament at room temperature and taking the temperature co-efficient for tungsten as 0.0058 K^{-1} [6]. The threshold for the formation of a transverse discharge never occurred on any electrode below 170 mA. The electrode temperature began to flatten above 200 mA, indicating decreasing gains in electrode temperature above this current. Note that as the heater current decreased, so the time to reach the corresponding temperature increased. At a heater current of 50 mA the thermal delay with some lamps was as high as 15 seconds.

3.6 Lamp Ignition

Lamp ignition is dependant upon many factors besides starting voltage amplitude. These include:

- Lamp temperature.
- Humidity.
- Electrode temperature.
- Presence of a transverse discharge.
- Starting voltage *dv/dt* and bandwidth.

Because of the above influences it is not possible to define a minimum starting scenario for all ballast designs. Rather, this investigation attempts to describe basic phenomenon and trends with some indication of starting requirements.

3.6.1 Test Method

Various dc voltages were applied across the lamps. The heater current was then initiated and the ignition voltage noted. It was important to consider that heater current raised the temperature of the lamp and hence the gas pressure. This meant that the ignition voltage had to be applied before initiating heater current and that after every test the lamp had to be allowed to cool for approximately 5 minutes. A constant current sources supplied heating current to the cathode.

3.6.2 Test Results

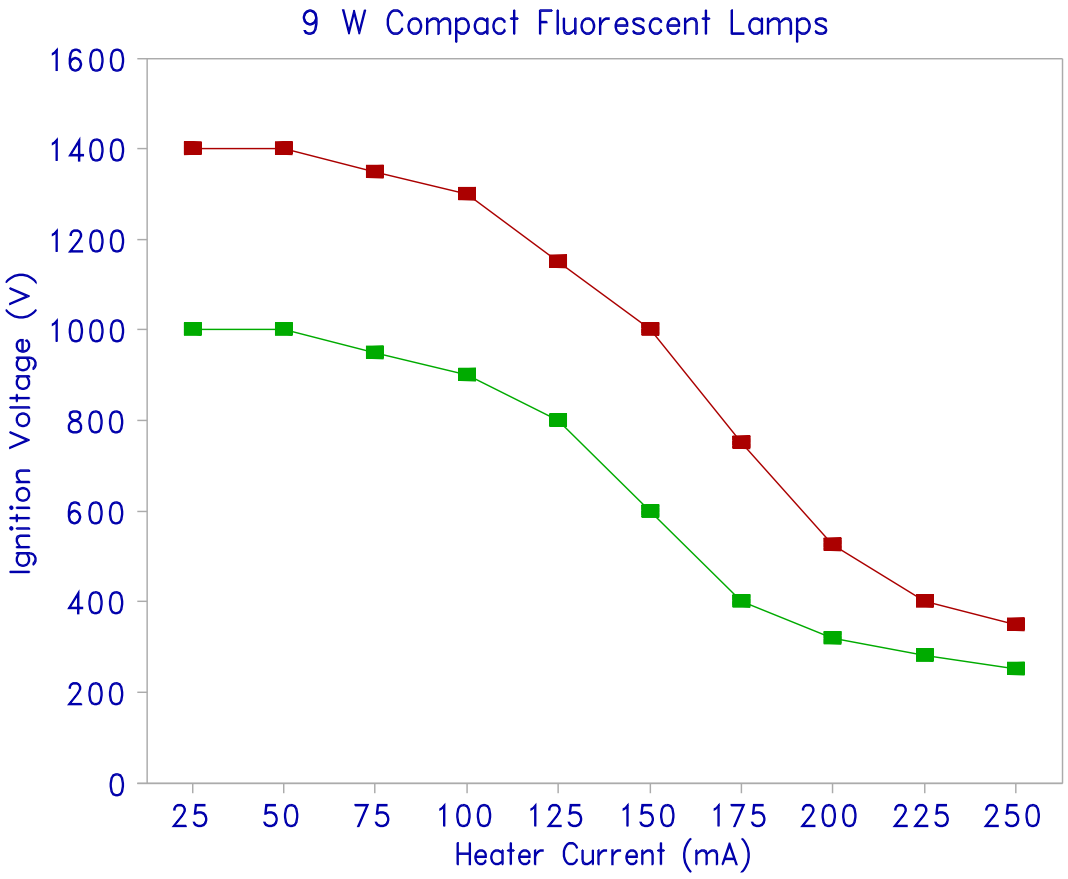

Figure 3.9: Measured extremes of required dc ignition voltage plotted against cathode heater current.

Figure 3.9 plots the extremes of lamp ignition voltage for each value of heater current. Variations in required ignition voltage increase with decreasing heater

current and, conversely, lamp ignition becomes more predictable at high heater currents. This is also true for an individual lamp's performance. Elenbaas[1] swamped this variation in his measurements by using an earthing strip. The ignition voltage requirement for any lamp rarely decreased below 250 V. The formation of a transverse discharge reduced the starting voltage requirement for individual lamps by more than 100 V. This phenomenon occurred above 200 mA with all lamps. The results indicate that it is desirable to obtain

a transverse discharge before applying the starting voltage in order to both reduce the starting voltage requirement and provide reliable starting.

3.7 Starter Assembly Tests

When powered from a mains supply the starter assembly is essential. It provides electrode heating, a starting voltage surge and EMI suppression. With regard to electronic ballasts, the starter assembly poses many problems. The suppression capacitor impedance reduces with frequency thereby attenuating starting voltage surges and it causes an increase in electrode losses during an arc discharge. The starter itself provides an additional load to the inverter especially during contact closure. It is for these reasons that compact fluorescent lamp manufacturers also provide an `electronic' version of their lamps without the starter assemblies. These lamps have four pins; two for each electrode.

Although the `electronic' version seems to the obvious choice for use with an electronic ballast there are applications where the standard version is more suitable. Maintained[5] emergency lighting applications require that the lamp be energised from mains and switch over to battery backup during a mains failure. Using an `electronic' lamp for this application would require further switching complexity, for four pins as opposed to two, and an external starter for mains operation. Another economic consideration is that the standard version is generally more readily available and is therefore cheaper.

Starter performance figures are generally company confidential and as most electronic ballasts use the `electronic' lamp, few relevant articles have been published. This section attempts to characterise the operation of the starter separately from the lamp in order to optimise the design of the electronic ballast.

Four starter assemblies were tested, two from Philips lamps and two from Osram lamps. As the sample batch was small, no attempt has been made to analyse performance distributions. Rather, range as a percentage of the mean is stated. The model presented is therefore type characteristic and not definitive. The performance of starters from 18 W and 26 W lamps have been included in certain sections to draw comparisons.

All the glow starters tested were of similar internal construction in that the contacts consisted of a metal pin and a single bimetal element. Heat generated by the glow discharge causes the bimetal element to bend and touch the metal pin.

3.8 Glow Starter 50 Hz Performance

The aim was to gain insight into the normal operation of the starters connected to a 50 Hz mains supply. Each starter, with its suppression capacitor, was connected to a variable mains supply via an 18 W ballast. Voltage, current and visual effects within the starters were noted.

3.8.1 Transition to Glow Discharge

At a certain supply potential the onset of a glow discharge occurs when electrons are liberated from the cathode by impinging ions. The liberated electrons will then collide with atoms in the buffer gas and thereby create new ions. This classical negative resistance transition to glow discharge is limited by the surface area of the cathode[4]. Once the entire cathode is covered by a glow discharge further increases in current density must be accompanied by increases in the supply potential. The transition to glow discharge occurs quickly, *i.e.* within microseconds, if the sum of the supply internal resistance and the glow starter characteristic resistance is negative.

3.8.2 Glow Discharge Threshold

The threshold for glow discharge for the various starters was between 70 V and 86 V rms. This corresponds to a peak voltage of between 99 V and 121 V. There was no correlation

between manufacturers and threshold voltages. The peak voltage range was 20% of the mean. Peak voltage measurement is more meaningful as the glow discharge responds to the instantaneous value of the applied voltage.

The threshold voltage has been chosen by the manufacturers to exceed the maximum operating voltage of a single lamp (60 V) and to ensure reliable glow starter function when two lamps are connected in series with a single ballast. Series operation results in less supply voltage available for starter operation if the one lamp has already ignited. Under these conditions, with a low mains voltage, only 150 V may be available across the starter. Not only must this voltage exceed the glow threshold, but it must also ensure sufficient heating in the starter to close its contacts. For these reasons the dynamic resistance of starters in the 9 W lamps is lower than that of starters used in 18 W or 26 W lamps.

It is interesting to note that as the supply voltage was increased, the glow discharge forms around the metal pin first, in all cases. The glow discharge formed around the bimetal element on average 5 V rms higher than the metal pin. This voltage difference is due to dissimilar work functions of the two electrodes.

3.8.3 Measurement of Dynamic Resistance

Once a glow discharge completely covers the cathode, further increases in supply voltage result in increases in current density and luminous intensity of the glow. The V/I characteristic is therefore positive and so the glow starter has a certain dynamic resistance.

As the supply voltage was increased from zero, current flowed through the glow starter only during that portion of the voltage waveform which exceeded the glow discharge threshold, in this case 100 V. The glow discharge extinguished rapidly after the instantaneous supply voltage decreased below the glow discharge threshold as there are no storage effects at 50 Hz.

As glow starters operate in the positive region of discharge V/I characteristic curve, a model comprising two back to back zener diodes in series with a resistor adequately simulates the load at 50 Hz, see Figure 2.11. The zener voltages equal the glow threshold voltage and the series resistance equals the dynamic resistance of the starter, which in this case is approximately 1000 Ω.

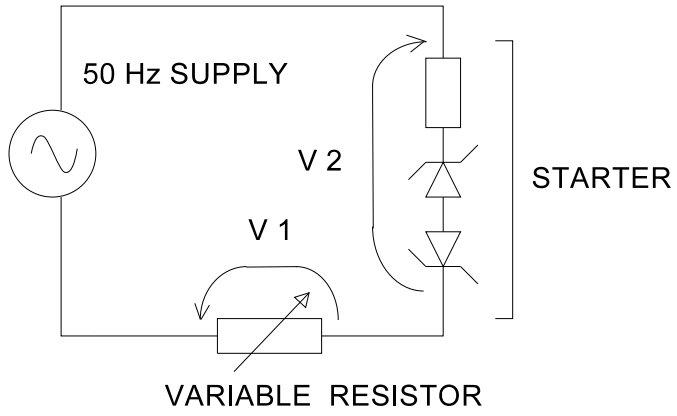

Figure 3.10: The test circuit used to determine the dynamic resistance of the glow starters.

To determine the dynamic resistance of the starter, the circuit in Figure 3.10 was used. The voltage across the starter, V2, was measured by one channel of the oscilloscope. The voltage across the variable resistor, V1, was measured by the other channel. The oscilloscope waveform of voltage V2, during the period of conduction, represented the glow discharge threshold plus the glow current multiplied by the dynamic resistance. The voltage across the variable resistor represented the glow current multiplied by its resistance. The two waveforms were added and the variable resistance was adjusted so that the resultant waveform was flat topped. The variable resistor value was now equal to the dynamic resistance of the starter.

Although there was some decrease in dynamic resistance with increasing current, this variation was swamped by sample spread. Although the dynamic resistance was asymmetrical due to dissimilar work functions of the electrodes, this variation was also exceeded by sample spread. The dynamic resistance of the four starters varied from 800 Ω to 2000 Ω. The resistance range was 80 % of the mean. There was correlation between manufacturer and dynamic resistance. The Osram starters were 800 Ω and 1000 Ω, whilst those from Philips lamps were both 2000 Ω. In comparison, the dynamic resistance of starters measured from 18 W and 26 W compact fluorescent lamps were 6000 Ω and 3000 Ω respectively, which confirms the requirement of a low dynamic resistance for 9 W starters to facilitate series mains operation.

3.8.4 Minimum Power Requirement

The above test setup was again used. The voltage across the variable resistor represented glow current and as the glow threshold was known the power dissipated in the starter was calculated. The criteria for determining minimum power for switch closure was defined as closure within five seconds after the voltage was applied. It is of little importance to record powers which require in excess of five seconds because these values would vary substantially with ambient temperature and would therefore be unreliable. The minimum power required for switch closure varied between 700 mW and 900 mW. The power range was 25 % of the mean.

3.9 Glow Starter DC Performance

The aim was to verify the ac performance results, to ascertain why compact fluorescent lamps exhibit an asymmetrical ignition requirement with a dc supply, and to determine why this phenomenon sometimes causes unreliable lamp ignition with certain ballasts. Both current and voltage were monitored as the variable dc supply was increased. Visual effects were also noted.

3.9.1 Glow Discharge Threshold

The glow discharge threshold varied between starters from 100 V to 120 V dc when the metal pin was cathode. The threshold range was 20% of the mean. The threshold voltage with the bimetal element as cathode was on average 6 volts higher, due to dissimilar work functions of the two elements. The difference was only approximately 10% of the glow threshold voltage and should not alone affect starting performance using dc voltages. These results correlate well with the 50 Hz tests.

3.9.2 Minimum Power Requirement

The minimum power required to close the switch varied considerably depending on whether the metal pin was the cathode or the bimetal element was the cathode. When the bimetal element was the cathode then the starters required 300 to 400 mW to close. The power range was 30% of the mean. However, when the metal pin was the cathode the starters required 1400 mW to 2200 mW for switch closure within five seconds. The power range was 40% of the mean in this case.

Heat is generated in the cathode fall of the glow discharge and so when the bimetal element

is the cathode rapid heat transfer occurs from the cathode fall to the bimetal element which results in prompt switch closure. When the bimetal element is the anode inefficient heat transfer through the gas results and hence switch closure is delayed. This phenomenon is responsible for the polarity sensitive starting performance when using a dc lamp supply. The time difference varies with glow discharge current but the following results further illustrate the point.

3.9.3 Delay Before Contact Closure

The glow starter requires more energy to close its contacts if the metal pin is the cathode due to the indirect heating of the bimetal element. At a discharge power of one watt the starters required 1 s to 2 s to close when the bimetal element was the cathode. However, the starters required 12 s to 15 s to close when dissipating the same power but with the metal pin as cathode.

3.9.4 The Closure Period

This test was conducted without the suppression capacitor connected across the glow starter. The period that the glow starter contacts remain closed is also dependant upon polarity. The glow discharge heat is generated in the cathode fall region and so when the bimetal element is the cathode then heat is readily transferred and switch closure is effected before the gas in the starter has the opportunity to heat up. The period that the switch remains closed is therefore dependant upon the thermal inertia of the bimetal element.

When the metal pin is the cathode then heat transfers to the bimetal element via the gas and the glass envelope also heats up appreciably. The period that the switch remains closed is now approximately dependant upon the energy dissipated prior to switch closure. The energy required for switch closure is substantially greater than that required when the

bimetal element is cathode and so starter temperature also rises. The switch contacts therefore remain closed for a longer period. A starter's switch closure times vary considerably during normal operation.

Closure times varied in the tests from tens of milliseconds to seconds so an accurate assessment of time closures for the different polarities was impossible. However, observations revealed that the ratio of the different polarity closure times was approximately 2:1.

3.9.5 Variation of Dynamic Resistance with Proximity

The glow discharge characteristics vary as the glow switch elements close. As the contact separation becomes less than the cathode fall the glow discharge extinguishes. At the instant just before the switch contacts close, the glow discharge will be sustained only by those portions of the switch electrodes whose separation exceeds that of the cathode fall. The dynamic resistance of the glow starter therefore decreases just before contact closure.

Figure 3.11, on the following page, illustrates this phenomenon. The upper trace shows the voltage across the glow starter and the lower trace shows the resulting glow current, measured across 80 Ω. The second division from the bottom of the graticule is zero volts for both traces. The glow current decreased before contact closure, indicated by large voltage excursions on the upper trace, even though the voltage across the glow starter increased.

The initial dynamic resistance of this particular glow starter was 2 kΩ. The dynamic resistance then decreased to 3 kΩ just prior to contact closure.

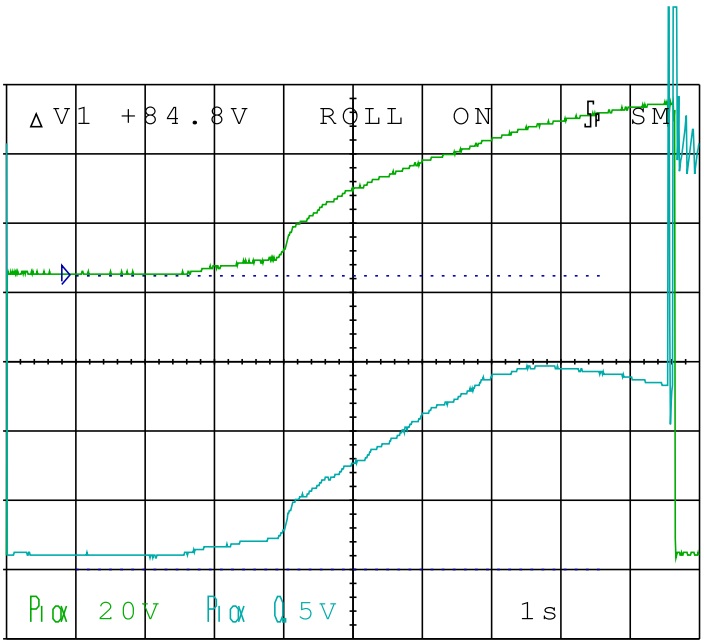

Figure 3.11: Measured relationship between applied voltage and resulting glow current with respect to time.

3.10 High Frequency Performance

The aim was to observe the performance of the starters when subjected to transient voltages in order to optimise the electronic ballast ignition.

3.10.1 Test Method

The test circuit consisted of a flyback inverter with the facility to vary pulse width, amplitude and duty cycle. A 120 Ω resistor was connected in series with the loads to record currents. The applied pulse amplitude was approximately 150 V and of 5 µs duration. The rising edge overshoot of 350 V and 1 µs duration was due to the pulse generator, which was a clamped flyback inverter.

The results were compared to the performance of the model to verify that salient points of the transient response were due to the starter and not due to the test fixture.

3.10.2 Test Results

Figure 3.12 and Figure 3.13, on the following page, show an applied voltage pulse across a starter and the starter model respectively.

The initial voltage peak of 1 μs duration can be seen in Figure 3.12. The amplitude of this peak is similar to that occurring without the starter present and so the resistivity of the starter was initially high. The voltage sag thereafter was due to the decreasing resistivity of the glow discharge as its plasma formed.

Figure 3.13 shows the response of the circuit model to the same transient. The dynamic resistance chosen was 800 Ω, similar to that of the starter used in these tests. Two series connected 68 V zener diodes were used in the model. Note that the overvoltage in Figure 3.12 is not present in Figure 3.13 as the zener diodes responded rapidly to clamp the applied voltage.

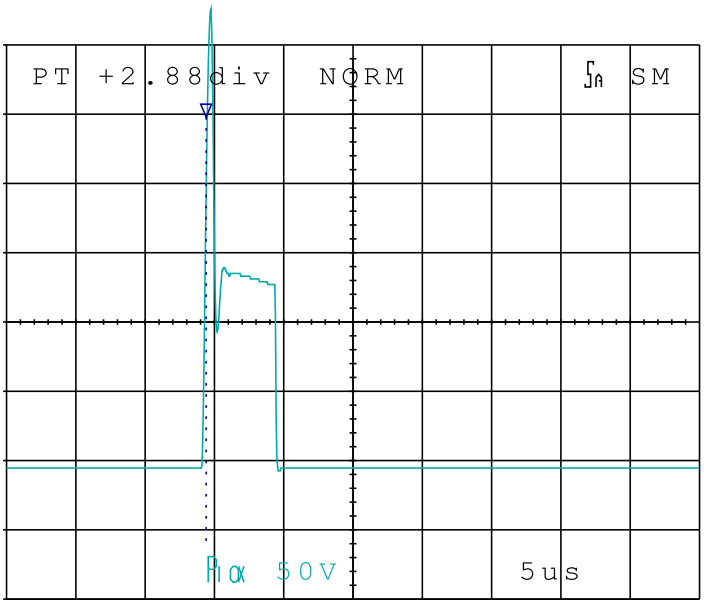

Figure 3.12: Typical measured response of a glow starter to a 350 V pulse.

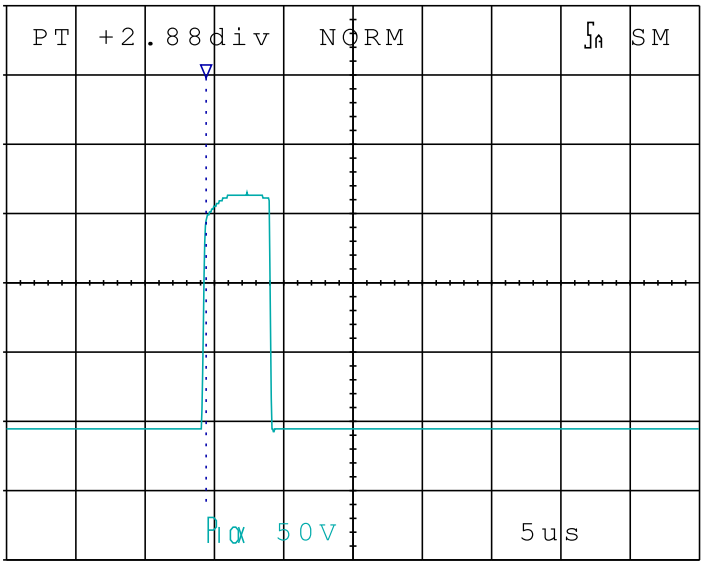

Figure 3.13: Measured response of the starter model to a 350 V pulse.

The current waveforms of the starter and model are shown, on the following page, in Figure 3.14 and Figure 3.15 respectively. The waveforms were measured across a 120 Ω resistor in series with the load. The same voltage was applied in both cases.
The cursor was positioned at the rising edge of the voltage transient. The initial current peak, in Figure 3.14, occurred at the same instant as the transition to glow discharge occurred and on the trailing edge of the applied voltage overshoot. It is therefore of little importance. Note the gradual increase in current through the glow starter which is not evident when using the model. This was due to the finite formation period of the glow discharge.

The glow discharge therefore requires approximately 3 μs to reach its steady state resistivity. During the tests it was noted that if the applied voltage transient amplitude was below the glow threshold then no current flowed through the starter, regardless of pulse form.

3.10.3 Summary of High Frequency Tests

If the instantaneous lamp operating voltage does not exceed the glow threshold, the glow starter resistivity will remain high.

The starter conductivity increases from zero to its steady state value after 3 μs. There may therefore be an advantage in ensuring glow starter switch closure during ignition because when the contacts open the plasma resistivity is initially high and would not load the starting voltage transient. Also, the steady state plasma resistivity is highest at small switch contact separations.

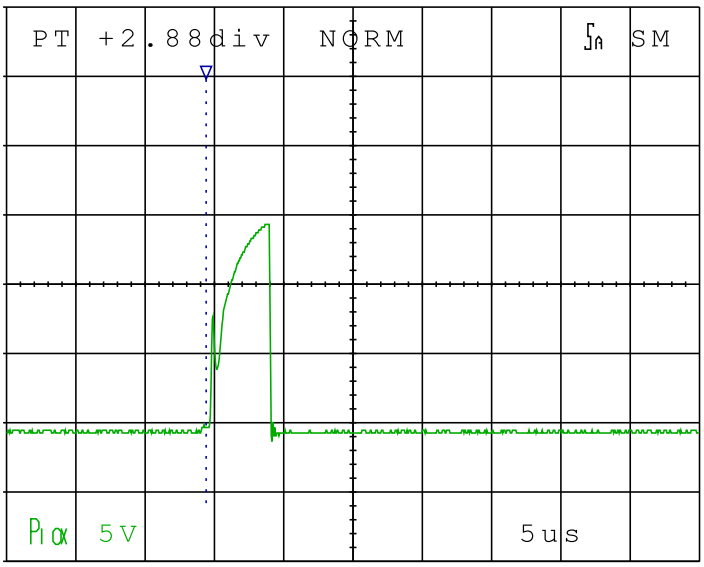

Figure 3.14: Measured transient current response of a glow starter measured across 120 Ω.

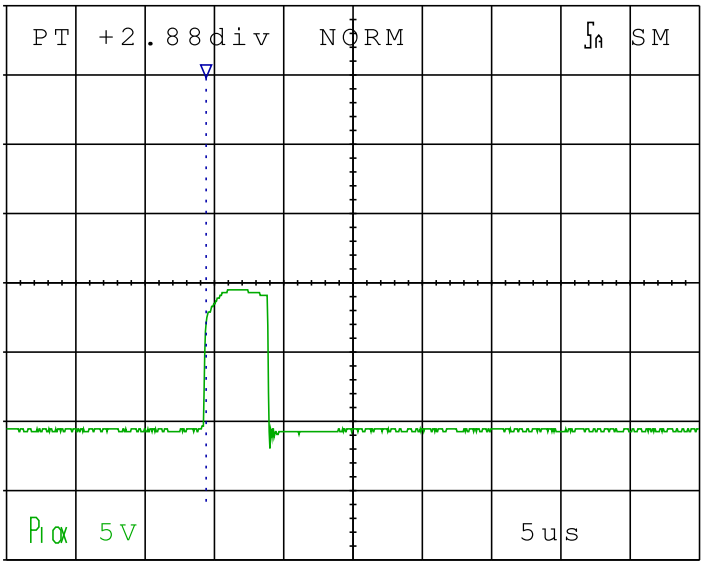

Figure 3.15: Measured transient current response of the glow starter model.

3.11 The Suppression Capacitor

Meyer *et al*[2] states that "The purpose of the suppression capacitor is to limit the bandwidth of voltage transients and hence EMI, and to increase the time that the switch contacts remain closed". The author could find no explanation as to how the capacitor assists in keeping the contacts closed.

The measured values of the suppression capacitors varied from 2,8 nF to 3,4 nF. The Philips suppression capacitors had the inscription `302' (= 3000 pF). The Osram capacitors had no value markings.

The cathode fall of the glow discharge in the starter produces the heat which causes the bimetal element to bend closed. As the bimetal element touches the metal pin the glow discharge extinguishes and heating ceases. The period the contacts remain closed is now determined by the thermal time constant of the bimetal element and, the author proposes, by the strength of a weld formed between the contacts as the switch closed. The suppression capacitor value has been chosen to both limit the voltage transients and to store energy to assist in the formation of the weld. The following tests conducted confirm this theory.

3.11.1 Effects of Capacitor Value on Closure Times

The starters were connected to a high voltage supply with an internal resistance of 1 kΩ. The supply voltage was increased until the switch contacts began closing intermittently. The bimetal element was the cathode.

Without the suppression capacitor connected across the glow starter the time closed averaged 20 ms. With the suppression capacitor connected this time increased to 100 ms. By adding an additional 1 μF capacitor the average time closed increased to seconds. When

the suppression capacitance was increased to 2 μF the starter contacts of both starters welded firmly together. This test was only conducted on two starters.

3.11.2 Measurement of Bimetal Characteristics

This experiment was performed to prove that the increase in contact closure times with increasing suppression capacitor value is not due the discharge capacitor current causing increased element deflection.

The element was assumed to be of homogeneous brass construction for the purposes of resistance calculation. The bimetal element cross sectional area and length were measured and its resistance then calculated from

$$R = \rho \frac{l}{A} \quad [\Omega] \ , \tag{3.1}$$

where ρ is the resistivity, l is the length and A the cross sectional area of the material. The bimetal element resistance for the sample was calculated to be 1.3 mΩ.

The contact resistance was measured using a four wire low resistance meter whilst externally heating a sealed glow starter until the contacts closed. The measurement of the contact resistance of the sample varied between 0.2 and 0.35 Ω.

It is evident from the above resistance values that insignificant energy is dissipated in the bimetal element during switch closure, the energy being dissipated mainly in the switch contacts. The high current density at the point of contact causes the contact material to melt and form metal bridges[14]. Contact erosion then results when the contacts are forcibly separated. This roughening of the contact surface was visible through a microscope. Also, the sound of the weld breaking is audible during lamp starting.

3.12 Mains Ballast Measurements

In order to reduce the cost of the emergency ballast it is desirable to omit the change over relay in maintained fittings[5,31]. The electronic ballast would then be permanently connected to the lamp during mains operation. For reliable operation under these circumstances the following conditions must be met:

- The electronic ballast load must not affect normal mains operation appreciably.
- The electronic ballast must function reliably with the mains ballast connected across the lamp as it can be assumed that during a mains failure other appliances would provide a return path to the lamp neutral pin.
- The electronic ballast must withstand large voltage transients during mains ignition.

In order to investigate the feasibility of connecting the electronic ballast permanently to the lamp a mains ballast, DECALIGHT type: EC 18 W A27, was measured. Although only one ballast was tested, the results were expected to return typical characteristics and not definitive values.

Figure 3.16 shows the ballast impedance vs frequency. The ballast inductance was measured at 1.9 mH and the winding self capacitance was 180 pF. No other effects were noted up to 100 kHz.

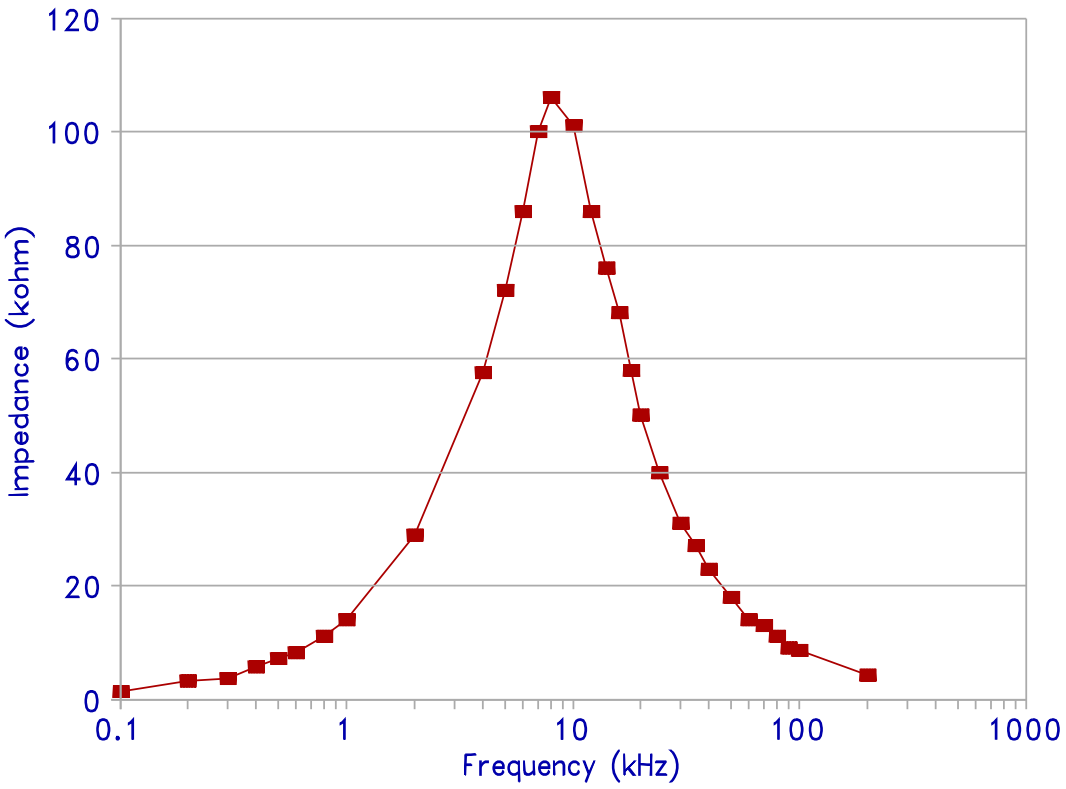

Figure 3.16: Measured impedance of a 18 W mains ballast.

The winding self capacitance of the mains ballast may allow mains borne transients to appear across the lamp and therefore across the output of the electronic ballast, if there is no change over relay. These high voltage transients may then be reflected to the primary circuit of the electronic ballast and damage components there. The connection of additional suppression capacitors across the lamp to reduce the effects of mains borne transients may, however, affect starting performance. Reliable operation using this type of connection can only be confirmed after exhaustive tests which must include simulated lightning strikes.

3.13 Summary

The electrical characteristics of the lamps tested are virtually identical. Although the sample batch was small, this may indicated that lamp brand name should not be a consideration during electronic ballast development. The tube ends of the "No Name Brand" lamps had, however, blackened more than the other lamps by the end of the tests which may mean that its performance parameters were beginning to shift.

The deviation in performance between different brand name starters with respect to glow threshold and power required for switch closure was within 30%. This may be due to the narrow performance restrictions imposed by the requirement of series operation from a single ballast. It is notable that the ac power requirement results yield lower distributions than the individual dc performance of each polarity. This could be due to the manufacturers ac based performance criteria.

Other starter parameters are covered by a wider distribution. These parameters include dynamic resistance, closing time and the period the switches remained closed. The period which the starter contacts remained closed varied from tens of milliseconds to seconds. During normal mains operation lamp ignition is normally accomplished after one or more switch closures during which the electrodes of the lamp are heated to some degree.

From the above it follows that, in order to achieve glow starter switching action, the inverter performance must be tested in terms of minimum glow threshold and power. A model comprising two back to back 100 V zener diodes in series with an 1→2 kΩ resistor could be used to simulate the load of a starter. The finite formation period of the glow discharge inside the starter may be of assistance if the starting conditions use narrow pulses. The decrease in glow discharge conductivity when the contacts are nearly closed may be of assistance as well.

It is possible that the suppression capacitor value has been set by an industry standard at

3 nF.

The low dynamic resistance and the existence of the suppression capacitor indicate that lamp ignition should be accomplished by additional means than by relying solely on a voltage transient after electrode heating. A high frequency design could affect electrode heating by relying on the suppression capacitor to shunt current through the electrodes before the starter closes. Lamp ignition could then be accomplished by the subsequent application of a semi-resonant transient. The operating frequency upper limit is determined by lumen efficiency as electrode losses rise with frequency. Lamp life due to electrode evaporation must also be a consideration.

If a dc supply is used to power the lamp then ignition must be possible with both polarities and the design must include resistance or inductance between the lamp and the smoothing capacitor in order to protect the starter from excessive current surges during switch closure.

The starters require at least 1 W of power for switch closure. 2 W could be considered as being safe for ac operation. A minimum of 3 W is required for dc operation to ensure reliable starter action with both lamp (starter) polarities.

As the glow starter responds to lamp voltage excursions which exceed its glow threshold the lamp voltage form therefore determines the minimum lamp power if ac is used. Assuming that the lamp voltage is a perfect sinusoid and that the glow threshold is 100 V, then the maximum lamp voltage is 70 Vrms. This limits the minimum lamp power to approximately 4 W. Lamp dimming is therefore not feasible using compact fluorescent lamps with built in starters unless dc or low frequencies are used.

4 Ballast Performance Requirements

4.1 General

The electronic ballast must convert power from a dc power supply, in this case a battery, to the required voltage necessary to correctly start and drive the fluorescent lamp. In order to achieve a high conversion efficiency switch mode power supply (SMPS) techniques are used. Electronic ballasts for fluorescent lamps have been used for many years and are evolving as switching device and lamp technology improve. Initially transistor and thyristor switching speeds limited inversion frequencies to the audio band, however, the advent of the power FET has enabled switching frequencies to be increased without significant increases in losses. It is now possible to develop efficient inverters to drive the fluorescent lamp at 100 kHz where it is most efficient[17].

In today's fiercely competitive market place, the most important reason for choosing an inverter design is cost. The second most important reason is reliability and other issues are efficiency, starting conditions and operating waveform. This chapter will analyse designs currently used and new circuit ideas in an attempt to provide a baseline for the design an optimal ballast.

Battery powered ballasts can be used for both portable and emergency lighting. Portable lighting systems include caravan light fittings and solar panel charged remote lighting. Emergency lighting applications include both maintained and non-maintained systems[5,31]. A maintained light fitting includes the facility to power the lamp from mains, and then to switch over to battery power during a mains failure. A non-maintained fitting is a dedicated emergency light with no mains powered lighting option. Maintained fittings include numerous variations: Automatic and manual changeover to battery power, changeover

dependant upon ambient light levels and permanent connection of emergency ballast. The latter is perhaps the most demanding of designs because the electronic ballast and the mains ballast are permanently connected to the same lamp, negating the need for a changeover relay or switch. In this case the electronic ballast must withstand the ignition transients developed by the mains circuit. Also, the mains ballast may present a load to the electronic ballast during a mains failure.

Another problem with maintained systems is that a mains failure may occur when the lamp has been burning and the electronic ignition will have to cope with starting a hot lamp.

4.2 Requirements

In order to develop an electronic ballast it is essential to first specify the requirements and then review current industry designs and trends. These requirements, biased to achieve success in the South African market, are listed in order of importance below.

4.2.1 Manufacturing Cost

A design which comfortably satisfies lamp drive requirements through complex circuitry would be of pure academic interest if it is not commercially attractive. Electrical requirements must be achieved through a trade off between component cost, producibility and lamp life. A major cost driver in electronic ballasts is the ferrite transformer. The number of windings, insulation, leakage inductance and turns ratio requirements all contribute substantially to the cost of manufacture. For these reasons it is important to limit the number of transformers to one and to limit the number of windings and turns ratio in order to facilitate the use of the smallest bobbin.

Another cost driver is the switching element. Besides the cost of the additional device, the

choice of a push pull arrangement usually requires additional drive circuitry and associated cost. Further considerations are reproducibility and testing requirements. Designs whose performance are too dependant upon transistor gains and bandwidths result in low yields and subsequent high reworkings.

4.2.2 Reliability

Reliability is second only to unit cost in terms of importance. In the author's experience, electronic component failure is caused mostly through unusual conditions such as the full power being applied with no lamp present, or endless ignition cycles due to the presence of an old lamp. Both conditions may cause increased circuit dissipation which sometimes results in component failure.

4.2.3 Ballast Efficiency

An important requirement of a portable or emergency luminaire is to provide illumination for extended periods. Also, battery dimensions, and hence energy capacity, are usually restricted so power conversion efficiency is very important.
A high conversion efficiency is not only important to extend emergency battery life, but also to reduce manufacturing costs. High switching device dissipation requires adequate heat sinking and ventilation. The optimum ballast would not require any form of heat sinking. The minimum emergency lamp lighting duration required by SANCI is 60 minutes[31].

4.2.4 Operating Temperature Range

The ballast starting and arc discharge performance must be reliable for all expected ambient temperatures. Problems may be experienced whilst starting at temperature

extremes and ballast failure may occur at high ambient temperatures. Middlecote[37] specifies the operating ambient temperature range for luminaires to be between -5°C and +40°C. The author proposes that the ballast electronics should be capable of operating at an ambient temperature of 60°C. This may be the temperature rise inside a sealed luminaire due the combined effects of a high ambient temperature and heat supplied by the lamp. Another worst case scenario is re-ignition of a hot lamp.

4.2.5 Lumen Efficacy

Alling[20] specifies the following test scenario for an electronic ballast which is intended to replace the mains ballast. "The light output of seasoned lamps (100 hours) is measured in an integrating sphere at 25°C using a reference ballast from a mains supply. This output is then divided by the light output when driven from the electronic ballast. This ratio, the BF, should lie in the region of 0.94". Although this figure is not directly applicable to battery powered ballasts it does indicate that an improvement in lumen efficacy, of approximately 6%, over mains operation should be achieved. Bedocs[35] specifies that a luminous efficacy improvement of approximately 10% is possible by increasing the lamp current frequency from 50 Hz to the region of 20→50 kHz.

Lumen efficacy is dependent upon ambient temperature and mounting position. Performance of PL 9W lamps is optimised for the base up or horizontal positions. A base down position will raise the temperature of the cold spot, increase mercury vapour pressure and so decrease efficiency.

4.2.6 Current Crest Factor

The crest factor (CF) must be less than 1.7 at mains frequencies[1]. Alling[20] states "The ideal situation is to drive the lamp with a pure sine wave without distortion". Analysis by Bouwknegt *et al*[3] suggests otherwise: Electrode thermal delay results in excessive ion

bombardment during the lamp current peak so it seems that the optimum crest factor used should be unity. This is only possible with a square current waveform or dc. At high frequencies, above 1 kHz, the electrodes do not follow periodic fluctuations in current and so electron emission is constant. Also, due to the inertia of the mercury ions, their kinetic energy reduces with frequency therefore the energy they may impart at electrode impact decreases. The crest factor limit may therefore be exceeded at high frequencies without decreasing lamp life.

4.2.7 Lamp Current Frequency

The minimum operating frequency must be above the audio band, approximately 17 kHz, and the maximum is limited by electromagnetic interference considerations to about 50 kHz[2]. A dc lamp supply should not be used otherwise lamp life will be significantly reduced through electrophoresis[1,5].

4.2.8 Starting Scenario

Starting conditions and crest factor are the two of the main criteria determining lamp life. The electrodes should be heated before an attempt is made to start the lamp in order to reduce cathode sputtering. The glow current, *i.e.* the lamp current which flows before ignition, should be limited to the region of 10 - 15 mA[20] to minimise sputtering.

The starting voltage should be the minimum necessary to properly start the lamp. The minimum starting voltage requirement cannot be specified due to its dependence upon many conditions (see Chapter 2) but the basic requirement is to design the ballast with a minimum open circuit voltage, plus margin, necessary to consistently start all the intended lamp types at nominal input centre voltage and at rated lamp temperature[20]. The starting voltage should not be excessive as this would lead to excessive electrode sputtering during

starting. These criteria seems vague but such is the nature of ballast design. A fluorescent lamp has no absolute maximum rating specifications as do semiconductors. The art of ballast design is to provide reliable starting and to extend lamp life by providing sound operating conditions.

4.2.9 Lamp Power

If the lamp is operated at 50% or less than the rated power then the electrodes must be heated by some external means otherwise there will be a significant reduction in lamp life[2]. There is also a decrease in efficiency when the lamp is operated below its rated power[1].

4.2.10 Open Circuit Voltage

In the development of electronic ballasts for compact fluorescent lamps with internal starters, the open circuit voltage is different to the starting voltage due to the load presented by the starter assembly. This figure is of importance if the lamp is removed or is not present during starting. Excessive voltages, greater than 2000 V, could develop across the terminals if a flyback inverter is used. This could result in breakdown of the switching device or failure of the step up transformer or transformer secondary components.

4.2.11 Mains Insulation

The changeover circuitry must prevent flash-over during mode changes in maintained emergency applications from either power source; from mains to battery or from battery to mains. Worst case scenarios occur during changeover. Excessive voltage conditions can occur after a power failure when the mains voltage is restored. At this instant the inverter is operating at full power. The changeover relay may be energised before the inverter

power is shut off and the voltage across the relay contacts will be the sum of the mains voltage and the inverter open circuit voltage. This problem is compounded if the electronic ballast is directly coupled to the mains ballast.

4.2.12 Safety

In order to prevent electric shock all metal components of the luminaire must be earthed and no dangerous voltages must be user accessible[37].

4.3 Basic Principles[27,28]

A fluorescent lamp presents a complex load with specific requirements for both ignition and arc discharge and, as stated previously, the characteristic of an arc discharge is negative. It is therefore essential that it is either driven from a constant current source or there must be a series limiting impedance. In this case the combined characteristics of the ballast and the lamp must be positive to ensure stable operation.

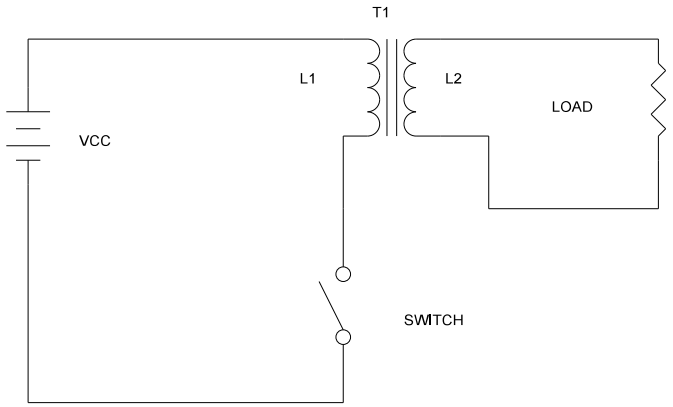

Figure 4.1: A basic inverter circuit.

Power conversion is accomplished in flyback inverters by repeatedly switching a primary winding of a transformer across a dc power source, see Figure 4.1. The current flowing through the primary winding produces a magnetic field and at each instant of switch opening the collapsing magnetic field induces a voltage across the secondary winding. Current then flows through the load. The secondary voltage generated during switch closure may also cause current to flow through the load in some designs.

As the switching element closes the current which flows through the primary (I_p) is given by

$$I = \frac{Vcc}{R}\left(1 - e^{(-t_{on}R/L)}\right) \quad [A] , \qquad \textbf{(4.1)}$$

where Vcc is the supply voltage, R is the primary resistance and t_{on} is the period the switch is closed.

The slope of the current is

$$\frac{di}{dt} = \frac{Vcc}{L} e^{(-t_{on}R/L)} \quad [As^{-1}] . \tag{4.2}$$

As t_{on} is usually much smaller than L/R so that $I_p << I_{max}$ (as t→0) the slope of the current may be approximated by Vcc/L. The slope is therefore nearly constant for small values of t_{on} facilitating the use of piecewise linear analysis[29]. When the switching element opens the energy (E) stored in the primary winding (L1) is

$$E = \frac{1}{2}L(I_{pk})^2 \quad [J] , \tag{4.3}$$

where L is the primary inductance and I_p is the peak current at switch opening. The theoretical maximum conversion power is given by

$$P_o = \frac{1}{2}L(I_{pk})^2 f_s \quad [W] , \tag{4.4}$$

where f_s is the switching frequency. In practice, conversion power losses besides those due to circuit resistance are incurred. These include capacitor dielectric losses and switching device losses.

Losses in the storage capacitor result from power dissipated in the equivalent series resistance (ESR). These losses can be reduced by using low ESR capacitors. For EMI considerations it is also important that a close coupled storage capacitor present the lowest impedance supply to the switching device.

Two types of loss occur in the switching device, namely switching conduction losses. Switching losses arise due to the finite turn on and turn off time of the switching device.

During each switching transition energy is lost in the form of heat in the switching device. Switching losses limit the switching frequency as the power dissipated in the switching device increases with frequency.

The relation between switching power loss and frequency is given by

$$P_{sw} = E_{sw} f_s \ , \qquad \textbf{(4.5)}$$

where P_{sw} is the power dissipated in the switch and E_{sw} is the energy loss at each switching transition.

Conduction losses arise in BJT devices due to their saturation voltage and in FET devices due to their finite `on' resistance.

Another source of considerable power loss in flyback inverters is the ferrite transformer. Ferrite, or core, losses are caused by eddy currents, hysteresis and magnetic drag[30]. Copper losses are incurred because to the finite resistance of the windings.

4.4 Designs Currently Used in Industry

Battery powered ballasts for both compact and linear fluorescent lamps were obtained from industry for analysis. Some of the ballasts tested are not included here either because their designs are too complex, and are therefore not economical to produce, or because their designs are particularly poor.

Where no samples of published ballasts could be obtained, their design is analysed in terms of published performance data or circuit topology.

4.5 Single Transistor Oscillators

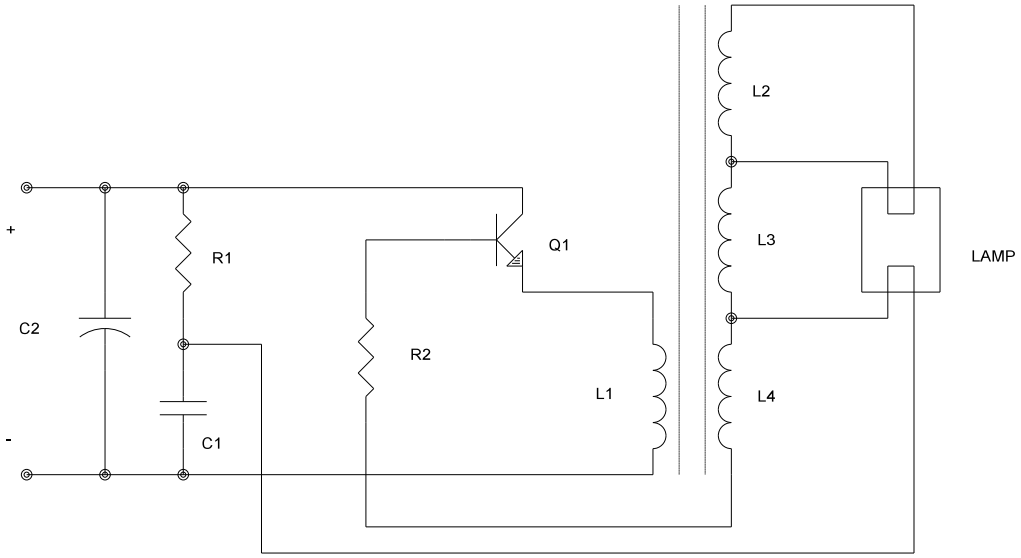

Figure 4.2: A fluorescent lamp ballast using a single transistor blocking oscillator.

This basic configuration[1,5,34] is perhaps the most widely used. Variations of this design and can be found in caravans, elevator emergency lights and portable lighting equipment. It is both cheap and simple.

Feedback via L1 and C1 provides oscillatory operation. During starting the lamp breakdown voltage is high so the only secondary load is provided by the electrodes. Electrode heating is therefore accomplished during lamp ignition. Oscillator frequency is high with no load thereby assisting starting. Note that the one electrode forms part of the base drive circuit. This ensures that the inverter does not operate when the lamp is

removed. The base current also produces electrode heating thereby assisting lamp ignition.

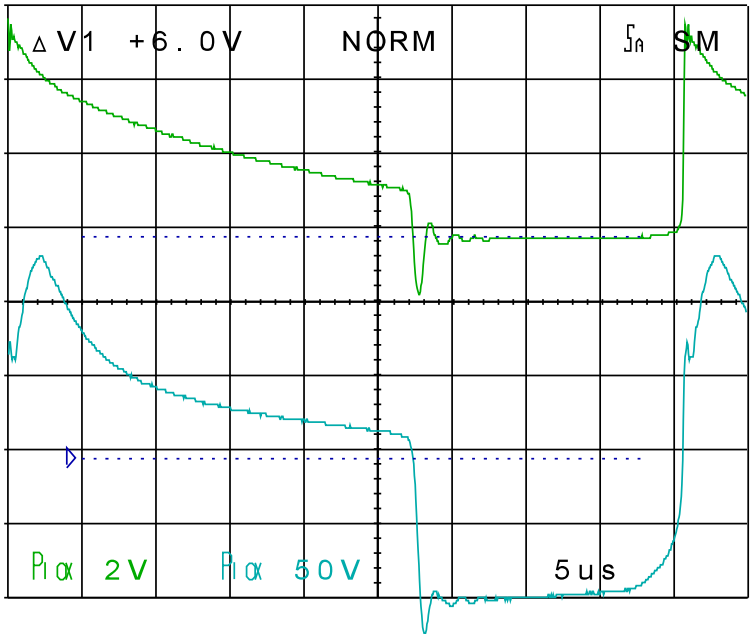

Figure 4.3: Lamp current (upper trace) and voltage (lower trace) waveforms for a simple blocking oscillator ballast. Current was measured across 10 Ω.

Figure 4.3 shows the lamp current and voltage waveforms. The positive voltage half cycle is derived from the flyback cycle whilst the negative voltage half cycle is produced during the conduction period. The secondary voltage during the conduction period is simply the supply voltage multiplied by the turns ratio. The turns ratio in this case was 8.75. The cursors are positioned at zero volts for both traces.

Note that the lamp reignites at 70 V during the positive half cycle but fails to ignite during the negative half cycle even although this voltage reaches 100 V. The reason for this phenomenon is that the *dv/dt* of the flyback cycle is greater than that of the other half cycle. The faster rise time during the flyback cycle causes additional ignition current through

nearby metal parts, *i.e.* the luminaire, assisting ignition. The net result is a large dc lamp current component which causes electrophoresis and hence reduced lamp life.

4.5.1 Advantages

- Simplicity and hence low cost.

4.5.2 Disadvantages

- High crest factor and poor waveform symmetry result in low lamp life.
- Lamp ignition relies on high overvoltages on the secondary whose amplitude is only limited by parasitic capacitance in the secondary circuit and the electrodes. In this way a modest turns ratio is used to achieve ignition. It is therefore not easily adapted to drive lamps with internal starters.
- Output power depends upon both transistor gain and switching speed. Usually this results in the reliance on devices made one particular manufacturer. Performance variations documented from production data between transistors from the same batch typically cause lamp powers to vary by as much as 20%. It is generally accepted in the industry that TIP 3055 transistors manufactured by MOSPEC are most suitable for this application. Other brand name TIP 3055 transistors may require higher turns ratios to achieve either lamp ignition and a reliable arc discharge.
- Cayless[5] states "It is not suitable for maintained operation due to its poor current waveform."

4.6 DC-DC Converters

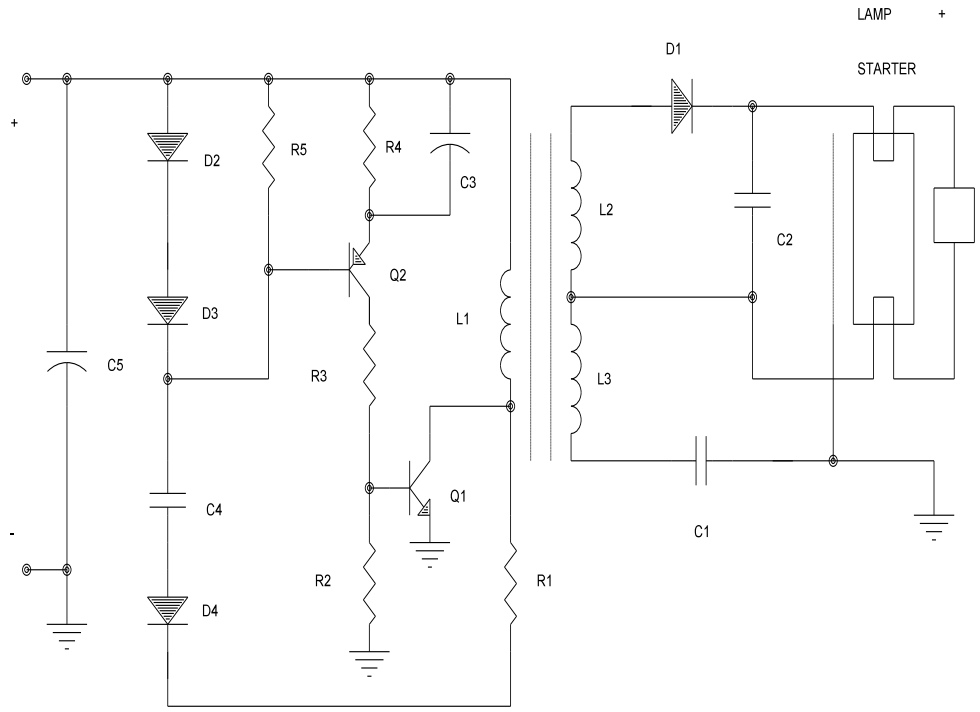

Figure 4.4: A fluorescent lamp ballast which supplies dc lamp current.

DC lamp current is the obvious choice in order to overcome the load presented by the built in suppression capacitor. Figure 4.4 shows the basic circuit. This particular design is used to drive a pair of 9 W compact lamps or a single `2D' 16 W lamp.

Feedback from the collector of Q1 via C4 to the base of Q2 results in oscillatory action. The secondary loading affects the basic frequency. During starting the secondary is lightly loaded which results in a high oscillator frequency which assists starting. The collector current of Q1, and hence output power, is limited by constant current base drive provided by Q2. This is achieved by D2 and D3 providing a constant voltage across R5. The

feedback resistor, R4, then controls the current through Q2 by

$$I_C = \frac{V_{R5} - V_{be}}{R_4} [A] , \qquad \textbf{(4.6)}$$

where V_{be} is the emitter base voltage of the transistor.

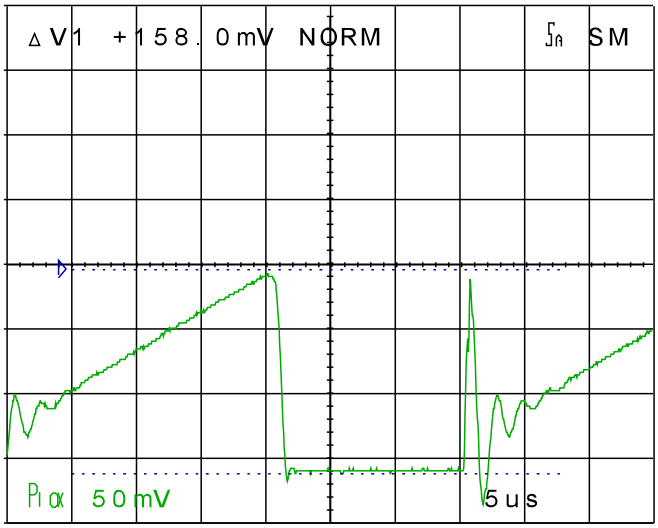

Figure 4.5: The primary current measured across 50 mΩ.
This waveform is typical of single ended ballasts.

C3 is added to reduce switch on losses by negate constant current action during turn on instants. R2 has a low value (47 Ω) to reduce switch off losses by removing the base storage charge of Q1. D1 half wave rectifies the secondary voltage and C2 provides smoothing. The extra winding is used to provide a near field voltage to the lamp and thereby assist starting. C1 limits the lamp current to this field. C5 is included to reduce the supply impedance.

Note the classic ramp build up of primary current in Figure 4.5, on the previous page. The peak current is 3.16 A and as the primary inductance is 49 μH, the output power is 7 W. The initial overcurrents, at the start of each conduction cycle, are due to secondary self capacitance and rectifier diode capacitance. Secondary self capacitance and high turns ratios are often a cause of switch overcurrents in fluorescent ballasts. The problem is usually overcome by adding a primary circuit series inductor.

4.6.1 Advantages

- The loading effects of the suppression capacitor is negated by using dc.
- Reliable starting has been ensured by using a near field voltage.
- Circuit modelling is facilitated as this power conversion process is common[27,28,29].

4.6.2 Disadvantages

- A major disadvantage with this design that there is no lamp current reversal. This results in phosphoresis and reduced lamp life.
- There is no current limiting between C2 and the lamp so as the starter closes high transient currents flow through both the electrodes and the starter. This has resulted in both glow starter and electrode failure. The glow starter switch contacts weld together and sometimes the high transient currents cause filament rupture. The inclusion of a current limiting resistor, however, reduces efficiency.
- Lamp removal sometimes results in the failure of either D1 or C2 through excessive voltages.

4.7 Class C Inverters

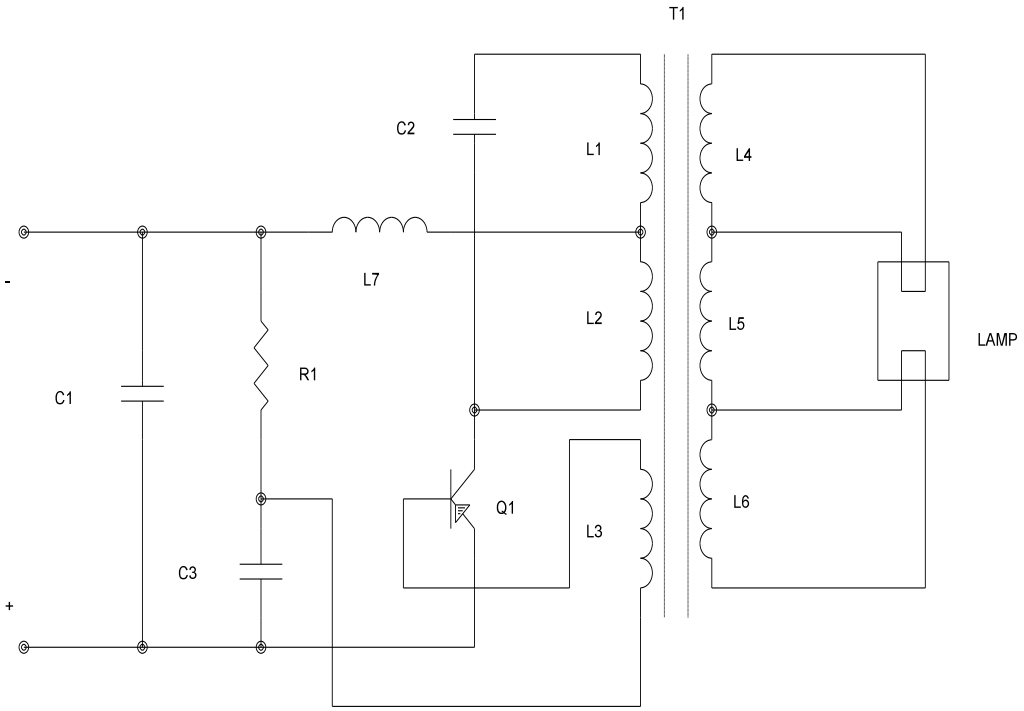

Figure 4.6: A class C battery operated fluorescent lamp ballast.

This circuit[4,5] is an improvement on the simple blocking oscillator. C2, L1 and L2 form a resonant circuit. This reduces lamp current distortion and hence lowers the crest factor. The transformer secondary is loosely coupled to the primary, the secondary leakage inductance acting as a ballast. The turns ratio has been chosen so that during ignition the voltage developed across L5 is sufficient to start the lamp when the electrodes are hot. The voltage developed across L4 and L6 provide rated heater current.

During arc discharge the secondary voltage across both the lamp and the electrodes decreases due to the secondary leakage reactance. The leakage reactance counters the

negative resistance of the lamp resulting in stable operation. L7 is included to help the transistor act as a switch by reducing turn-on losses.

4.7.1 Advantages

- Low cost.
- Class C operation provides less current distortion than a simple flyback inverter. This reduces the dc current component through the lamp.

4.7.2 Disadvantages

- Although the circuit is simple two inductive components are required and the transformer has too many windings, *i.e.* six. The requirement of a loosely coupled secondary complicates the coil winding procedure.
- A major disadvantage of single ended bipolar transistor (BJT) oscillator designs is performance dependence on transistor parameters.
- Another problem with transistor oscillators is initiation of oscillation if used in emergency applications. It is preferable to have the dc power connected to the inverter permanently and to initiate operation under certain conditions; correct battery voltage, low ambient light *etc*.. No simple electronic solution will inhibit oscillation with these designs. The power must be removed or the base current must be interrupted. This requires the additional expense of a relay or another high current transistor.
- The secondary leakage reactance may make this design unsuitable for use with lamps with internal starters because the suppression capacitor limits the starting voltage transient.

4.8 Push Pull Inverters

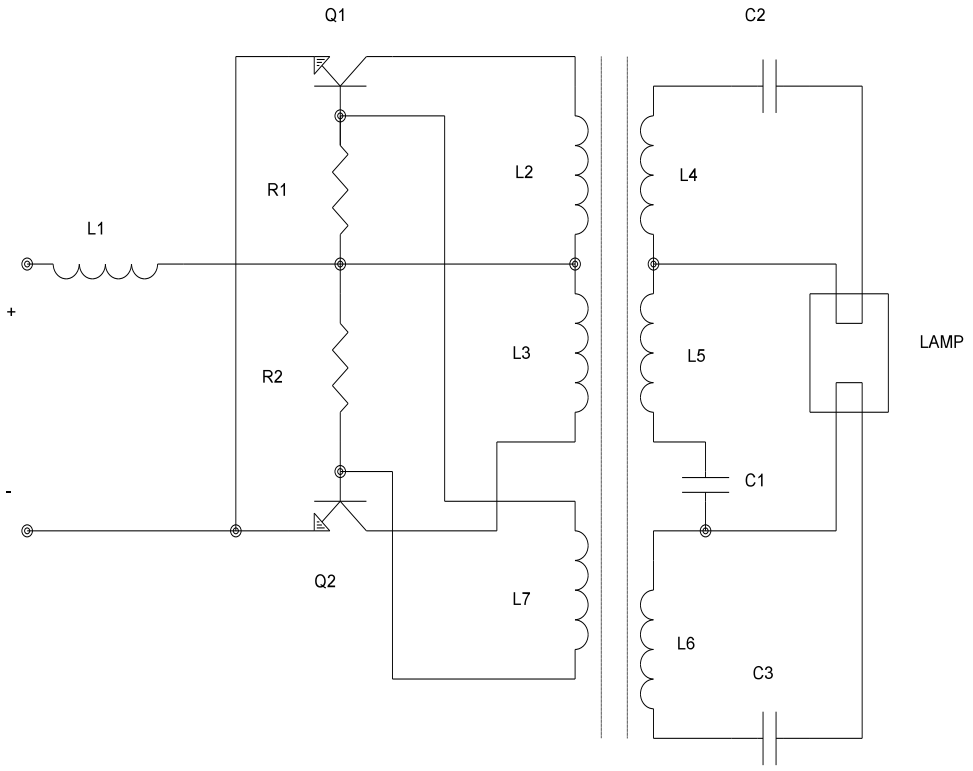

Figure 4.7: The Baxandall push-pull fluorescent lamp ballast[5].

This Baxandall class D circuit[5] and other variations[1] achieves a higher efficiency than that of a flyback inverter due to the push-pull action. The output impedance of the circuit is also lower and is thus more suitable to overcome the loading effects of the starter assembly. This type of circuit is used as an alternative to the flyback inverter to provide a low current crest factor and to improve efficiency. Variations of this circuit are used to drive both fluorescent lamps with and without internal starters.

The feedback coil (L7) provides base drive to Q1 and Q2. The polarity of the drive is dependant upon whether L2 or L3 was energised. In many battery powered ballasts, the

combined effects of both high turns ratios and secondary self capacitances result in a high primary circuit capacitive load being presented to the switching devices. This increases switching losses during the turn on transition. L1 is included to overcome this problem and reduce switching losses, by allowing the transistors to saturate rapidly.

When unloaded the oscillator runs at high frequency. This assists lamp ignition and provides electrode heater current. After ignition the secondary voltage falls and the frequency decreases thereby reducing heater current. C1 acts as a ballast and serves as a tuning capacitor. A circuit efficiency of up to 90% is claimed with the Baxandall circuit[5].

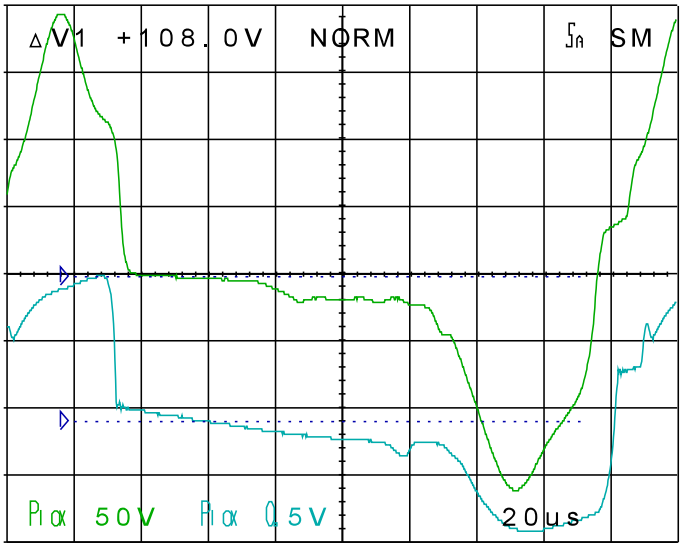

Figure 4.8: Measured lamp voltage (upper trace) and current (lower trace across 10 Ω) of a typical push-pull inverter.

Figure 4.8 shows the lamp current and voltage waveforms of a typical push-pull inverter described by Elenbaas[1]. Efficiencies of up to 80% are possible when using this circuit at 15 kHz and higher[1]. However, at approximately 8 kHz the measured efficiency of this

particular ballast was only between 50 and 60%, which compares well with the published performance of this type of circuit at this frequency[1].

The high current crest factor of approximately 3, coupled with a low switching frequency, will result in a low lamp life. The poor symmetry of the waveforms is due to different transistor parameters.

4.8.1 Advantages

- The circuit is simple to manufacture.
- No electrophoresis will result due to a near symmetrical lamp drive.
- The symmetrical drive provides a low output impedance.
- High efficiencies are possible with the Baxandall circuit.

4.8.2 Disadvantages

- Extra cost incurred by using two switching elements instead of one.
- A relay or high current transistor is required to interrupt the power in emergency lighting applications, adding to cost. There is no simple, low cost, means of interrupting oscillatory action.
- The output power is device dependent.
- This particular circuit operated at a frequency well within the audio band which proved irritating.

4.9 Simple Flyback Inverters

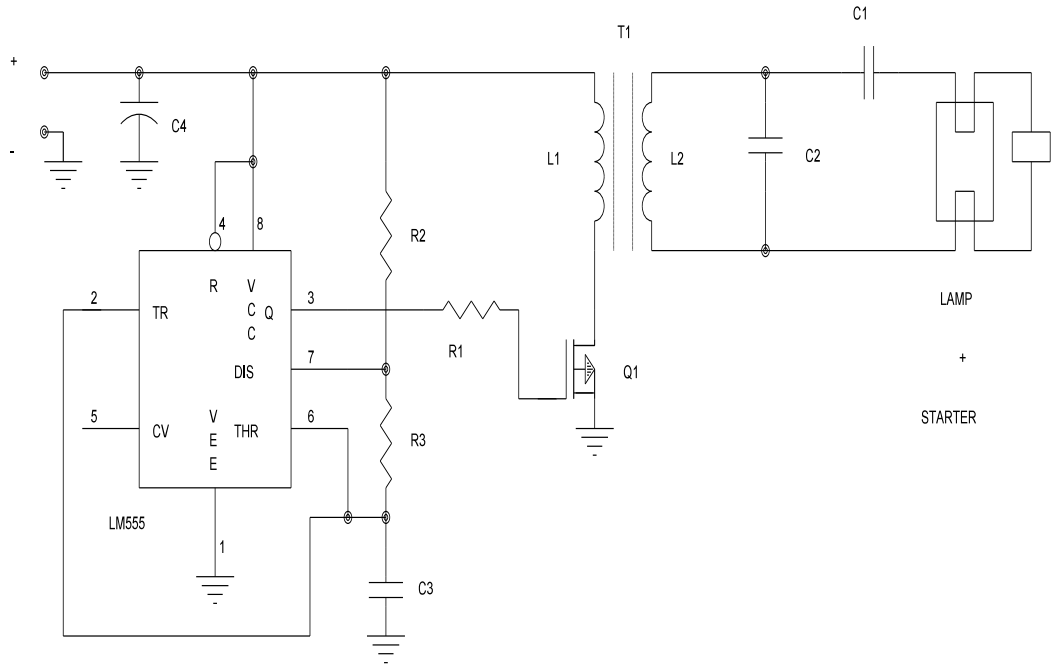

Figure 4.9: A simple flyback lamp inverter designed for compact fluorescent lamps with built in starters.

The circuit shown in Figure 4.9 is probably one of the simplest configurations of a flyback inverter. This particular circuit is used to drive compact lamps with internal starters. The output power can be readily controlled by varying the duty cycle. The LM 555 connected in the astable mode provides the gate drive to the FET. C1 is included as a ballast. C2 is included to minimise the secondary voltages and switching element overvoltage if the lamp is removed, without substantially degrading starting performance.

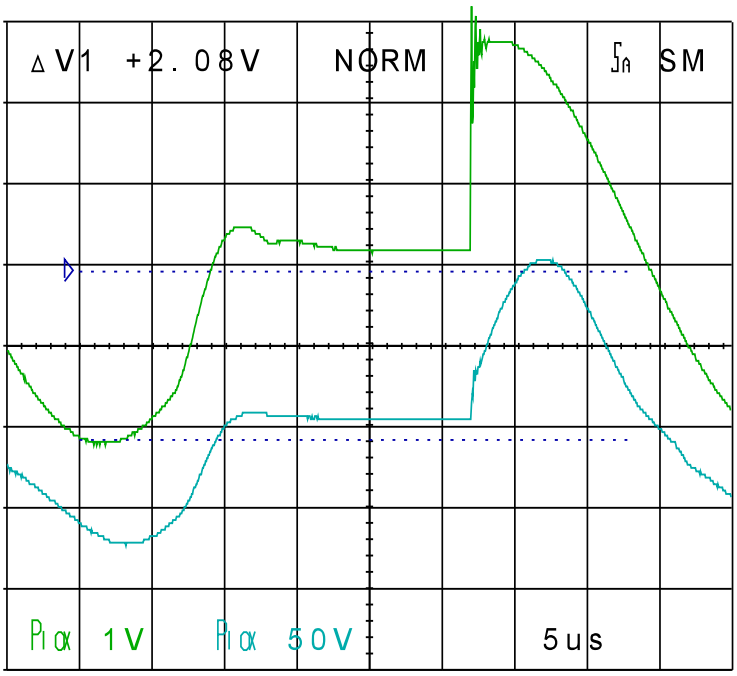

Figure 4.10: Current (upper trace) and voltage waveforms for a simple flyback inverter. Current was measured across 10 Ω.

The lamp current, see Figure 4.10 on the following page, is appreciably distorted during switch conduction. The measured rms lamp current is 130 mA. The peak lamp current in Figure 4.10 is 260 mA. The lamp current crest factor is therefore approximately 2. The only method of reducing the crest factor using this circuit is to reduce the conduction period.

The primary current waveform was similar to that shown in Figure 4.5, but the peak primary current is 7 A. The conduction period is 17 μs and the switching period is 45 μs. The primary inductance was measured to be 15.3 μH. Based on these figures, the output power is therefore approximately 8 W. As energy conversion relies almost entirely on stored magnetic energy, the output power can be simply controlled by varying the

conduction period. From Equation 4.2 the peak current, using piecewise linear analysis, is given by

$$I_{pk} \approx \frac{\left(Vcc - V_{sat}\right) t_{on}}{L} . \qquad \textbf{(4.7)}$$

The peak current is therefore proportional to the conduction period. However, the output power is proportional to the peak current squared, from equation (4.4). The output power is therefore proportional to the conduction period squared. It is not possible to reduce the switch conduction period with this design as the conversion power would decrease disproportionately. The initial primary current peak due to secondary self capacitance results in switching losses which are therefore incurred during both switch on and switch off instants. Switch conduction losses are incurred during the entire conduction period of 17 μs. The measured power conversion efficiency is 70%. The FET temperature exceeded 110°C without its heat sink so device dissipation must account for a significant portion of the total circuit losses.

4.9.1 Advantages

- Low cost due to a simple transformer winding configuration and single ended design.
- Output power is easily controlled.

4.9.2 Disadvantages

- Substantial secondary voltages of greater than 3000 V, and therefore large primary voltages, are generated when no lamp is present.
- Poor efficiency.
- High crest factor due to the high duty cycle (D = 0.4).

- Poor starting scenario due to high starting voltages.
- Poor starting reliability with low dynamic resistance starters (PL 9W).

4.10 Pulse Width Modulation Inverters

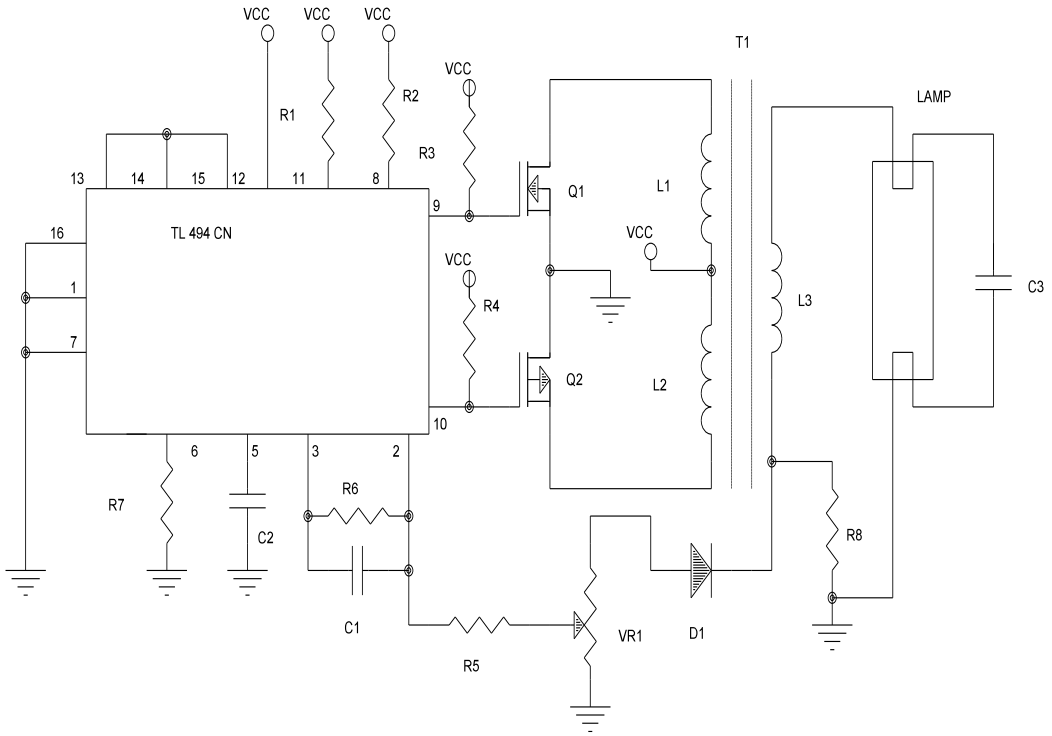

Figure 4.11: A push-pull fluorescent lamp ballast using pulse width modulation to control output power[18].

This particular circuit[18] uses pulse width modulation to drive a pair of push-pull switching devices. The drive frequency is set by passive components whilst the on period of the switching devices is controlled by a feedback arrangement. The mean tube power is given by

$$P = V.I.\frac{\tau}{T/2} \quad [W] \ ,$$

Size A	Document Number **(4.8)**
Date:	September 24, 1994

where V and I are the peak tube voltage and current, τ is the transistor on period and T is

the switching period. Lamp current is the feedback parameter. Too little lamp current results in the on pulse width being extended and *vice versa*. As the transformer is being used in a traditional manner, the required turns ratio is given by

$$n = \frac{V_{\text{sec}}}{V_{pri}}, \qquad \textbf{(4.9)}$$

where V_{sec} is the required peak secondary voltage to ensure reliable starting.

Starting is assisted by ringing due to a loosely coupled secondary winding. The secondary leakage inductance and C3 produce an underdamped series resonant circuit.

4.10.1 Advantages

- Low lamp current crest factor. The published oscillograms indicate a crest factor of approximately 1.2.
- The push-pull circuit produces symmetrical output waveforms and will therefore not cause electrophoresis.
- The feedback enables accurate output power control.

4.10.2 Disadvantages

- Additional cost is incurred in using two switching devices.
- The TL 494 is expensive relative to the usual LM 555 switch driver.
- Lamp ignition relies on an underdamped series resonance of C3 and output leakage reactance of the transformer. The starter glow discharge will load this resonance and may inhibit ignition when using PL type lamps.

4.11 Summary

Other designs reviewed but not included here are multiple ferrite designs that ensure low distortion lamp current and other high frequency designs[33] whose complexity and high cost result in little market share.

An indication of power conversion efficiency is the dissipation of the switching device. As the thermal resistance of the switching devices was known an attempt was made to remove the devices from their respective heat sinks, measure temperature rise and then compute dissipation. The temperatures of switches on all the designs, except that described in 3.4.1. which used a dc lamp supply, rose to dangerously high levels, above 110°C, and thus could not safely be measured in this manner. The transistor temperature in the dc lamp supply design rose to 90°C. The transistor dissipation was therefore 1 W. Power conversion efficiency with this design never exceeded 73% at any supply voltage. Other circuit losses therefore amounted to 800 mW. By virtue of device dissipation alone, none of the other designs tested were more efficient.

The low dynamic resistance of the PL 9 starter coupled with the potentially destructive effects of lamp removal indicate the use of a near field to assist lamp ignition is advantageous. The use of dc lamp current is not recommended due to the reduction in lamp life. Push-pull configurations are not cost effective due to the cost of the extra switching element and associated circuitry.

Unfortunately no class C inverters, single ended or push-pull, could be sourced for measurement. Perhaps this stems from the general belief in the industry that all single ended inverters provide poor lamp life and that all push-pull designs provide extended lamp life. It is only the large consumers of emergency lighting products who have the resources to accurately measure inverter performance.

5 Optimal Ballast Theory

5.1 General

The key to extended lamp life is current form. As it is not efficient to provide a symmetrical square wave current to the lamp using a single ended inverter, class C amplification must be used. Class C amplification involves pulsing a resonant circuit at its natural frequency. In this way the output current is a decaying sinusoid with aberrations during switch conduction cycles. The energy conversion during conduction cycles inevitably leads to current distortion and a method to reduce distortion is therefore to reduce the energy conversion time.

This chapter examines methods of effecting rapid energy conversion. A method is presented that relies on secondary reflected capacitance to effect energy conversion within the electron temperature relaxation period. The starter suppression capacitor now forms part of the energy conversion process whereas, in the case of conventional flyback techniques, it has a negative influence. The key to the operation of the new inverter can be seen in Figure 4.5. The initial primary circuit overcurrent caused by secondary reflected capacitance is usually problematic in fluorescent lamp inverter design, but here it is put to good use. In fact, it will be shown that energy conversion can be effected solely through secondary capacitance.

5.2 Secondary Capacitance Effects

Figure 5.1 (A) depicts a flyback inverter with a capacitive load. If the coupling coefficient of the transformer is unity, *i.e.* perfect coupling, then the secondary

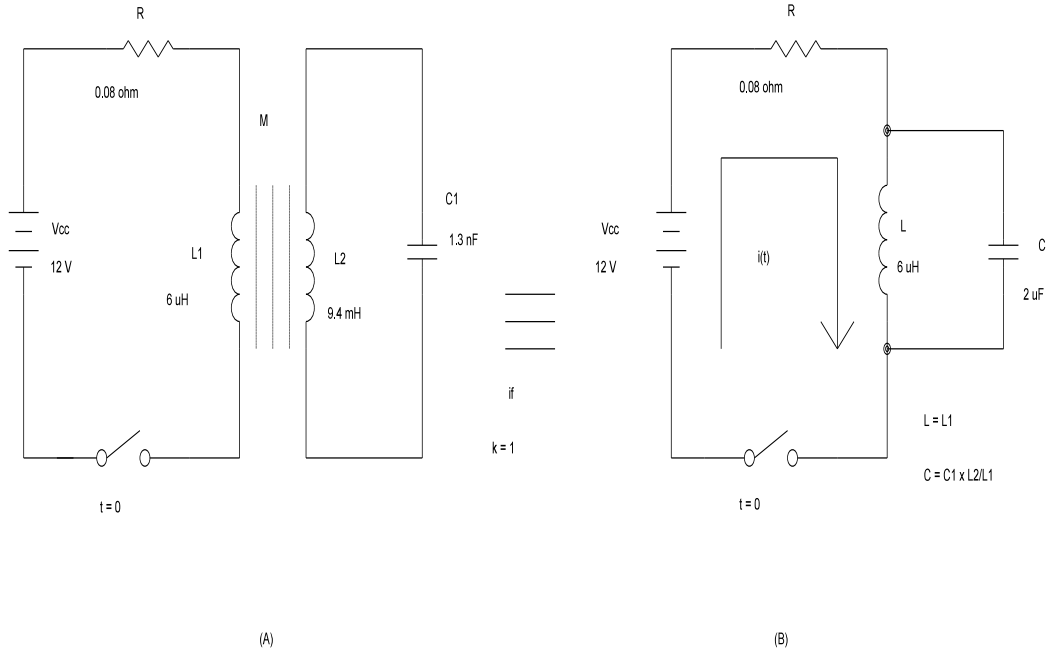

Figure 5.1: A single ended inverter with a capacitive load (A) and its equivalent (B) if perfect coupling is achieved (ie. if k = 1)

capacitance C_1 reflected back to the primary circuit is given by C as

$$C = \left(\frac{N_{\text{sec}}}{N_{pri}} \right)^2 C_1 \ ,$$

where N_{sec} and N_{pri} are the number of secondary and primary turns respectively. Also if perfect coupling is achieved then the circuit on the right (Figure 5.1 (B)) can be used to investigate the transient primary current as the switch closes. Perfect coupling can be approximated in practice by tightly winding both primary and secondary turns on a bobbin without any insulating layers.

Size	Document Number	R
A		
Date: April 19, 1995	Sheet of	

Using Kirchhoff's Voltage Law and writing an expression in the Laplace domain for current in the equivalent primary circuit (B)

$$\frac{Vcc}{s} = I(s)R + I(s)Z ,$$

where Z is the parallel connection of L and C. Rearranging the expression and substituting values for Z gives

$$I(s) = \frac{Vcc}{R}.\frac{(s^2LC + 1)}{s(s^2LC + sL/R + 1)} . \qquad \textbf{(5.1)}$$

The denominator second order polynomial is in the form

$$s^2(1/\omega_n^2) + s(2\zeta/\omega_n) + 1 ,$$

where ω_n is the natural frequency of oscillation and ζ is the damping ratio. The damping ratio provides an indication of system stability, where values exceeding one will result in an overdamped transient response and values of less than one will result in an oscillatory transient response at a frequency of $\omega_n/2\pi$. The damping ratio for the above circuit is given by

$$\zeta = \frac{1}{2R}\sqrt{\frac{L}{C}} . \qquad \textbf{(5.2)}$$

The roots of the polynomial can be computed from

$$s_1, s_2 = -\omega_n(\zeta \pm \sqrt{\zeta^2 - 1}) .$$

The primary and secondary turns on the prototype inverter are 5 and 200 respectively. The measured secondary self capacitance is of the order of 20 pF. The reflected secondary self capacitance to the primary is therefore 32 nF. The effect of the self secondary capacitance reflected back to the primary therefore provides a substantial transient load to the switching device. This is normally a problem with battery powered fluorescent lamp inverters due to the large turns ratios required.

The capacitive load across the secondary winding due to the ballast and suppression capacitors is, neglecting the lamp electrode resistance, approximately 1.3 nF. This combined secondary capacitance reflected to the primary is approximately 2 μF, which swamps the reflected self capacitance of 32 nF.

If

R = 0.08 Ω	:the resistance of the primary circuit
C = 2 μF	:secondary reflected capacitance
L = 6 μH	:the primary inductance
Vcc = 12 V	:battery supply voltage

then the Laplace domain expression for the primary current becomes

$$I(s) = 150.\frac{(s^2 + 8.3\times10^{10})}{s(s^2 + s(6.3\times10^6) + 8.3\times10^{10})} . \qquad \textbf{(5.3)}$$

Note that the discriminant ($[L/R]^2 - 4LC$) is positive so the roots will be real resulting in an overdamped response. When the denominator quadratic is factorised the expression yields

$$I(s) = 150\frac{(s^2 + 8.3\times10^{10})}{s(s + 13000)(s + 6.3\times10^6)} . \qquad \textbf{(5.4)}$$

The pole (s + 13000) is defined by the circuit inductance and resistance time constant where

$$\frac{L}{R} = \tau = \frac{1}{13000}\ s. \tag{5.5}$$

After separating into partial fractions and computing residuals, the inverse Laplace Transform yields the time domain transient response

$$i(t) = 150\left(1 - e^{-1.3\times10^{4}t} + e^{-6.3\times10^{6}t}\right)\ . \tag{5.6}$$

When $t = 0$ then $i(0) = 150$ A, which is expected as the initial charge on C is zero and the initial current is limited by the FET on resistance, circuit board track and primary winding resistances in series. The secondary capacitance is charged within one microsecond. Hence energy conversion can be accomplished more rapidly then by conventional flyback inverter techniques as the conversion time is only limited by primary resistance. When $t \rightarrow \infty$ then $i(\infty) \rightarrow 144$ A, which is also to be expected as the effects of the capacitor are negated with time and the inductor resistance is zero.

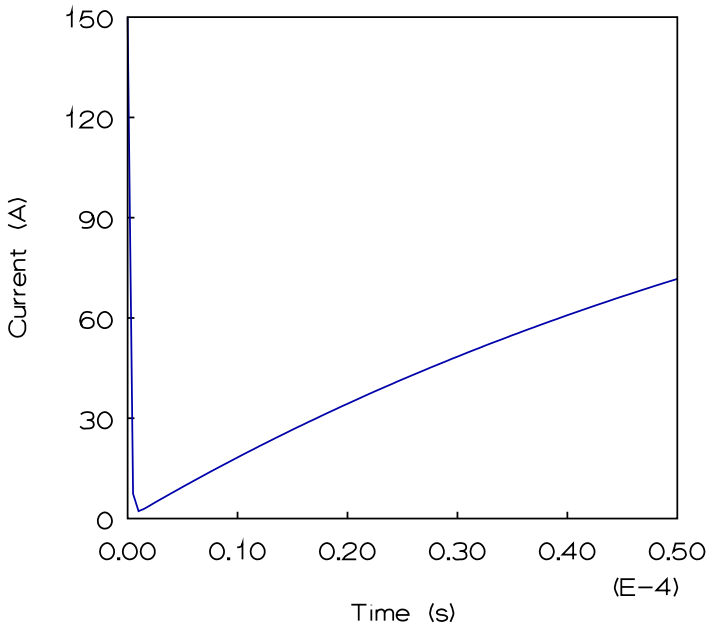

Figure 5.2: Calculated primary transient current showing the effects of secondary reflected capacitance.

Figure 5.2, on the following page, shows a plot of the resulting transient current/time relationship. Note that the response of the system will be overdamped until the primary circuit resistance becomes appreciable (0.87 Ω).

The current has its minimum value where

$$\frac{d}{dt}i(t) = 1.3\times10^{4}e^{-1.3\times10^{4}t} - 6.3\times10^{6}e^{-6.3\times10^{6}t} = 0 .$$

The current minimum value is determined by the magnitude of the discriminant. If its value is small then the minimum current will be large and *vice versa*.

At a time of 0.98 μs after switch closure the current has dropped from its initial peak of

150 A to a minimum of 2.2 A. If the switch is opened at this instant the secondary capacitor will be fully charged and the switch will open under low current conditions thereby reducing switching losses. The energy stored in the primary winding will also be low at this instant. This phenomenon assists with device overvoltage protection through primary leakage inductance derived transients.

At this point, however, it is evident that problems may arise if the core saturates causing initial overcurrents and increased switching losses during the turn on instant.

5.3 Transformer Coupling Effects

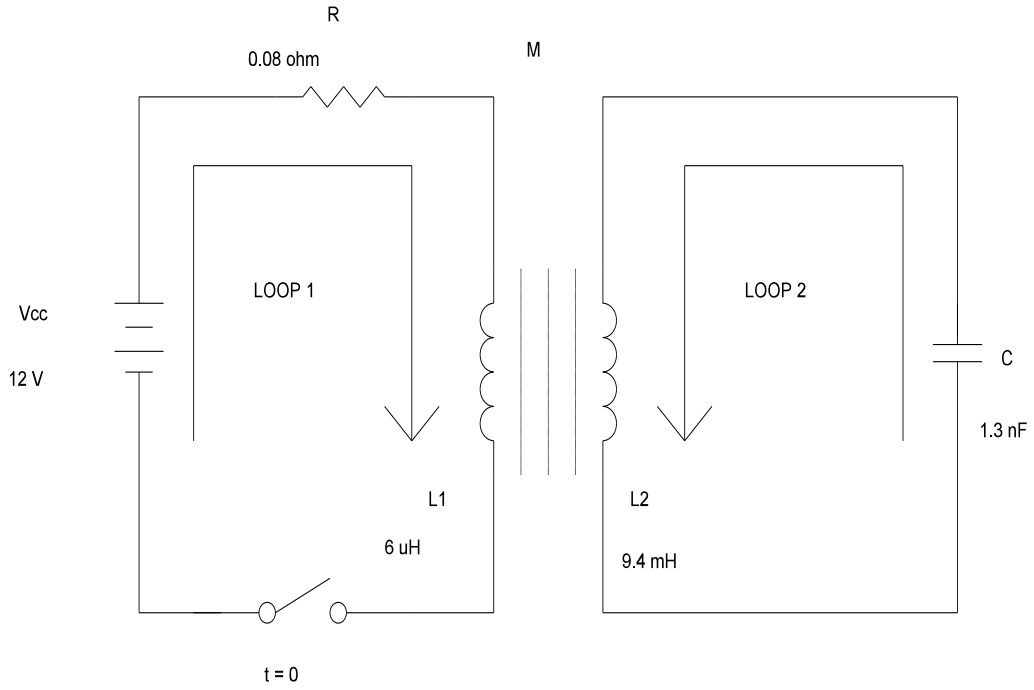

Figure 5.3: The equivalent circuit of a single ended inverter with a capacitive load.

Figure 5.3 shows the simplified circuit which includes the transformer but the load resistance and other components have been omitted. By Kirchhoff's Voltage Laws the sum of the voltages around loop 1 is given by

$$\frac{Vcc}{s} = I_1(R + sL_1) + I_2(sM) \ .$$

The sum of the voltages around loop 2 is

$$0 = I_1(sM) + I_2\left(sL_2 + \frac{1}{sC}\right) \ .$$

Cramer's Rule gives the loop 1 current as

$$I_1(s) = \frac{\begin{vmatrix} Vcc/s & sM \\ 0 & sL_2 + 1/sC \end{vmatrix}}{\begin{vmatrix} R + sL_1 & sM \\ sM & sL_2 + 1/sC \end{vmatrix}} .$$

Solving for the primary current yields

$$I_1(s) = \frac{Vcc}{R} \frac{(s^2(L_2C) + 1)}{s(s^3(L_1L_2 - M^2)(C/R) + s^2(L_2C) + s(L_1/R) + 1)} .$$

If the coupling coefficient (k) of the transformer is unity, *i.e.* perfect coupling is achieved, then $L_1L_2 = M^2$ where

$$M = k\sqrt{L_1L_2} . \qquad \textbf{(5.7)}$$

Assuming perfect coupling and re-arranging the terms yields

$$I_1(s) = \frac{Vcc}{R} \frac{(s^2 + 1/L_2C)}{s(s^2 + s(L_1/L_2)(1/CR) + 1/L_2C)} . \qquad \textbf{(5.8)}$$

The primary loop dynamics is now dictated by the secondary components with the primary resistance reflected to the secondary by the ratio

$$\frac{L_2}{L_1} = \left(\frac{N_{sec}}{N_{pri}}\right)^2 , \qquad \textbf{(5.9)}$$

The damping ratio is

$$\zeta = \frac{1}{2R}\sqrt{\frac{L_1}{C}\left(\frac{L_1}{L_2}\right)} \qquad \textbf{(5.10)}$$

In this case the damping can be compared to equation (5.2) above by the ratio of the primary and secondary inductances, *i.e.* the secondary reflected capacitance.

If	R = 0.08 Ω	:primary circuit resistance
	C = 1.3 nF	:secondary circuit capacitance
	L_1= 6 μH	:primary winding inductance
	L_2= 9.4 mH	:secondary winding inductance
	Vcc = 12 V	:battery supply voltage
	M = $(L_1.L_2)^{1/2}$ *i.e.* k = 1	:mutual inductance

then for perfect coupling

$$I_1(s) = 150\frac{(s^2 + 8.2\times10^{10})}{s(s^2 + s(6.4\times10^6) + 8.2\times10^{10})}, \qquad \textbf{(5.11)}$$

which yields the same time domain response as the previous theory given in Section 5.2. above. If, however, M = 0 then there would be no coupling between the primary and secondary circuits and C would not effect the dynamics of the primary loop. If M = 0 and C = 0 then the expression reduces to

$$I(s) = \frac{Vcc}{R}\frac{1}{s(s(L_1/R) + 1)},$$

which is a first order RL circuit with a time response given by

$$i(t) = I_{pk}\left(1 - e^{-tR/L_1}\right) .$$

In this case the current would rise exponentially from zero with no initial current peak.

The initial current peak can therefore be controlled by tuning the mutual inductance. Assuming imperfect coupling with M = 200 μH the Laplace Domain expression for the primary current $I_1(s)$ becomes

$$\frac{150(s^2 + 4.6\times10^4)}{s(s + 1.4\times10^4)(s + 1.6\times10^4 + j5.5\times10^5)(s + 1.6\times10^4 - j5.5\times10^5)} .$$

In this case the roots of the denominator polynomial are complex resulting in an underdamped or oscillatory response. The resulting time domain response is

$$i_1(t) = 150 - 150e^{-1.4\times10^4 t} + 9e^{-1.6\times10^4 t}\sin(5.5\times10^5 t) .$$

As $t \to 0$, $i \to 0$. The initial current through the switching device is therefore zero. The first two terms of the expression are those of a first order LR circuit ($150 - 150e^{(-tR/L)}$). The transient response of this type of circuit is therefore characterised by that of a first order LR onto which a third, oscillatory, term is superimposed. The transient response is shown in Figure 5.4, on the following page, together with plots for other values coupling.

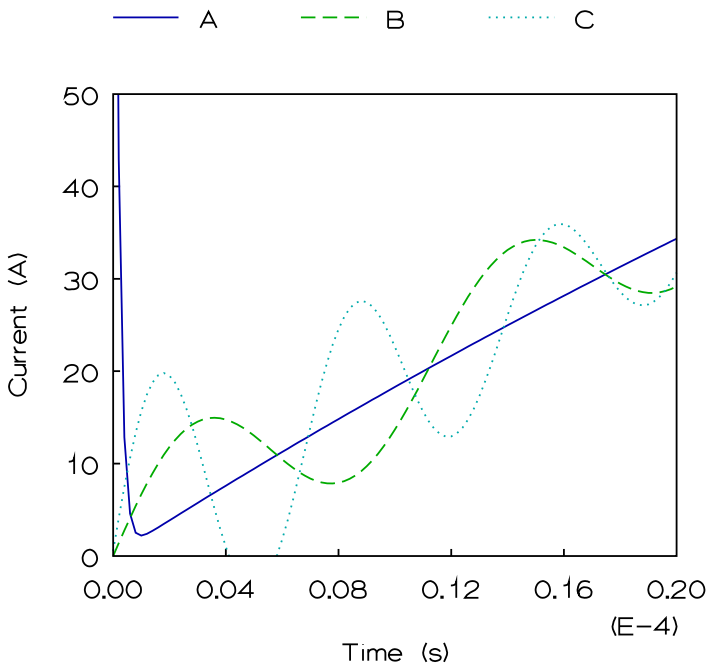

Figure 5.4: Calculated transient primary current for various coupling co-efficients. A: k = 1, B: k = 0.85, C: k = 0.95.

Note that in Figure 5.4 the first minimum does not correspond to zero amperes but if circuit parameters are tuned this minimum could occur at zero amperes. In both plots where $k < 1$ the initial current is also zero.

It is therefore possible to design a circuit which has zero switching losses because both switch on and switch off instants could be accomplished under zero current conditions. The traditional problems of primary leakage inductance and the resulting overvoltages would then be negated as at the end of every switching cycle no energy is stored in the magnetic circuit.

The conversion energy, stored in the secondary capacitor, given by

$$E = \frac{1}{2}CV^2 \quad [J] \ . \tag{5.12}$$

Conversion speed *i.e.* the period between primary current zeros, can be controlled by tuning the natural frequency of the secondary components.

5.4 Load Resistance Effects

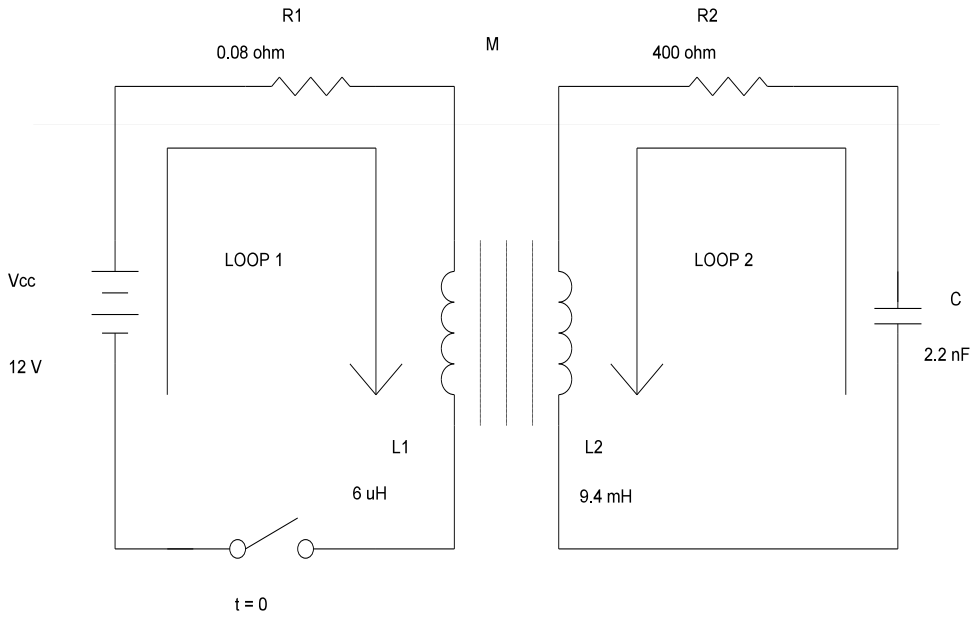

Figure 5.5: Equivalent circuit of a single ended inverter with a resistive load.

Figure 5.5 shows the simplified circuit including the load resistor, *i.e.* the lamp. The Laplace domain expression for the current in the primary loop, $I_1(s)$, is

$$\frac{Vcc}{R_1}\frac{(s^2(L_2C) + s(CR_2) + 1)}{s(s^3(L_1L_2 - M^2)(C/R_1) + s^2(L_2C + L_1CR_2/R_1) + s(L_1/R_1) + 1)}.$$

In order to negate the effects of varying mutual inductance the coupling coefficient is set at unity. The expression then becomes

$$I_1(s) = \frac{Vcc}{R} \frac{s^2(L_2C) + s(CR_2) + 1}{s(s^3(L_2C + L_1CR_2/R_1) + s(L_1/R_1) + 1)} .$$

Substituting values gives

$$I_1(s) = 150. \frac{s^2(0.23) + s(1\times10^4) + 1.9\times10^{10}}{s(s^2 + s(1.5\times10^6) + 1.9\times10^{10})} .$$

The time domain response of the primary current is given by

$$i(t) = 150\left(1 - 0.97e^{-1.3\times10^4 t} + 0.23e^{-1.5\times10^6 t}\right) .$$

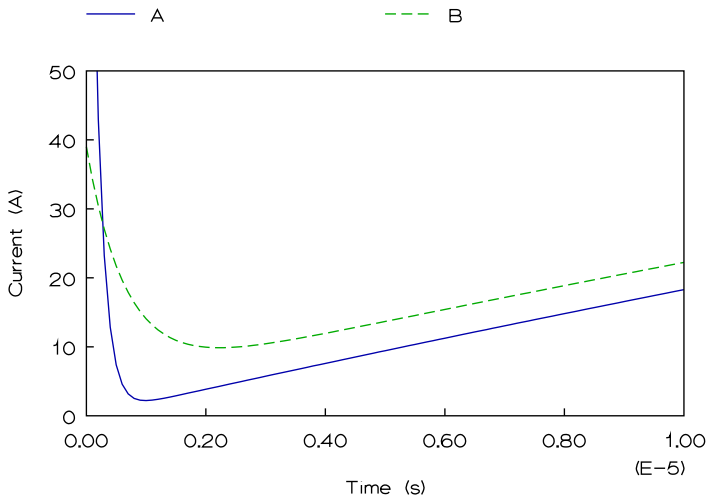

Figure 5.6: Calculated primary transient current with no secondary resistance (A) and with a secondary resistance of 400 Ω (B).

The effect of the load resistance on the transient primary current is to reduce the effects of the secondary capacitor, see Figure 5.6. The initial current (at *t=0*) is reduced and the current minimum is less pronounced. The design aim must therefore be to ensure a high secondary circuit Q thereby optimising the current minimum.

If k is reduced from zero to 0.97, *i.e.* M = 230 μH, then the Laplace domain expression for the current flowing in loop 1 becomes

$$I_1(s) = 150\frac{(s^2(2.1\times10^5) + s(9.1\times10^9) + 1.76\times10^{16})}{s(s^3 + s^2(9\times10^5) + s(1.3\times10^{12}) + 1.76\times10^{16})},$$

from which the time domain response is

$$i_1(t) = 150\left(1 - e^{-1.3\times10^4 t} + 0.16e^{-4.4\times10^5 t}\sin(1\times10^6 t)\right). \quad \textbf{(5.13)}$$

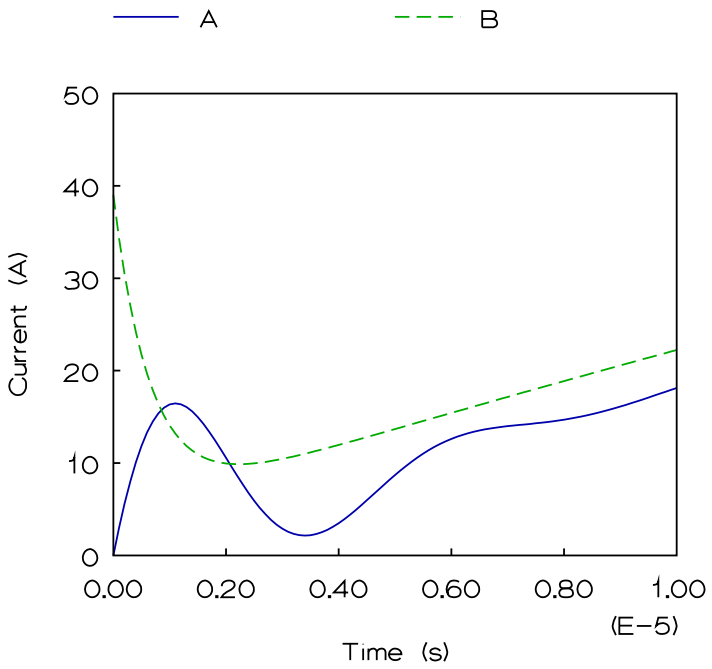

Figure 5.7: Calculated primary transient current with reduced mutual coupling (A) and with perfect coupling (B).

The time domain response in Figure 5.7 shows that it is still possible to obtain a current zero by tuning mutual inductance in spite of the presence of secondary resistance. The secondary resistance value was set at a realistic value of lamp discharge resistance.

The conversion and conversion time are, however, mutually dependent using this method of obtaining primary current zeroes.

5.5 Analysis of Component Dependency

The equivalent model shown in Figure 5.5 shall be used to examine variable dependency. Setting $L_1L_2 - M^2 = L_O$ and dividing through by the coefficient of s^3 yields

$$\frac{s^2\left(\frac{L_2R_1}{L_O}\right) + s\left(\frac{R_1R_2}{L_0}\right) + \left(\frac{R_1}{L_OC}\right)}{s^3 + s^2\left(\frac{L_2R_1}{L_O} + \frac{L_1R_2}{L_O}\right) + s\left(\frac{L_1}{L_OC}\right) + \left(\frac{R_1}{L_OC}\right)} .$$

The primary circuit topology is essentially a first order series LR network. This ensures that one of the partial fractions, *i.e.* a root of the denominator polynomial, will always be

$$\left(s + \frac{R_1}{L_1}\right) .$$

The time domain primary transient current will be characterised by an exponentially increasing current that is modulated by a damped oscillation.

After removing the above root, the polynomial is reduced to

$$s^2 + s\left(\frac{L_2R_1}{L_O} + \frac{L_1R_2}{L_O} - \frac{R_1}{L_1}\right) + \left(\frac{L_1}{L_OC}\right) .$$

The time domain response can then be approximated by

$$i(t) = \frac{Vcc}{R_1}\left[1 - e^{\left(-\frac{R_1}{L_1}t\right)} + \frac{L_2R_1}{2}\sqrt{\frac{C}{L_1L_0}}\, e^{\left(\frac{L_1L_2R_1 + L_1^2R_2 - R_1L_0}{2L_0L_1}\right)} \sin\sqrt{\frac{L_1}{L_OC}}t\right] . \qquad \textbf{(5.14)}$$

This expression was used to estimate primary current transient responses without the need to perform lengthy Laplace Transformations. However, none of the time domain responses in this thesis were obtained using this expression, numeric solutions to frequency domain expressions were computed by hand.

5.6 Initial Conditions

The previous sections have analysed the primary transient current with zero initial conditions. In practice there is usually residual energy from the previous switching cycle. This energy is stored in reactive components being either inductor current ($i_l(0)$) or capacitor voltage ($v_c(0)$).

This section examines the effects of initial conditions on the primary transient current using the simple case equivalent primary circuit shown in Figure 5.1 (B).

If the switching frequency is approximately equal to the natural frequency of the secondary circuit then it is possible to vary the initial capacitor voltage whilst keeping the initial current equal to zero. However, it is not feasible to vary the initial current whilst holding

the initial capacitor voltage at zero.

The analytical solution to the simplified circuit model, *i.e.* equation (5.1), including initial conditions, is given by

$$i_1(t) = \frac{Vcc}{R} - \left(\frac{Vcc}{R} + i_L(0)\right) e^{\left(-\frac{Rt}{L}\right)} + \left(\frac{Vcc - v_c}{R} + i_L(0)\right) e^{\left(-\frac{t}{RC}\right)} . \qquad \textbf{(5.15)}$$

This solution is only valid when $L/R >> CR$, which is always the case with this design. If the initial conditions ($i_L(0)$ *and* $v_c(0)$) are zero then both coefficients of e in the above expression are Vcc/R. A negative value for current is then not possible for any value of t. Providing that $L/R >> CR$ there are values of initial current and voltage which would result in the primary current passing through zero.

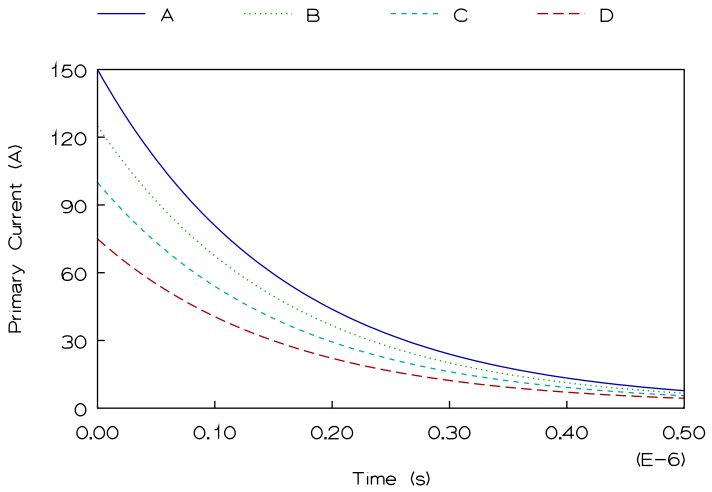

Figure 5.8: Calculated primary current for different initial voltages on the secondary capacitor. A: zero, B: 80 V, C: 160 V, D: 240 V.

Figure 5.8 shows the effect of varying initial capacitor voltage ($v_c(0)$) whilst setting $i_l(0)$

to zero. The effect is equivalent to reducing the supply voltage. The polarity of the secondary capacitor voltage will always effectively reduce the supply voltage at switching frequencies near to the secondary natural frequency. Also, it is not possible to cause negative primary current excursions by solely varying $v_c(0)$. During lamp ignition the lamp resistivity is high and the secondary capacitor is not charged substantially. The effect will therefore be higher peak primary currents.

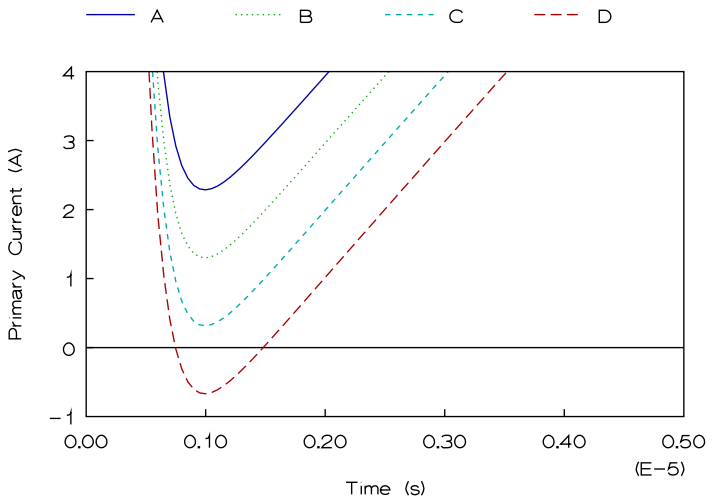

Figure 5.9: Calculated primary current for different values of initial secondary current. A: zero, B: 25 mA, C: 50 mA, D: 75 mA.

The effect of varying initial secondary current about zero depends upon the polarity of the current. If the current is positive *i.e.* the switching frequency is greater than the natural frequency of the secondary components, then a lower primary current minimum will result, as shown in Figure 5.9. The converse is true if the switching frequency is less than the natural frequency of the secondary components.

It is therefore possible to tune the switching frequency to obtain a primary current zero at the end of the conduction cycle without tuning mutual inductance. The mechanisms for providing current zeroes during turn on and turn off can be independent thereby facilitating flexibility in tuning conversion power. It is accepted that it may not always be possible to

guarantee switch off under zero current conditions due to component parameter shift. Some primary current may therefore be flowing at the switch off instant.

5.7 Complete Primary Current Transient Response

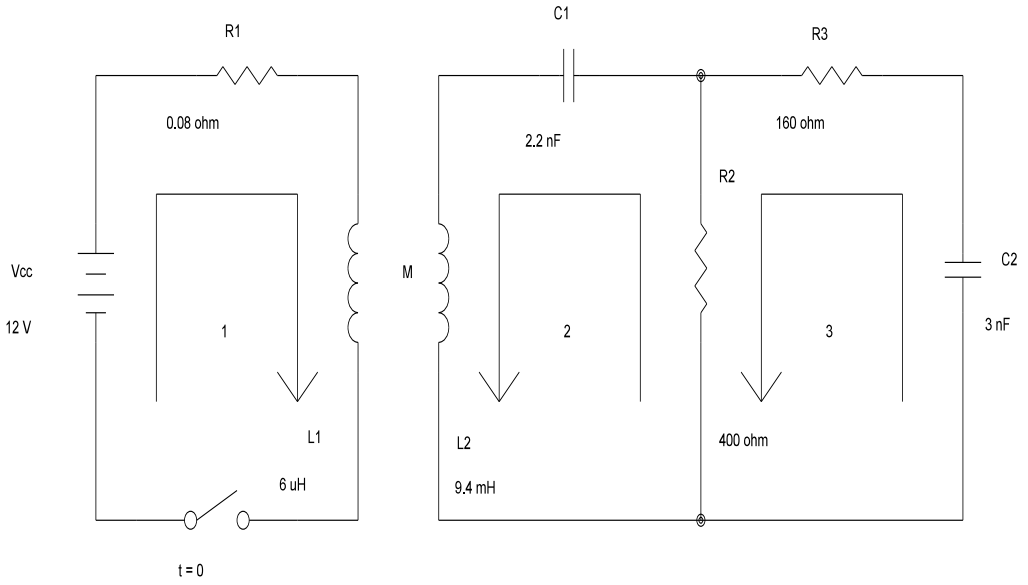

Figure 5.10: The equivalent circuit of the inverter including the suppression capacitor and the electrode resistance.

This analysis will examine the effects of both the combined electrode resistance (*R3*) and suppression capacitor (*C2*) on the primary transient current. Figure 5.10 shows the equivalent inverter circuit for analysis purposes. *R1* is the total series value of the FET on resistance, circuit board track resistance, primary winding resistance and decoupling capacitor ESR. The effects of the near field winding will be ignored due to its small contribution during an arc discharge. The lamp is represented by resistor *R2*, the value being determined by the operating point on the V/I discharge curve. *C1* and *C2* are the ballast and suppression capacitors respectively. *R3* represents the combined electrode resistance. The secondary winding self capacitance is ignored because it is swamped by *C1* and *C2*.

By Cramer's rule the current flowing in the primary is given by

$$I_1(s) = \frac{\begin{vmatrix} Vcc/s & sM & 0 \\ 0 & sL_2 + 1/SC_1 + R_2 & -R_2 \\ 0 & -R_2 & R_2 + R_3 + 1/sC_2 \end{vmatrix}}{\begin{vmatrix} sL_1 + R_1 & sM & 0 \\ sM & sL_2 + 1/sC_1 + R_2 & -R_2 \\ 0 & -R_2 & R_2 + R_3 + 1/sC_2 \end{vmatrix}} .$$

The primary loop current, $I_1(s)$, in the Laplace domain is given by the following single ratio

$$Vcc\ [\ s^3(R_2 + R_3)(C_1C_2L_2) + s^2(C_1L_2 + C_1C_2R_2R_3) +$$

$$\frac{}{}$$

$$R_1\ [\ s(s^4(C_1C_2/R_1)(L_1L_2 - M^2)(R_2 + R_3) + s^3(C_1/R_1)(L_1L_2 - M^2 + C_2L_1R_2R_3 +$$

$$s(C_2R_2 + C_2R_3 + C_1R_1) +$$

$$\frac{}{}$$

$$C_2L_2R_1R_2 + C_2L_2R_1R_3 + C_2L_1R_2^2) + s^2(C_1L_1R_2/R_1 + C_1L_2 + C_1C_2R_2R_3$$

$$1\ ]$$

$$\frac{}{}$$

$$+C_1C_2R_2^2 + C_2L_1R_2/R_1 + C_2L_1R_3/R_1) + s(L_1/R_1 + C_2R_2 + C_2R_3 + C_1R_3) + 1\ ]$$

If tight coupling between primary and secondary windings is achieved, *i.e.* $L_1L_2 = M^2$, then the time domain response is

$$i_1(t) = 150\left(1 - e^{-1.3\times10^4 t} + 0.23e^{-6.5\times10^5 t}\sin(3\times10^5 t + 1.9)\right) . \qquad \textbf{(5.16)}$$

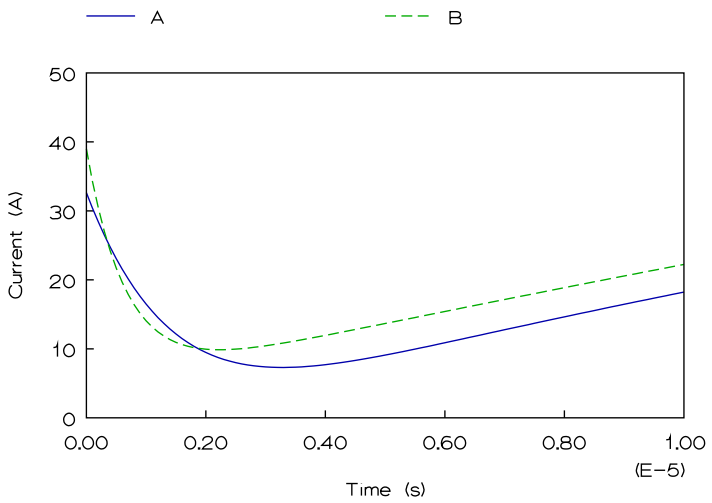

Figure 5.11: Calculated primary transient current including the suppression capacitor (A) and neglecting these components (B).

The complete transient current response is shown in Figure 5.11 above. The simplified case is include for comparison. The primary current transient response may therefore be calculated with little error by disregarding the suppression capacitor and equivalent electrode resistance.

5.8 Secondary Circuit Analysis

The use of a low duty cycle facilitates the analysis of the secondary circuit as the power dissipated in the load during switch conduction is less than the total and can be ignored initially. Load current is provided mainly by energy stored in the secondary reactive components between switch conduction periods. The switching frequency is tuned to the secondary natural frequency to provide class C operation. The load current therefore consists of single whole cycles of decaying sinusoids between conduction periods.

5.8.1 Load Current

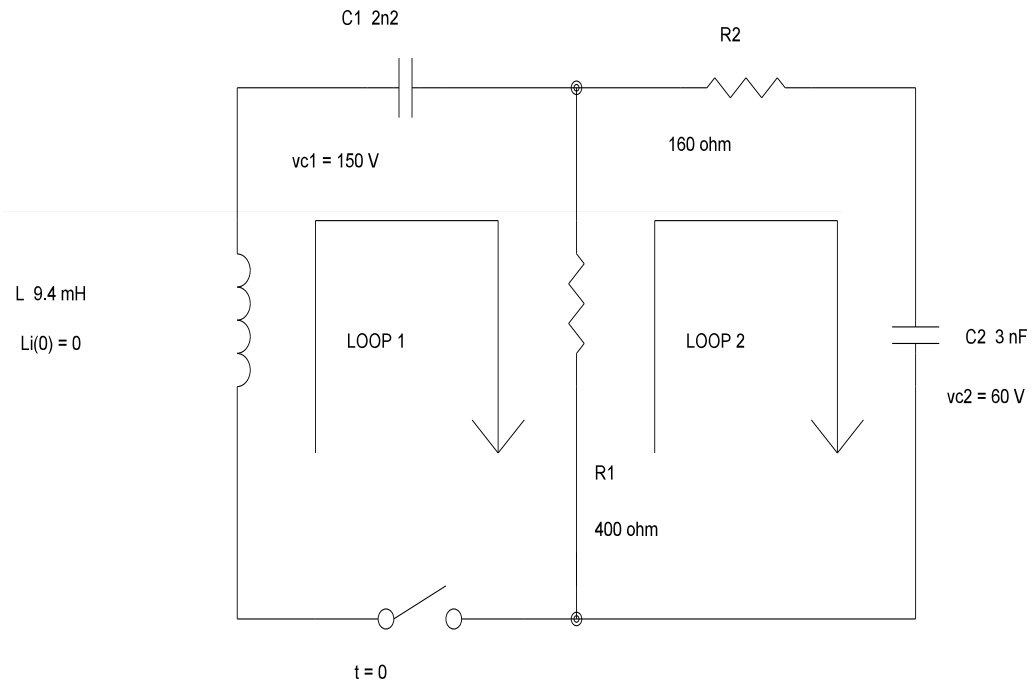

Figure 5.12: Equivalent secondary circuit with initial condition generators v_{C1}, v_{C2} and Li(0).

Figure 5.12 shows the equivalent secondary circuit with initial condition generators. In this case it is assumed that switch opening is achieved under zero current conditions so the initial conditions do not include any current component. The initial condition voltages across C_1 and C_2 are given by v_{C1} and v_{C2} respectively.

The Laplace domain expression for the current, $I_1(s)$, flowing in loop 1 is given by

$$\frac{s(C_1C_2)(v_{C1}R_1 + v_{C1}R_2 + v_{C2}R_1) + v_{C1}C_1}{s^3(C_1C_2L)(R_1 + R_2) + s^2(C_1L + C_1C_2R_1R_2) + s(C_2R_1 + C_2R_2 + C_1R_1) + 1}.$$

The time domain response of loop 1 is

$$i_1(t) = 0.074e^{-2\times10^4 t}\sin(2.3\times10^5 t + 0.07) - 0.005e^{-5.6\times10^5 t} . \quad \textbf{(5.17)}$$

The natural frequency of oscillation is 230 krads^{-1} (36.6 khz). The sinusoid envelope decrement is given by $e^{(-Rt/2L)}$. Perfect current symmetry is therefore not possible because the second current peak will be smaller than the first by a factor of

$$\frac{I_2}{I_1} = e^{\left(-\frac{\pi R}{L\omega_n}\right)} .$$

The time domain response neglecting the suppression capacitor yields a simple RLC response of

$$i(t) = 0.072e^{-2\times10^4 t}\sin(2.2\times10^5 t) . \quad \textbf{(5.18)}$$

Figure 5.13, on the following page, shows a comparison between the response of the simple case and that including the suppression capacitor. The error obtained by computing component values using the simple case is therefore minimal. The values of natural frequency and damping ratio are computed in the normal manner.

The current due to the suppression capacitor in loop 1 is negligible but the load current is the sum of the currents in loops 1 and 2. As the effective electrode resistance, of approximately 160 Ω, is not accessible in practice, it is important to note any deviation from current measured solely in loops 1 or 2. The Laplace domain expression for the current flowing in loop 2 ($I_2(s)$) is given by

$$\frac{s^2(C_1C_2Lv_{C2}) + s(C_1C_2R_1)(v_{C1} + v_{C2}) + v_{C2}C_2}{s^3(C_1C_2L)(R_1 + R_2) + s^2(C_1L + C_1C_2R_1R_2) + s(C_2R_1 + C_2R_2 + C_1R_1) + 1}.$$

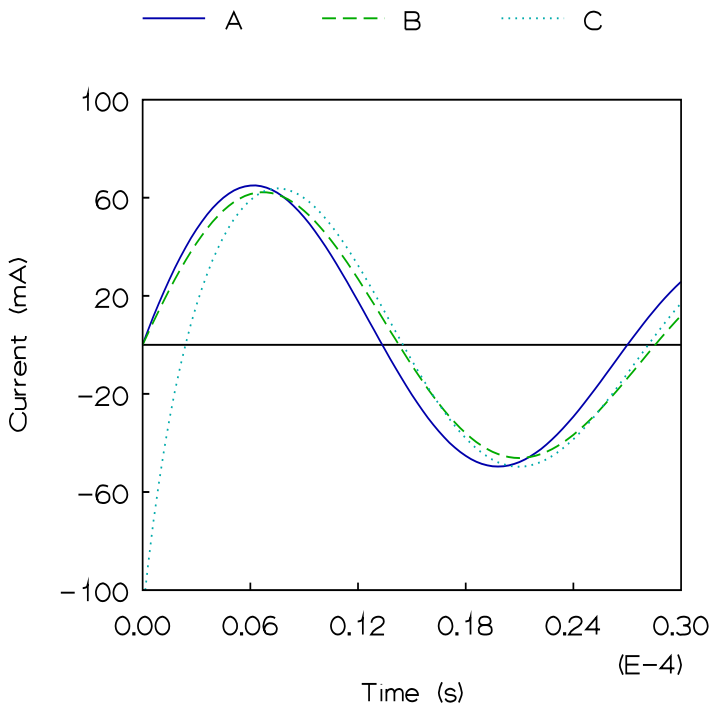

Figure 5.13: Calculated secondary current in loop 1 (A). Secondary current in loop 1 neglecting the suppression capacitor (B). Current through the load (C).

The time domain response of the transient current in loop 2 is

$$i_2(t) = 0.09e^{-5.6\times10^5 t} + 0.02e^{-2\times10^4 t}\sin(2.3\times10^5 t + \pi/2)\ . \qquad \textbf{(5.19)}$$

The sum of the two currents in the load is therefore

$$i_{LOAD}(t) = -0.09e^{-5.6\times10^5 t} - 0.02e^{-2\times10^4 t}\sin(2.3\times10^5 t + \pi/2) - 0.005e^{-5.6\times10^5 t} + 0.074e^{-2\times10^4 t}\sin(2.3\times10^5 t + 0.07) \quad \textbf{(5.20)}$$

Note in Figure 5.13 the initial load overcurrent due to the energy stored in the suppression capacitor. This current peak is given by

$$i_{peak} = \frac{peak\ suppression\ capacitor\ voltage}{lamp\ resistance + equivalent\ electrode\ resistance} .$$

It is therefore important that the energy stored in the suppression capacitor be minimised otherwise substantial lamp current transients will occur. This circuit is inaccessible as the suppression and glow starter are housed in the base of the lamp.

5.8.2 Ballast Capacitor and Secondary Voltages

By Kirchhoff, the sum of the voltages around loop 1 is given by

$$v_c + v_{load} + v_L = 0 .$$

This expression can be written in the form

$$i(t)_{load}R + L\frac{d}{dt}i(t) = -v_C(t) .$$

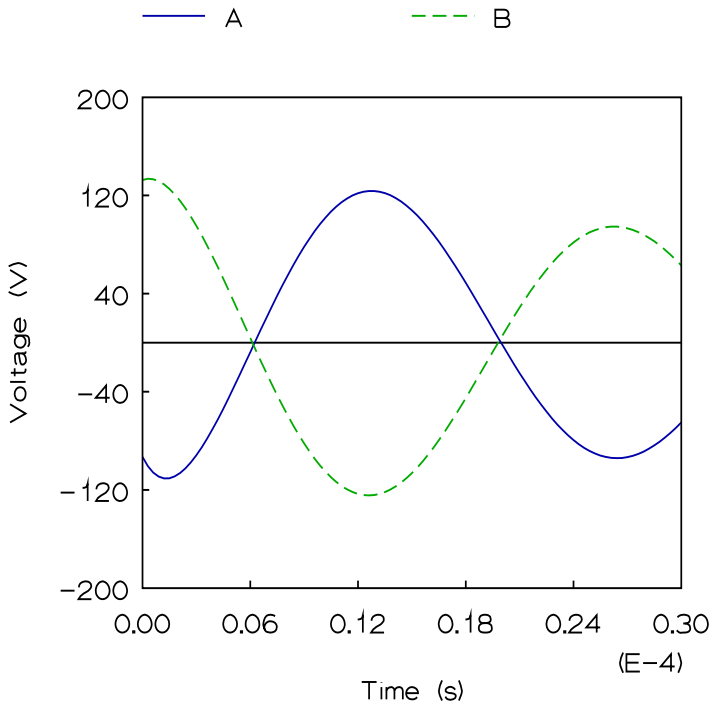

Figure 5.14: Calculated ballast capacitor voltage (A) and secondary (B) instantaneous voltages.

Figure 5.14, on the following page, shows the relationship between the ballast capacitor and transformer secondary voltages. These voltages are exactly 180° out of phase. This demonstrates classical resonant action. The secondary current lags the inductor voltage by 90° and leads the capacitor voltage by 90° so that when the energy stored in the capacitor is at its maximum, at its voltage peak, then the energy stored in the inductor is zero and *vice versa*.

5.9 Efficiency

The efficiency of a class C amplifier is given by[38]

$$\eta = \frac{\theta - \sin\theta}{4\sin\left(\frac{\theta}{2}\right) - 2\theta\cos\left(\frac{\theta}{2}\right)}, \qquad \textbf{(5.24)}$$

where Θ is the conduction angle. If $\Theta = \pi$ then the circuit will be functioning as a class B amplifier with a maximum theoretical efficiency of 78.5%. As $\Theta \rightarrow 0$, $\eta \rightarrow 1$ and so efficiency increases with decreasing duty cycle. Figure 5.15 shows that efficiencies exceeding 90% are only possible when the duty cycle is less than 0.3.

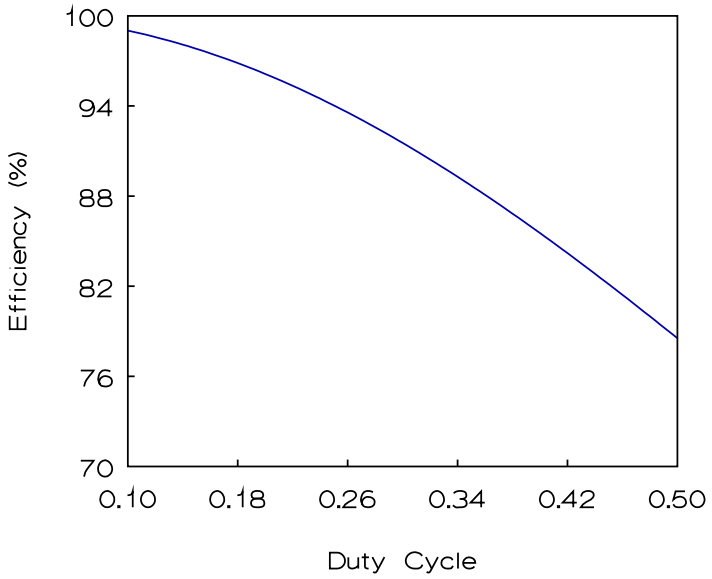

Figure 5.15: Computed maximum possible efficiency of a class C amplifier plotted against duty cycle.

As the duty cycle decreases, however, so the peak current increases, given the same output power. The design aim must be to use the lowest possible duty cycle to both improve efficiency and to place the bandwidth of current abberations outside that which can be followed by the plasma.

5.10 Summary

It has been shown that careful design can eliminate switching losses, improve efficiency and effect rapid energy conversion. This can be achieved by utilising secondary capacitance, including the lamp suppression capacitor, in the energy conversion process. The secondary capacitance could thereafter form part of a resonant circuit which would provide an almost sinusoidal lamp current.

6 Optimal Ballast Design

6.1 Circuit Description

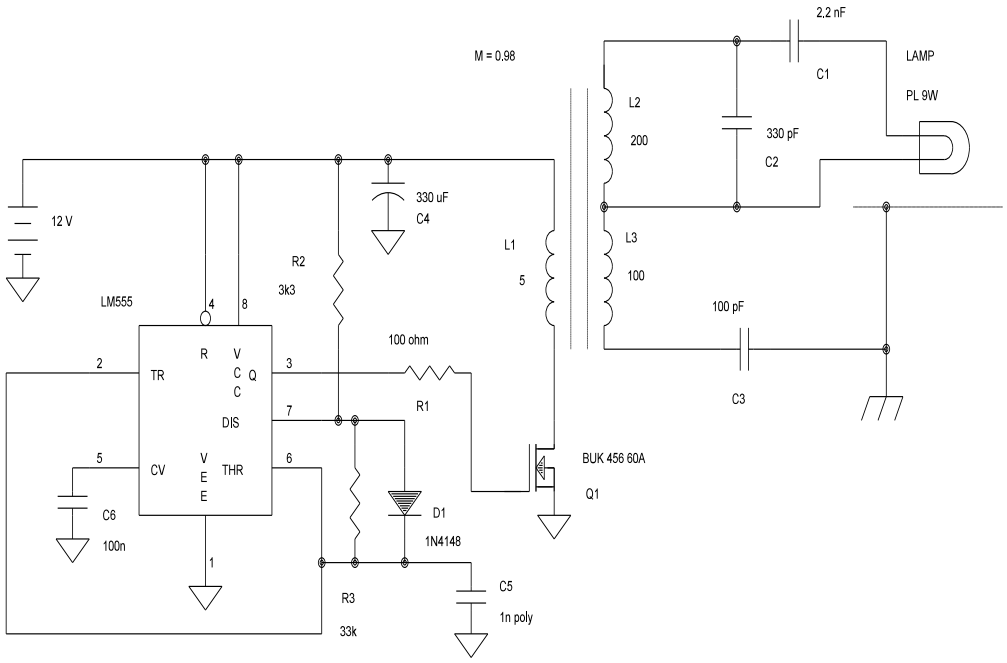

Figure 6.1: The optimal battery powered ballast.

Figure 6.1 shows the basic circuit. Housekeeping circuitry has been omitted for clarity. The circuit is similar to that described in Section 4.9 but the mode of operation and transformer details differ considerably. Whereas the circuit in Section 4.9 relies on classical flyback techniques for energy conversion, this circuit uses energy conversion techniques described in the previous chapter.

Size	Document Number	REV
A		
Date: August 1, 1995	Sheet of	

The LM 555 provides the basic oscillation frequency. L3 provides a near field voltage to assist starting. The voltage is connected to the lamp housing which is earthed. The secondary circuit is therefore elevated above earth by the near field voltage. C3 limits the capacitive coupled glow current through the lamp. C2 provides a load to the inverter in the event of lamp removal. C1 is the ballast capacitor which, together with L2, forms a resonant circuit. C4 is the supply bypass capacitor. The measured capacitance between the lamp and the chassis on the prototype is 150 pF.

An improved current waveform has been achieved by using class C operation. The switching frequency has been tuned to the natural frequency of the secondary RLC circuit and, as the circuit is underdamped, the load current is a near symmetrical sinusoid between switching periods. Waveform distortion is further reduced by using a low duty cycle. The prototype circuit switching period and conduction times are 30 μs and 3 μs respectively.

This circuit relies on the presence of the suppression capacitor to increase secondary capacitance and to heat the electrodes. This feature improves lamp life because heating is initiated immediately during starting. This also improves starting reliability because the circuit is less reliant on the glow starter closure times.

The use of a near field to assist starting provides greater flexibility in the design, as L2 need not provide excessive overvoltages for lamp ignition. This feature is particularly important when attempting to start PL 9 lamps because the dynamic resistance of their glow starters is lower than that of other PL lamps.

The battery supply of 12 V was chosen because the most popular range of sealed lead-acid batteries provide 12 V, and the techniques discussed are readily applied to other supply voltages.

6.2 Component Dependency Relationships

The conversion power in a conventional flyback inverter is given by

$$P = \frac{1}{2} L_{pri} (I_{pk})^2 f_s \ , \qquad \textbf{(6.1)}$$

where I_{pk} is the peak current at switch opening. No simple expression can describe the conversion power of this inverter because the above expression assumes that no other energy conversion processes occur during current build up in the primary winding. For this design, the energy available for conversion at switch opening is energy stored in the ballast and suppression capacitors, and some energy may be stored in the magnetic field of the transformer. The energy process is further complicated because energy is also dissipated in the load during the switch conduction period. In the ideal case no energy is stored in the magnetic field at the switch off instant. In practice this condition is attainable with temperature stable oscillator components. The energy stored in the ballast capacitor is typically ten times that stored in the suppression capacitor.

Assuming that no energy is stored in the magnetic field at switch opening (ideal case) and that all the secondary energy is stored in the ballast capacitor, then as the switch closes, the primary voltage reflected to the secondary is given by

$$V_{\text{sec}} = \frac{N_{\text{sec}}}{N_{pri}} (Vcc - V_{sat}) \ , \qquad \textbf{(6.2)}$$

where V_{sat} is the combined volt drops of switch saturation and primary circuit resistance losses. Written in terms of primary and secondary inductances

$$V_{\text{sec}} = \sqrt{\frac{L_{\text{sec}}}{L_{pri}}} \ (Vcc - V_{sat}) \ . \qquad \textbf{(6.3)}$$

The output power from the energy stored in the ballast capacitor is given by

$$P_o = \frac{1}{2} C_b (V_b)^2 f_s \ . \tag{6.4}$$

The peak voltage across the ballast capacitor can be expressed as

$$V_b = \sqrt{\frac{2P_o}{f_s C_b}} \ . \tag{6.5}$$

The peak lamp voltage in terms of output power and lamp resistance is given by

$$V_{lamp} = \sqrt{2P_o R_{lamp}} \ . \tag{6.6}$$

The secondary peak voltage equals the sum of the peak ballast capacitor and peak lamp voltages. Hence

$$\sqrt{\frac{L_{\sec}}{L_{pri}}} (Vcc - V_{sat}) = \sqrt{\frac{2P_o}{f_s C_b}} + \sqrt{2P_o R_{lamp}} \ . \tag{6.7}$$

However, the secondary circuit must operate at its resonant frequency. Therefore the secondary inductance is related to the ballast capacitance and switching frequency by

$$C_b L_{\sec} = \frac{1}{(\omega_n)^2} = \frac{1}{(2\pi f_s)^2} \ . \tag{6.8}$$

Therefore, primary inductance can be computed from

$$L_{pri} = \frac{(Vcc - V_{sat})^2}{8\pi^2 P_o f_s (1 + f_s C_b R_{lamp})} \ . \tag{6.9}$$

Note that because C_b is not yet known, the term $f_s C_b R_{lamp}$ may be omitted with little error in primary inductance. A typical value for $f_s C_b R_{lamp}$ is 0.03.

Figure 3.9 shows the dc starting characteristics with no near field. The art of ballast design

is to supply both the minimum near field current and lowest starting voltage to prolong the life of the lamp. In this case the minimum starting voltage is approximately 250 V. Lower starting voltages require excessive glow currents from the near field.

There are three requirements of the main secondary winding. It must provide the specified voltage and current for reliable glow starter operation, reliable starting and arc discharge at rated power. Reliable glow starter function is easily achieved as the glow starters will operate at 120 V rms. For optimum operating conditions the starting voltage and the arc voltage must be supplied without the need for complex circuitry. From equation (6.7) the peak voltage across the lamp can be expressed as

$$V_{lamp} = \sqrt{\frac{L_{\text{sec}}}{L_{pri}}}\left(Vcc - V_{sat}\right) - \sqrt{\frac{2P_o}{f_s C_b}} \; . \qquad \textbf{(6.10)}$$

Rearranging the above expression in terms of the ballast capacitor yields

$$C_b = \frac{2P_o}{f_s\left(\frac{L_{\text{sec}}}{L_{pri}}\left(Vcc - V_{sat}\right)^2 - V_{lamp}\right)} \; . \qquad \textbf{(6.11)}$$

For stable operation in both arc discharge and starting modes the solution of the above equation must be the same for both cases. Hence

$$\frac{L_{\text{sec}}}{L_{pri}} = \frac{P_{\text{arc}}\left(V_{ign}\right)^2 - P_{ign}\left(V_{\text{arc}}\right)^2}{\left(Vcc - V_{sat}\right)^2\left(P_{\text{arc}} - P_{ign}\right)} \; . \qquad \textbf{(6.12)}$$

This equation defines a ratio of inductances which will satisfy both starting and arc discharge conditions. The expression is sensitive to supply voltage squared, $(Vcc - V_{sat})^2$, so provision must be made for operation from a flat battery at 10 V.

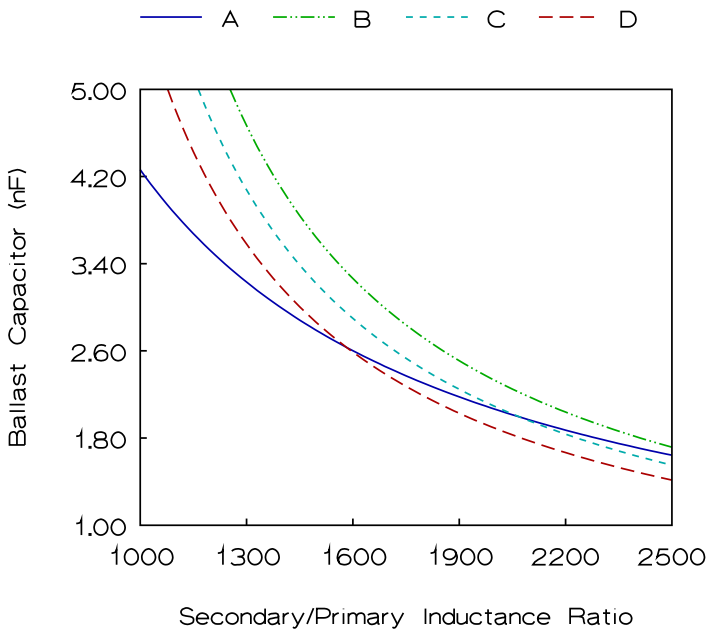

Figure 6.2: Computed ballast capacitor vs ratio of secondary to primary inductances. A: Arc discharge of 8 W. B: Starting peak voltage of 270 V. C: Starting peak voltage of 260 V. D: Starting peak voltage of 250 V.

Figure 6.2 compares the capacitor and inductance ratios for arc discharge and various starting voltage requirements. The interception of the arc discharge curve *A* and the starting voltage curves *B,C,D* defines where both starting and arc conditions will be met. It is evident that as the starting voltage requirement increases the turns ratio required increases to a greater degree. An inductance ratio of 1600 satisfies both requirements of a minimum starting voltage and a low turns ratio, to reduce manufacturing cost.

6.3 Design Example

6.3.1 Selection of Switching Frequency

The choice of switching frequency and duty cycle are the first considerations. The switching frequency is limited by excessive electrode dissipation via the suppression capacitor, and EMI considerations (>50 kHz).

If the lamp is operated at full power then the suppression capacitor current must be minimal so that the electrodes do not operate above their rated temperature. If the lamp is operated at reduced powers then this current must be increased so that the electrodes operate at rated temperature.

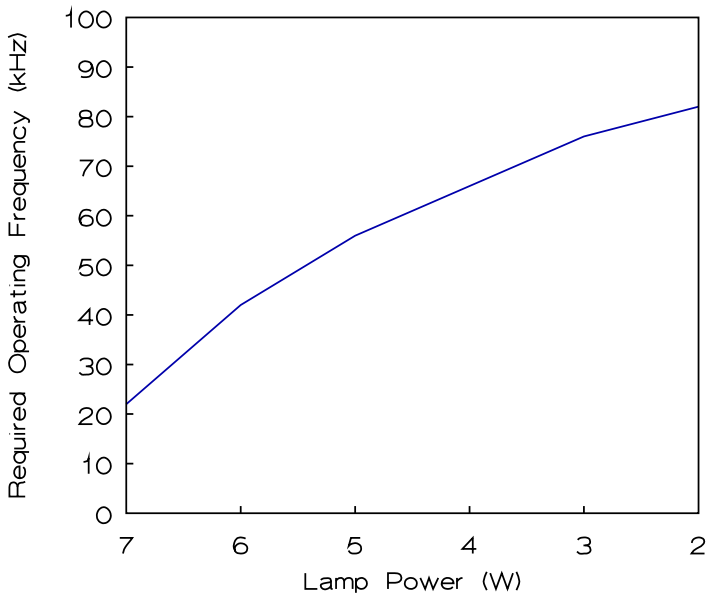

Figure 6.3: Computed operating frequency required to maintain rated electrode temperature. The rated lamp operating power is 8.2 W.

The lower frequency limit is an audible switching frequency of approximately 16 kHz.

Lamp efficiency improves with frequency and there is evidence that improvements can be gained up to 100 kHz[17], therefore the highest feasible operating frequency must be used. Increased electrode dissipation will occur, however, at any frequency above 100 Hz if the lamp is operated at full power due to current flowing through the suppression capacitor. When the supply battery is fully charged this could be a problem, but as the supply voltage drops the power to the lamp decreases from 8 W to approximately 6 W at 10 V, which is the minimum battery voltage. At 6 W an operating frequency of 40 kHz is required to provide rated electrode temperature, see Figure 6.3.

Switching frequencies in the region of 25-35 kHz suit these requirements and optimise lamp lumen efficacy (lmW^{-1}). A switching frequency of 33 kHz is selected for this design example.

It is inevitable that lamp current waveform distortion will result in class C operation due to the energy conversion period. The conduction period should therefore be kept to a minimum so that current aberrations during conversion are not followed by the discharge. Ideally, the conduction period should be less than the minimum period of ion oscillations to ensure that sputtering is minimised, but this would mean a maximum conduction period of 100 μs. In order to achieve the same energy conversion within a shorter period of time, the current amplitude must increase. This would reduce efficiency as I^2R losses would increase.

Although this design lends itself to exploring this possibility it would ultimately result in a higher unit cost. In order to reduce circuit complexity a conduction period of 3 μs was selected for this design. Pulse widths below this value require careful design to reduce primary inductance and increase primary transient currents. Higher transient currents result in increased supply bypass capacitor dissipation and higher core flux densities.

6.3.2 Calculation of Primary Inductance

The output power required (P_o) to provide rated lamp dissipation at high frequency is 8 W[9]. The battery supply voltage (Vcc) is 12 V and the volt drops (V_{sat}) around the primary circuit are estimated to be 1 V. As the chosen secondary resonant frequency (f_s) is 33 kHz, the required value of primary inductance (L_{pri}) computed from equation (6.9) is therefore 5.8 μH.

6.3.3 Calculation of the Turns Ratio

The minimum required starting voltage (V_{ign}) from Figure 3.9 is 250 V. The power dissipated in the glow starter (P_{ign}), computed from the starting lamp voltage and the starter equivalent model, is 5.6 W. The required lamp power (P_{arc}) is 8 W. The corresponding peak lamp voltage (V_{arc}) during arc discharge, from Figure 3.4, is 85 V. From equation (6.12) the required ratio of secondary to primary inductances is therefore 1580. As the primary inductance is 5.8 μH, the secondary inductance is 9.2 mH and the turns ratio is 40.

6.3.4 Calculation of the Near Field Turns Ratio

The near field voltage is only relevant during starting. However, during starting the secondary load (L2) varies according to the glow starter state. Energy translation during starting is not achieved solely through secondary capacitive voltage as the inverter functions more like a classical flyback inverter during this time. Energy storage elements during starting include the suppression capacitor, ballast capacitor and the secondary winding. The rms value of the near field voltage can not therefore be easily computed.

The required turns ratio for the prototype was derived by experiment. The capacitance between the lamp and the chassis was measured to be 150 pF and the maximum glow

current permitted is 10 mA[17]. A near field winding of 100 turns provided an adequate voltage during ignition, but a series capacitor of 100 pF is required to limit the glow current below 10 mA. The near field to primary inductance ratio of 400:1 should satisfy most requirements.

6.3.5 The Ballast Capacitor Value

Using equation (6.11), the required ballast capacitor value is 2.5 nF. The nearest standard value is 2.2 nF. The ballast capacitor value can be checked using equation (6.11) during either starting or arc discharge conditions.

6.3.6 Calculation of the Peak Primary Current

Energy is transferred from the primary circuit to the ballast capacitor during every switching cycle. Assuming that the primary current pulse is an impulse, *i.e.* zero width, then

$$\frac{1}{2} L_{pri} \left(I_{pri}\right)^2 = \frac{1}{2} C_b \left(V_b\right)^2 . \qquad \textbf{(6.13)}$$

Hence the peak primary current expressed in terms of output power is given by

$$I_{pri} = \sqrt{\frac{2\ P_o}{f_s\ L_{pri}}} . \qquad \textbf{(6.14)}$$

The calculated peak primary current, for an output power of 8 W at 33 kHz, with a primary inductance of 5.8 μH, is 9 A.

6.4 Magnetic Circuit Design

6.4.1 Theory

The relationship

$$N_{\text{sec}} = N_{pri}\left(\frac{V_{\text{sec}}}{V_{pri}}\right), \tag{6.15}$$

may be used to determine winding ratios for this inverter. The inverter charges the ballast capacitor to a voltage of approximately

$$V_b = Vcc\left(\frac{N_{\text{sec}}}{N_{pri}}\right). \tag{6.16}$$

The total energy, stored mainly in the ballast capacitor, is then dissipated in the load. However, the fluorescent lamp ballast must function reliably with different loads, *viz.* no load (lamp removed), high impedance or capacitive loads during starting, short circuits whilst the glow starter closes and quasi resistive loading during arc conduction. Under some of these conditions *viz.* starting and lamp absent, the instantaneous secondary voltage ($v_{sec}(t)$) is given by

$$v_{\text{sec}}(t) = -M\frac{d}{dt}\left(i_{pri}\right), \tag{6.17}$$

where M is the mutual inductance and i_{pri} is instantaneous primary current. In these cases the secondary voltage is determined by the bandwidth of the primary current. The secondary voltage is then only limited by parasitic capacitance and leakage resistance. This is an important consideration in the development of flyback fluorescent lamp inverters as thousands of volts may be generated when no lamp is present leading to interwinding breakdown, switching device overvoltage, intertrack arcing and changeover relay failure. These considerations place an upper limit on the turns ratio.

It is also important that the core does not saturate under any load conditions. Under conditions of core saturation the primary inductance reduces sharply as the permeability of the magnetic circuit reduces to that of free space. This leads to a rapid increase in current. Other considerations in core selection are window area and cost. The high turns ratios and interwinding insulation requirements normally associated with lamp inverters, necessary for starting, preclude the use of small bobbins.

6.4.2 Core Selection

The E20 series bobbin was too small for any of the attempted winding configurations so the E25 series is used. The core material (type J2) was chosen for financial reasons as this seems to be a popular choice of manufacturers from the Far East. The maximum power throughput for the E25 core at 100 kHz is 50 W, and as this application requires a throughput of only 8 W, core dissipation is not a problem. The core has the following specifications:

Initial Permeability (μ_i):	2800
Working frequency:	< 0.4 MHz
Maximum flux density (B_{max}):	0.5 T
A_L value:	2.3 μH
Effective area (A_e):	52.5 mm^2

For operation in only one quadrant of the B-H characteristic the operating flux density must be limited to[30]

$$B_{opp} \leq 0.4\ B_{\max} \ . \qquad \textbf{(6.18)}$$

The maximum operating flux density must therefore be limited to 0.2 T.

The A_L of a core is related to the inductance (L) of a winding with N turns, with no core air gap (tightly clamped), by

$$L = N^2 A_L \,, \tag{6.19}$$

where

$$A_L = \frac{\mu_0 \mu_r A_e}{l_e} \,. \tag{6.20}$$

The constants μ_0, μ_r, A_e and l_e are the absolute permeability of free space ($4\pi x10^{-7}$ Hm^{-1}), relative permeability of the core, effective core cross sectional area and effective magnetic path length respectively.

The A_L values are only specified to an accuracy of 25% and its value varies with temperature, magnetic field strength and frequency. Over a temperature range of 0 to 100°C the initial permeability, *i.e.* at a low flux density, may increase by 50%. The energy conversion in this case does not contribute significantly to the core temperature due to the low conversion power.

The permeability reduces at frequencies above 400 kHz. Although the switching frequencies used here are below 100 kHz, the current pulse has a bandwidth of approximately 300 kHz.

In order to swamp ferrite permeability variations and reduce manufacturing dispersion, an air gap is introduced into the magnetic circuit. The length of the air gap depends upon the application, but a prerequisite is that it is repeatable. It is not practical to compute a value for the air gap and then proceed to find the correct thickness material. The air gap should be a material which is not compressible or else production runs will see large performance variations.

In the prototype the air gap is made from two pieces of transformer insulating tape in each leg of the core. The air gap is therefore a total of four pieces of transformer insulating tape. The total measured air gap length of four pieces of transformer winding tape is 0.4 mm.

It is also easiest to determine what the new A_L value is by measurement than by calculation, because small errors in air gap measurement result in large errors in computation. By winding approximately 20 turns onto the core with the proposed air gap the new A_L value is readily determined. The new measured air gap A_L value on the prototype is 230 nH. Using equation (6.19), five turns is required to achieve a primary inductance of 5.8 μH.

The maximum flux density is given by

$$B_{\max} = \frac{I_{pri}\, A_L\, N_{pri}}{A_e} \quad . \tag{6.21}$$

In this case the computed maximum operating flux density is 0.2 T, which is equal to the maximum permissable flux density calculated from equation (6.18) above. These values were confirmed during the design of the prototype by using Hanna Curves[30].

As the required primary to secondary turns ratio is 40, the secondary winding inductance, using the new A_L value of 230 nH, is 9.2 mH.

6.4.3 Wire diameters

The peak primary current is approximately 10 A. In order to reduce copper losses 0.63 mm diameter wire with a resistance of 0.055 Ωm^{-1} is used in the prototype. As the primary wire length is 350 mm the calculated resistance of the primary is 0.019 Ω, which will result in a voltage drop of 0.2 V. Besides reducing efficiency, the primary resistance also reduces the effective supply voltage. The primary copper loss at a peak current of 10 A and a duty cycle of 0.1, is 190 mW.

The secondary wire diameter is chosen so that voltage between adjacent winding layers is less than the puncture voltage of the enamel insulation. The need for additional interlayer insulation is therefore avoided.

6.4.4 Equivalent Transformer Model

The ideal transformer has a coupling coefficient of unity, no leakage reactances and no self capacitance. In reality these anomalies can have a profound effect upon the function of this circuit due to the wide bandwidth of conversion frequencies. It is therefore important to measure the transformer parameters accurately for modelling and design purposes.

The number of primary, main secondary and near field secondary turns are 5, 200 and 100 respectively. The measured total secondary self capacitance across both secondaries on the prototype is 20 pF. The secondary self capacitance referred to the primary is therefore 74 nF. The measured inductances of the primary, main secondary (n = 200) and near field secondary (n = 100) are 6 μH, 9.4 mH and 2.3 mH respectively.

The primary leakage inductance is measured by shorting the secondary and swamping primary self capacitance with a capacitor of known value. The resonant frequency of the drain voltage is then related to the primary leakage inductance. This was measured to be approximately 400 nH. The energy stored at a peak current of 10 A is therefore 20 μJ. The switching device must therefore be capable of dissipating this energy during overvoltage breakdown. The main secondary (200 turns) leakage inductance was measured to be 36 μH. This value of leakage inductance is inconsequential compared to the secondary inductance.

6.4.5 Measurement of Mutual Inductance

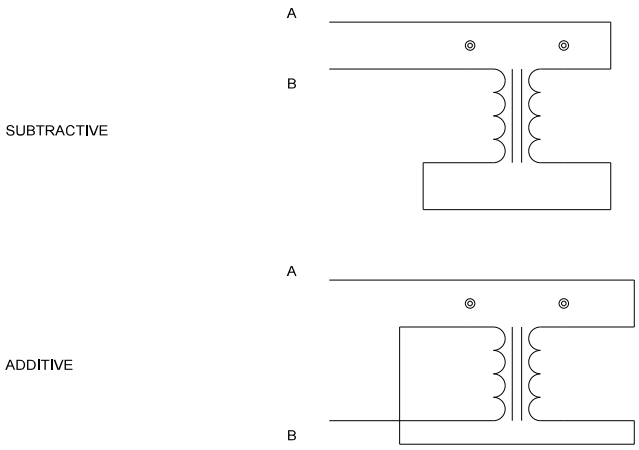

Figure 6.4: The connections used to determine mutual inductance.

The mutual inductance between the primary and secondary of the transformer is an important parameter in the development of the inverter model. Two methods of measuring mutual inductance are presented because the large turns ratio complicates measurement.

One method of mutual inductance measurement entails the measurement of cross connected total inductances. The inductance across the terminals in the subtractive connection in Figure 6.4 is given by

$$L_{subtractive} = L_{pri} + L_{\sec} - 2M\,, \qquad \textbf{(6.22)}$$

as the magnetic fields produced by the two windings oppose one another. The inductance across the terminals of the additive connection is given by

$$L_{additive} = L_{pri} + L_{\sec} + 2M\,. \qquad \textbf{(6.23)}$$

In this design where L_p and L_s are 6 μH and 9.4 mH respectively, measurement using both

connections yielded values between 275 μH and 195 μH. The reason for the measurement inaccuracy was that the mutual inductance was swamped by the secondary inductance.

In order to obtain more accuracy another method was used. The relationship between mutual inductance and primary current in a transformer is given by

$$v_{\text{sec}} = -M\frac{d}{dt}\left(i_{pri}\right), \tag{6.24}$$

where v_{sec} is the instantaneous secondary voltage, M is the mutual inductance and i_{pri} the instantaneous primary current. If the primary current is sinusoidal then

$$v_{\text{sec}} = -M\frac{d}{dt}\left[I_{pk}\sin(\omega t)\right], \tag{6.25}$$

which reduces to

$$v_{\text{sec}} = -M\omega I_{pk}\cos(\omega t), \tag{6.26}$$

where I_{pk} is the peak primary current. At t = 0 the value of M equals

$$M = -\frac{v_{\text{sec}}}{\omega I_{pk}}. \tag{6.27}$$

This equation facilitates measurement because at t = 0 both primary current and secondary voltage waveforms are at their maximum amplitudes. The value of mutual inductance for the final iteration transformer, measured using this method, is 233 μH. The coupling coefficient of the windings is therefore approximately 0.98. If the coupling coefficient is less than 0.98 then the peak primary current is reduced and conversion power decreases. Conversely, if the coupling coefficient exceeds 0.98 then switching and circuit I^2R losses will increase. The primary transient current response was observed using different coupling

coefficients in order to verify conformance to the theory presented in Chapter 5. A coupling coefficient of 0.98 is achieved by using one layer of transformer insulating tape between the primary and secondary windings. This provides optimum efficiency with the present gate drive circuitry.

6.5 Component Selection

6.5.1 Switching Device

BJT's are unsuitable for this design due to restrictions of current gain. The current gain of BJT's decrease when the device is used near to or in saturation. Under these circumstances their current gain, *i.e.* their forced gain[29], may be in the region of 3 to 10. Using this design concept primary peak currents can exceed 10 A and may approach 20 A. The base current will then be between 1 and 6.7 A. Also, high switching speeds are essential for high efficiency.

The FET used in the prototype is a Philips BUK 456-60A. The TO-220 package device is well suited for this application with the following specifications

Maximum drain-source voltage (V_{DS})	60 V
Maximum continuous drain current (I_D)	52 A
Maximum peak drain current (I_{DM})	208 A
Junction to ambient thermal resistance (θ_{ja})	60 KW^{-1}
Drain-source on-state resistance ($R_{ds\ on}$)	0.028 Ω
Input capacitance (C_{iss})	2 nF
Maximum switching delay	220 ns
Peak reverse drain current (I_{DRM})	208 A

This device is fairly common and has an equivalent manufactured by International

Rectifier, the IFRZ 34.

6.5.2 Supply Bypass Capacitor

To obtain high efficiency, consideration must be given to potential losses in the primary circuit caused by high transient currents. The bypass capacitor I^2R_{ESR} losses can account for a considerable loss of power. The Equivalent Series Resistance (ESR) of a capacitor at low frequencies is given by

$$ESR = \frac{\tan \delta}{\omega C} \quad [\Omega] \ .$$

The dissipation factor, tan δ, for the 330 μF 35V capacitor used is 0.16 at 100 Hz. The bandwidth of the current pulse is approximately 330 kHz and so, accounting for the rise in dissipation factor with frequency, the ESR at 100 kHz is 18 mΩ. The computed capacitor dissipation is 180 mW with a primary peak current of 10 A and a duty cycle of 0.1.

7 Measured Ballast Performance

7.1 Measurement Techniques

As power conversion efficiency is an important parameter, it was necessary to measure temperature rise of the switching element and supply bypass capacitor to confirm measurements. The temperature rise of the FET was monitored because the thermal resistance of the other devices was not known, and the switching device losses usually account for most of the total circuit losses in inverters. The thermal resistance of the FET is specified as: $\Theta_{j\text{-}a} = 60\ KW^{-1}$. The device dissipation could simply be computed as

$$P_{device} = \frac{(T_{device} - T_{ambient})}{\theta_{j-a}} . \qquad \textbf{(7.1)}$$

A bare thermocouple junction (FLUKE) was pressed onto the FET, with a blob of heat sink paste. The measurement point on the FET was the metal tab as it offered the lowest thermal resistance to the thermocouple. Consideration was given to ensure that both minimal heat was conducted from the FET and that the device radiation was not significantly impaired.

The accurate measurement of switching device current also required careful consideration. In order to reduce the volt drop, and hence its effect on circuit operation, a 180 mm length of 0.63 mm diameter wire was first used (= 10 mΩ). However, even if the wire was wound in a bifilar arrangement, the resultant waveforms were unacceptably differentiated due to inductance. The ultimate method used to obtain accurate current waveforms was to use twenty, one ohm resistors in parallel (= 50 mΩ) in the primary circuit. The oscilloscope probe was connected as close as possible either side of one of the resistors.

7.2 Performance with a Resistive Load

The performance of the final circuit was evaluated with both resistive and lamp loads. The aim of the former was to facilitate modelling and hence understanding of the circuit.

7.2.1 Test Method

The network shown in Figure 2.11 was used to simulate the lamp. The current sensing resistor was placed in series with the complete network so current measurement would include current flowing through the suppression capacitor. The supply voltage used in all cases was 12 V. To simulate the lamp during arc discharge at full power, a 450 Ω resistor was used. This corresponds to the plasma resistance of the lamp at a power of 8 W, as shown in Figure 3.5. The electrodes were simulated by a single 150 Ω resistor.

7.2.2 Results

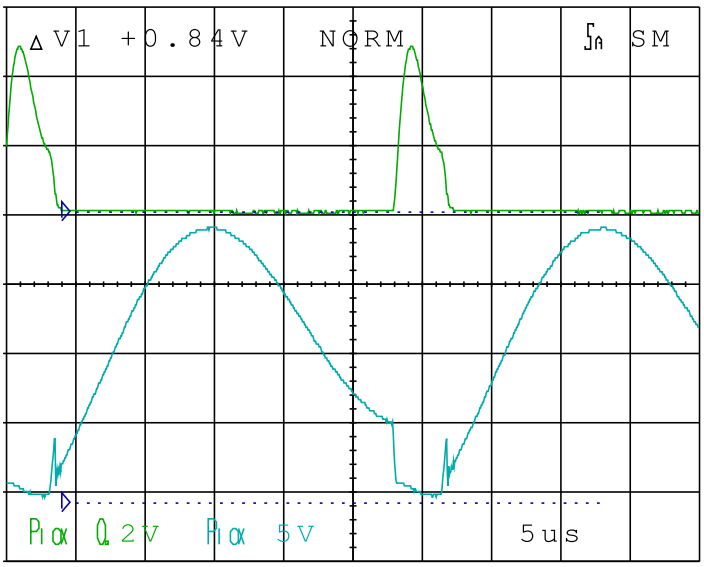

Figure 7.1: Measured primary current (upper trace) and voltage (lower trace) waveforms with a 450 Ω load.

Figure 7.1 shows the primary current, upper trace across 50 mΩ, and drain voltage waveforms. The dashed cursors indicate zero for their respective traces. The drain current peaks at 10 A and drops to 3.6 A at the switch opening. The rise time of the leading edge of the current pulse is approximately 0.5 µs, being limited by the gate drive circuit and primary leakage inductance. The drain voltage is offset from zero volts due to the current sensing resistor in the FET source circuit. During the current peak, the drain voltage is approximately 1 V. This translates to an FET `on' resistance of 100 mΩ, which is well above the specified value of 30 mΩ. The reason for this discrepancy is the limited gate voltage rise time. Although the gate threshold voltage for the FET is 4 V, the FET does not achieve 30 mΩ `on'

resistance until the gate voltage is above 8 V. The gate voltage is internally limited by the 555 to approximately 10 V, and takes some time to reach 8 V, due to internal slew rate

limitations and the FET gate capacitance load. The output of the 555 must drive the gate-source capacitance (C_{gs} = 2 nF) and the gate-drain capacitance (C_{gd} = 1 nF). Although the output impedance of the LM 555 is low, it is prone to erratic operation with capacitive loads. A 100 Ω resistor is the lowest gate series resistance tolerated by the 555. The time constant of the gate drive circuit is therefore 0.3 μs. With a primary leakage inductance of 400 nH the FET drain current rises to 2 A by the time the device has turned on completely, *i.e.* zero volts. Increasing the mutual inductance or using series drain inductance does not improve switching appreciably due to a distorted gate drive pulse from the 555. A method of improving the efficiency would be to reduce the switching losses during turn on by inserting a current amplifier between the 555 and the FET.

The initial peak current has a maximum theoretical value, see Chapter 6, of

$$I_{pk} = \frac{Vcc}{R_{ds\ on} + C_{ESR} + R_{circuit} + R_{pri}} \equiv 140\ A\ , \qquad \textbf{(7.2)}$$

assuming no secondary resistance, zero energy initial conditions and no primary leakage inductance, *i.e.* perfect transformer coupling. The maximum theoretical current, in this case, can be obtained by extrapolating the current negative slope to the *y* axis. The current would intercept the *y* axis at only 16 A because the circuit initial conditions reduce the primary current amplitude.

The drain voltage between switching periods consists of the reflected secondary voltage superimposed on the supply voltage, but 180° out of phase. The secondary voltage between switching periods is therefore

$$15\ V_{p-p} \times \frac{200}{5} \approx 600\ V_{p-p}\ . \qquad \textbf{(7.3)}$$

The small voltage overshoot accompanying switch off is due to the primary leakage

inductance. The value of this primary leakage inductance was measured to be 400 nH. The energy stored in the leakage inductance at switch off is therefore 3.2 μJ. The maximum drain-source voltage for the FET is 60 V, a figure never exceeded under any conditions. However, in the event of the drain voltage being exceeded then the energy dissipated during avalanche breakdown must be contained within certain limits otherwise device destruction could result.

The BUK 456-60A has no specified avalanche limiting energy, but a similar device, the BUK 455-100A is rated at 100 mJ. Perhaps it was an oversight on behalf of the manufacturer not to quote a figure for the BUK 465-60A, but for this circuit the leakage inductive energy is well below the 100 mJ rating.

The duty cycle is

$$D = \frac{t_{on}}{T_S} = \frac{3\ \mu s}{29\ \mu s} \approx 0.1\ . \qquad \textbf{(7.4)}$$

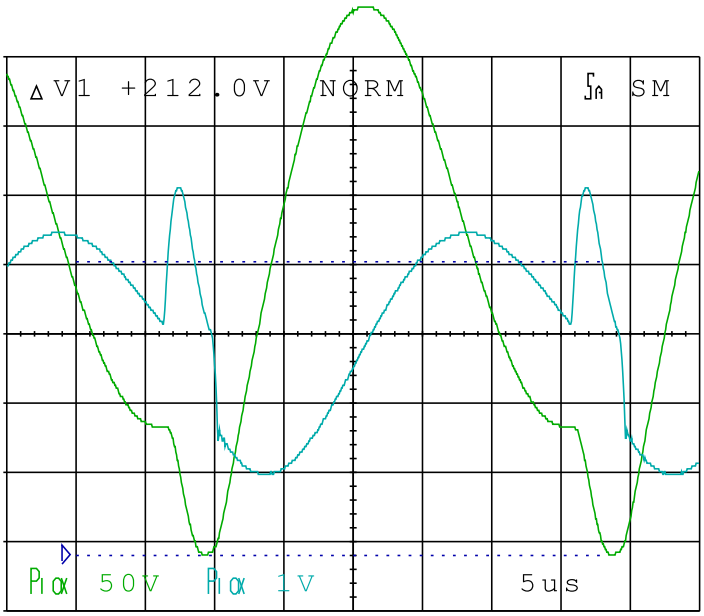

Figure 7.2: The larger waveform shows the secondary voltage (x2), the upper dashed line indicates zero volts. The smaller waveform shows the load current (measured across 10 Ω), the centre graticule indicates zero amperes.

Figure 7.2 shows the instantaneous secondary voltage and current waveforms. At the instant of switch opening the primary current is 3.6 A. The primary inductive energy at the instant of switch opening is therefore

$$\frac{1}{2} L_{pri} I^2 = \frac{1}{2} \cdot 5.8\times10^{-6} \cdot (3.6)^2 = 38\ \mu J \ . \qquad \textbf{(7.5)}$$

Because the primary current is interrupted as the switch opens, the secondary current must change by 0.1 A to maintain the same stored energy. The instant of switch opening coincides with the secondary negative voltage peak. The rapid secondary current change, visible on the current waveform, occurs at this instant. The energy stored in the secondary at the instant of switch opening is therefore approximately 40 μJ.

The secondary voltage was measured via a voltage divider (2:1) to protect the oscilloscope from overvoltages. Compensating capacitors were not used in order to offer maximum transient protection to the oscilloscope. The voltage waveforms are therefore slightly bandwidth limited which resulted is low voltage measurements.

The secondary voltage reaches a minimum of -424 V during switch conduction (indicated by the voltage between the two cursors, multiplied by two). The peak voltage across the ballast capacitor is therefore the secondary voltage minus the load voltage which is -60 V. The ballast capacitor voltage is therefore -364 V. At the instant of switch opening the ballast capacitor energy is

$$E_b = \frac{1}{2} C_b V^2 \approx 150\ \mu J\ . \qquad \textbf{(7.6)}$$

However, at the end of every cycle the ballast capacitor voltage is not zero, and so all the energy is not used. The net energy supplied by the ballast capacitor during the cycle is therefore approximately 120 μJ.

The energy supplied by the suppression capacitor during the cycle is approximately 10 μJ.

During switch conduction, energy is supplied to the load. The current waveform is approximately sinusoidal so the energy supplied is

$$E_{sw} = \frac{(V_{load})^2}{2R_{load}} t_{on} \approx 38\ \mu J\ . \qquad \textbf{(7.7)}$$

The combined dissipated energies are 208 μJ and so the power dissipated in the load is

$$P = E_{total} f_s = 208\ \mu J \times 34\ kHz = 7.1\ W\ . \qquad \textbf{(7.8)}$$

The measured input power from the dc supply is 8.6 W (12 V @ 0.72 A). The circuit efficiency is therefore

$$\eta = \frac{output\ power}{input\ power} \approx 83\% \ . \qquad \textbf{(7.9)}$$

This efficiency calculation is pessimistic due to errors incurred in waveform voltage measurement.

The temperature of the FET rose to 41°C. As the ambient temperature was 25°C, the temperature increase was 16°C. Using $\Theta_{j\text{-}a} = 60KW^{-1}$, the FET dissipation was 266 mW. The temperature of the bypass capacitor rose by 10°C, due to dielectric loss, but no thermal resistance figures were specified by the manufacturer. The temperature rise of the FET was surprisingly low. To calibrate the results the author measured his body temperature, approximately 37°C, and confirmed that the FET temperature was comparable to normal body temperature. The efficiency of the inverter is thus very high. Besides high efficiency being desirable to extend battery life, it also translates to lower manufacturing cost, as the FET does not require any form of heat sinking.

The natural frequency of the secondary circuit can been calculated from the secondary current waveform. The natural frequency can also be computed, with a small error, by simply using the secondary inductance (9.4 mH) and the ballast capacitor (2.2 nF). For an under damped LCR network the natural frequency is given by

$$f_n = \frac{1}{2\pi\sqrt{LC}} \ . \qquad \textbf{(7.10)}$$

The natural frequency of the secondary circuit is therefore approximately 35 kHz. It is important to operate this circuit around the secondary circuit natural frequency to reduce

current harmonics and to improve efficiency. As the secondary current waveform is nearly sinusoidal between switching periods, current and hence power calculations can be simplified. For example, the load current from Figure 7.2 is approximately 180 mA peak and so the rms load current is 127 mA. The power dissipated in the 450 Ω resistor is therefore approximately 7.3 W. This figure compares well with that computed in equation (7.8) above. The balance of the input power is dissipated in the FET, supply bypass capacitor and the equivalent electrode resistor.

7.2.3 Power Conversion Efficiency

The rms to dc converter described by Richman[32] was used to measure the rms value of the inverter output current. By using high slew rate op-amps the converter bandwidth was extended to 3 MHz and so the inverter output current aberration during switch conduction is therefore included in the rms conversion computation. The power conversion efficiency from a 12 V supply, using a 450 Ω load resistor is 85%.

In order to optimise efficiency it is imperative to describe all circuit losses. FET dissipation, ferrite iron losses, drive circuit power, copper losses and supply bypass capacitor dielectric losses account for over 95% of the total power loss.

The FET temperature rise corresponds to a dissipation of 266 mW. This power loss is mainly due to conduction losses. It is possible to reduce the FET dissipation by achieving switch off under zero current, but power conversion efficiency reduces due to an increase in total circuit I^2R losses.

The core dissipation can be computed from a family of generic ferrite volumetric loss versus frequency curves by Williams[30]. In this case the maximum flux density of 0.2 T and an operating frequency of 34 kHz yields a volumetric loss of 100 $mWcm^{-3}$. The effective volume of the E25 core is 3.02 cm^{-3} so the ferrite dissipation is approximately

300 mW.

The LM555 quiescent current is 12 mA which corresponds to a 144 mW power loss, neglecting transitional output power.

The primary and secondary copper losses are 180 and 80 mW respectively.

The equivalent series resistance of the supply bypass capacitor at 300 kHz is approximately 18 mΩ. The capacitor dissipation is therefore 180 mW.

The total circuit losses are therefore 1150 mW. The dc input power is 8.6 W so the maximum possible power conversion efficiency is approximately 87%.

Improvements in efficiency could be achieved by reducing the core flux density. As the iron losses increase nonlinearly with increasing flux density, by halving the peak flux density the losses could be reduced by a third. This could only be achieved by increasing the air gap and increasing the turns ratio which would increase the copper losses. A less cost effective, but more efficient solution, is to increase to core size from E25 to E30. The larger core could operate at a lower flux density with the same number of turns.

The primary circuit copper losses could be reduced by increasing the surface area of the winding to counteract skin effects. This could be achieved by either using a thicker gauge wire or by using stranded wire. The secondary circuit losses could be reduced by simply using thicker wire.

By effecting these improvements, improving the gate oscillator drive and using a lower ESR capacitor, an efficiency of 90% is clearly achievable. This inverter's high power conversion efficiency is attributed to a reduction in switching device losses. The FET losses account for only 23% of the total circuit losses.

If the switching losses are reduced to zero then the only power dissipated in the FET would be that due to conduction losses. The rms current during switch conduction is approximately 10 A (see Figure 7.1). The FET $R_{DS\,(on)}$ is 30 mΩ. The averaged theoretical power loss would therefore be

$$P_{loss} = \left(i_{rms}\right)^2 R_{DS\,(on)}\, t_{on}\, f_s \approx 280\ mW\ .$$

This figure is close to that obtained when the circuit was operating under non ideal conditions and therefore indicates that the temperature measurements were slightly optimistic. However, the temperature of the FET in the prototype circuit was far cooler than any of the switching devices of the circuits evaluated in Chapter 4, whilst converting similar powers. The maximum theoretical power conversion efficiency with a duty cycle of 0.1, from Figure 5.15, is greater than 97%. Due to the low temperature rise of the FET, under all operating conditions, no heat sink is required.

7.2.4 Core Saturation

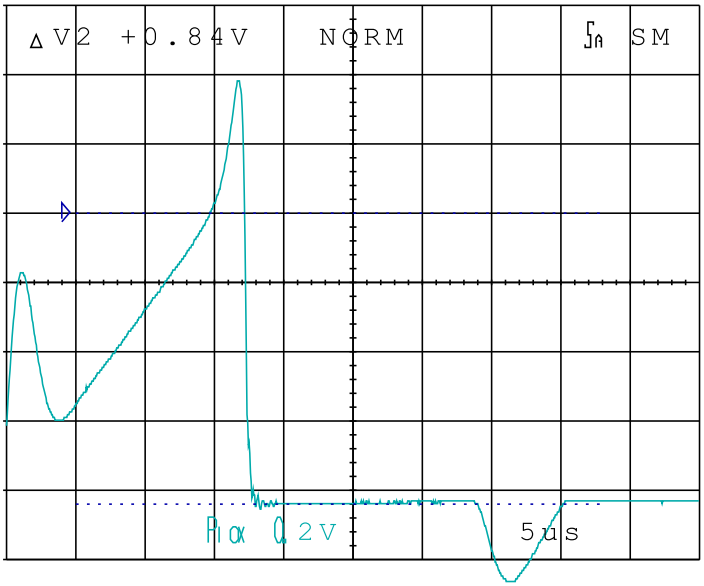

Figure 7.3: Measured primary current with increased conduction time illustrating the rapid increase in current at core saturation.

Figure 7.3 shows the primary current when the conduction time is extended to 18 μs. The switching frequency has been reduced to 2.2 kHz to ensure zero initial energy conditions. The supply voltage was reduced to 8 V to limit the peak drain voltage. Each vertical division represents 4 A. The characteristic initial overcurrent is clearly visible with a current minimum at 3.5 μs. The current gradient 5 μs after $t=0$ is 12 A/10 μs or 1.2 Aμs^{-1}. This corresponds closely to the theoretical slope of

$$\frac{d}{dt}i(t) = \frac{Vcc}{L_{pri}} = 1.3\ A\mu s^{-1}\ . \qquad \textbf{(7.12)}$$

After 15 μs the current increases rapidly, *i.e.* above 16 A, due to core saturation. The optimum performance will be obtained if the switch is opened at 3.5 μs where the current is lowest, thereby minimising switching losses.

7.2.5 Verification of the Lamp Model

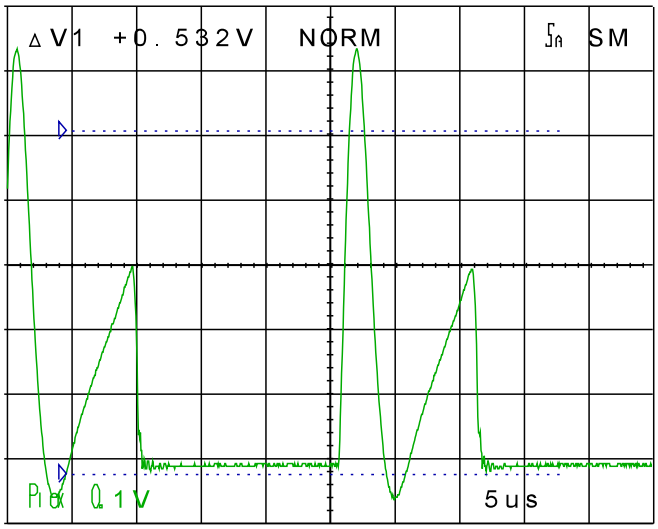

Figure 7.4: Measured primary current at high switching frequency illustrating the negative current phenomenon due to circuit initial conditions.

Figure 7.4 is included to illustrate that negative primary current excursions are possible. For this test the conduction period was increased to 11 μs and the switching frequency was increased to 40 kHz. The lower cursor position corresponds to zero amperes. Note the negative current excursion of -1 A after the initial current peak. Initial conditions can therefore be tuned to obtain zero switching losses at the end of the conduction cycle in the manner described in Section 5.6 above.

It should be noted, however, that excessive negative primary voltage excursions could cause the FET reverse limiting diode to conduct. This may reduce power conversion efficiency and increase EMI.

7.3 Performance with the Fluorescent Lamp

The following discharge performance measurements were conducted at an ambient temperature of 25°C with the prototype inverter. The starter components were connected to the lamp.

7.3.1 Arc Discharge Performance

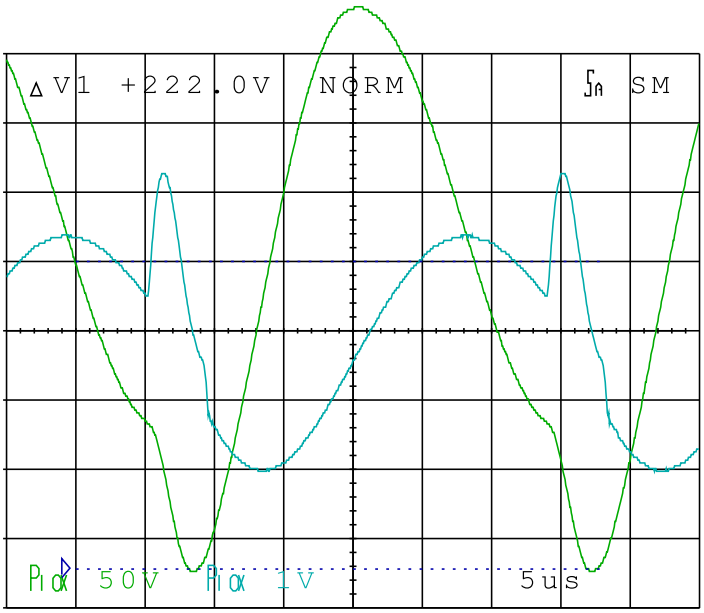

Figure 7.5: Measured secondary voltage (larger waveform) and lamp current (smaller waveform across 10 Ω) waveforms of the prototype circuit.

Zero volts, in Figure 7.5, is indicated by one division above the centre line for the larger trace and by the centre line for the smaller trace. The parameters measured after 10 minutes were:

DC input power:	8.6 W
Conduction pulse width:	3 µs
Relative luminous flux to 50 Hz performance at rated power:	100%
Switching frequency:	34 kHz
Switch dissipation:	260 mW
Bypass capacitor temperature rise:	10 K
Lamp current crest factor:	2

Lamp current distortion is considerably lower than any of the designs measured in Chapter 3. Current aberrations coincide with conduction periods and are only of 3 µs duration. The increased ion bombardment during this period will be minimal due to ion inertia. The current and voltage waveforms are almost identical to that of a resistive load shown in Figure 7.2, justifying the assumption that the lamp can be modelled as a resistor at high frequencies. The operating point on the lamp V/I characteristic, Figure 3.4, is therefore 60 V @ 135 mA.

The peak primary current during arc discharge is 9.5 A. The peak current during starting, when the starter switch open, is 16 A. The core saturates above 16 A, and so perhaps marginal headroom is allowed for component tolerances and production spread.

Shifts in chromacity coordinates were visually noted whilst varying the switching frequency or conduction period. As the crest factor increased so the lamp emission changed from its normal yellowish hue to white. This was possibly due to the phenomenon described by Polman[7], but this was not pursued any further.

The PL9 W lamp is rated at 8.2 W when operated at high frequency[9] so the lamp is operating near to rated power, approximately 90%. However, as the inverter has been designed for a battery supply, tests were also conducted to check circuit reliability below the recommended minimum lead acid voltage of 10.5 V. This minimum voltage has been specified by the battery manufacturers to prevent deep discharge. The dc input power drops

to 6.3 W at 10 V. Lamp extinction occurs when the supply voltage is between 7 and 8 V.

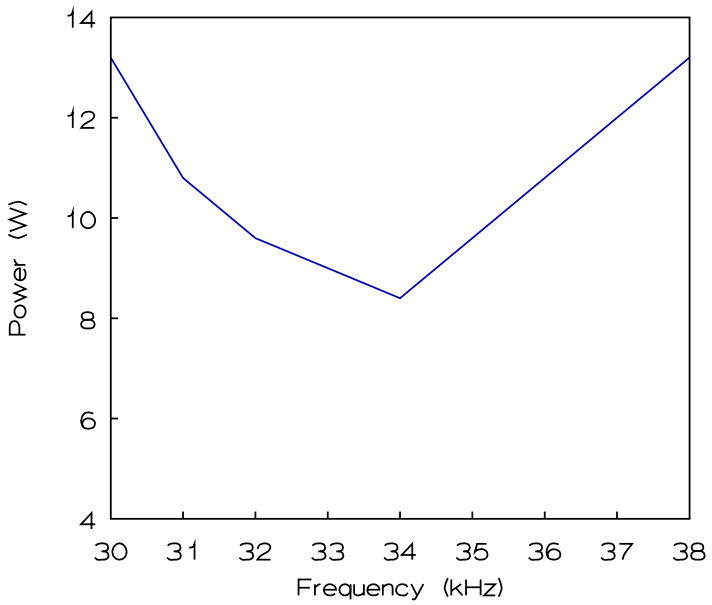

Figure 7.6: Measured dc input power plotted against switching frequency.

Figure 7.6 indicates that input power is at a minimum when the switching instant corresponds to the natural frequency of the secondary components. This is because the final ballast capacitor voltage is a maximum and so the primary peak current is reduced, see Figure 7.5.

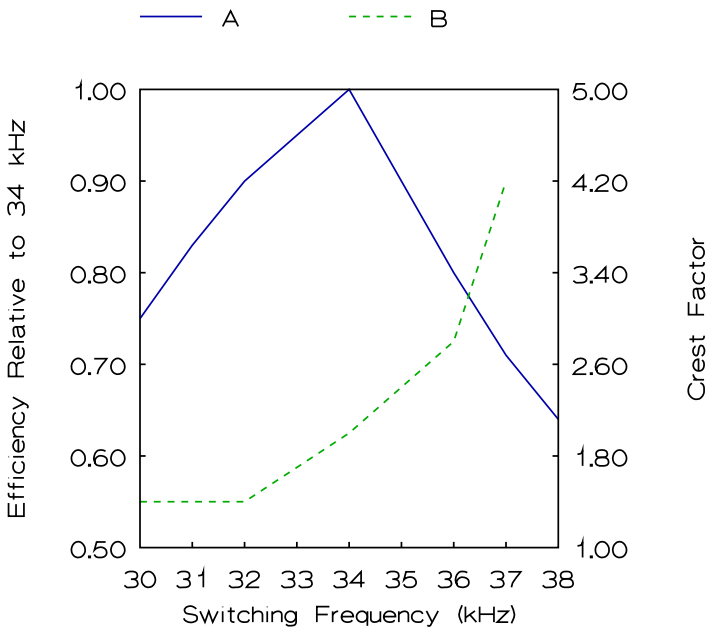

Figure 7.7: Graph A shows the relationship between measured lumen efficacy and switching frequency. Graph B show the relationship between measured current crest factor and switching frequency.

Graph A in Figure 7.7 shows how the lumen efficacy peaks at 34 kHz, which corresponds approximately to the natural frequency of the secondary circuit. The peak power efficiency does not occur when a primary current zero is achieved, at 36 kHz, because although the switching losses are reduced, the peak primary current increases and hence circuit I^2R losses.

The lamp current crest factor increases with increasing frequency and circuit efficiency worsens with decreasing frequency. The current crest factor worsens above 32 kHz as the switch conduction pulse exceeds the amplitude of the resonant peak as in Figure 7.9. Operation at 34 kHz is therefore a good compromise between efficiency and crest factor. The current crest factors shown in Figure 7.7 were measured with the starter components

connected. The actual lamp current crest factor is lower than that measured for the combined lamp and starter components.

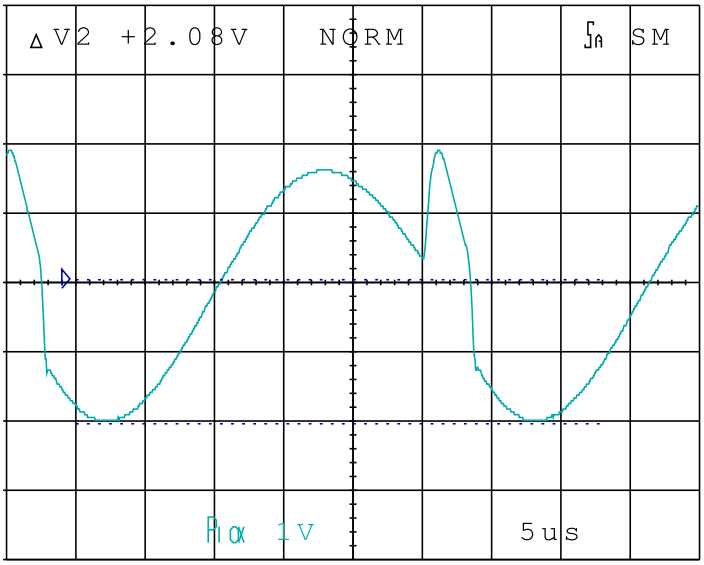

Figure 7.8: Lamp current (measured across 10 Ω) without a glow starter or suppression capacitor.

Figure 7.8 shows the effects of removing both the suppression capacitor and glow starter. The natural frequency of the secondary circuit has changed to 32 kHz. The current waveform retains its shape indicating that the plasma is almost purely resistive at these frequencies. Note that the CF has reduced from 2 to 1.4.

Besides heating the electrodes during starting, the suppression capacitor draws current through the electrodes during arc discharge. The rms voltage across the capacitor during an arc discharge is 49 V when the dc supply is 12 V. The suppression capacitor therefore causes a current of 31 mA to flow through the electrodes. Combined with the passage of the discharge current, the suppression capacitor current causes elevated electrode temperatures.

The electrode temperature vs current curve flattens above 180 mA, see Figure 3.8, and so increments in current thereafter do not cause proportional increases in temperature and hence evaporation. In the light of the above the suppression capacitor current is not considered to be excessive. Besides, at lower supply voltages the suppression capacitor current will assist with electrode heating.

7.3.2 Starting Performance

The starting requirements of fluorescent lamps cannot be accurately specified and so it follows that the starting scenario and starting reliability cannot be attained without experimentation. This inverter provides 250 V peak across the lamp, but this alone is insufficient to initiate an arc discharge. The suppression capacitor loads the starting overvoltage so other starting aids must be used.

This design uses a near field voltage of 650 V, applied between the lamp and the chassis, to initiate a glow discharge in the lamp. This voltage was not measured directly as the scope probe impedance is significant. The glow current was measured and the lamp voltage then computed. The distance between the mounting plate and the lamp is 12 mm. The capacitance between the lamp and the mounting plate was measured to be 150 pF. The peak glow current without a series capacitor is 20 mA which is above the acceptable glow current maximum of 10 to 15 mA[20]. The glow current with a 100 pF series capacitor is 8 mA. All starting performance tests were conducted with this capacitor. Safety is not a consideration with this design, because although the glow potential is applied between the lamp and the chassis, the chassis is earthed.

The ideal starting scenario would be to heat the electrodes to their operating temperature and then provide a high starting voltage to initiate starting. Glow currents cause sputtering of the electrodes because of the high cathode fall in a glow discharge. The glow discharge

with this circuit is initiated as the power is applied which means that sputtering is initiated immediately. However, the suppression capacitor provides a path for electrode current before the starter closes, and so electrode heating is also initiated immediately. The current during starting due to the suppression capacitor current alone is 180 mA rms. This current yields the minimum thermal delay and provides rated electrode heating. The heating current rises to 200 mA rms as the starter closes. The glow starter power during starting is 5.6 W. Glow starter switch closure is therefore ensured for both lamp polarities. Starting performance is reliable on all lamps at supply voltages above 10 V. Starting performance is also independent of lamp polarity. Lamp ignition is achieved within five seconds at any supply voltage between 10 and 13 V.

7.3.3 No Load Performance

No load conditions are important in the design of fluorescent ballasts as the lamp may be removed whilst the circuit is live. Although the secondary self capacitance is sufficient to limit the primary voltage to 70 V peak, the secondary voltage exceeds 2000 V under these conditions. This may cause insulation breakdown between windings and arcing between adjacent circuit board tracks. A 330 pF capacitor is added across the secondary winding to limit the primary voltage to 40 V peak and the lamp terminal voltage to 800 V peak, with no lamp present. The capacitor's effect on overall performance is negligible. With no lamp the FET dissipation is 400 mW and its temperature rises to 25°C above ambient. With continuous start attempts, as would happen with an old lamp, the FET temperature climbs to 35°C above ambient. Under all these conditions the FET and of all the other components are operating well within their maximum ratings.

7.3.4 Performance at Temperature Extremes

The high temperature worst case scenario is re-ignition of a hot lamp at a high ambient

temperature. For this test the prototype ballast was fitted inside a sealed luminaire. The unit was then placed inside a heating chamber and switched on. After 20 minutes, by which time the temperature inside the luminaire had stabilised, the ambient temperature inside the heating chamber was 40°C whilst the temperature inside the luminaire, measured next to the electronic ballast, was 60°C. The temperature of the FET rose to 80°C and its junction temperature was calculated to be 82°C, well below its maximum rated junction temperature of 175°C. Power was briefly interrupted and the re-ignition performance was noted. All six lamps re-ignited within three seconds.

For the low ambient temperature test the six lamps were cooled to -12°C. Each lamp was in turn removed from the cold chamber and tested before significant moisture formed on the tube walls. Ignition was accomplished with all six lamps within five seconds.

7.3.5 Lumen Efficacy

For these tests the reference light output was measured for each lamp using 50 Hz at rated power of 8.7 W, in an integrating sphere. The light output was then measured using the new ballast. The power conversion efficiency of the ballast with a fluorescent lamp load is estimated to be 85% and the dc input power is 8.6 W. The power dissipated in the lamp is therefore 7.3 W. The results are tabled below:

Lamp Sample Manufacturer and Number	**Illuminance at 50 Hz (lux)**	**Illuminance at 34 kHz (lux)**	**Increase in Lumen Efficacy (%)**
Osram (#3)	3000	2850	14
Osram (#4)	3230	2950	9
Philips (#5)	2470	2510	21

Philips (#6)	2730	2740	20

The average increase in lumen efficacy is 16%. Osram[9] claim that their mains powered ballasts achieve 15-52% increase in luminous efficacy over 50 Hz for starterless compact fluorescent lamps. These ballasts, however, do not incur electrode losses due to suppression capacitor current.

7.3.6 Zero Switching Losses with a Lamp Load

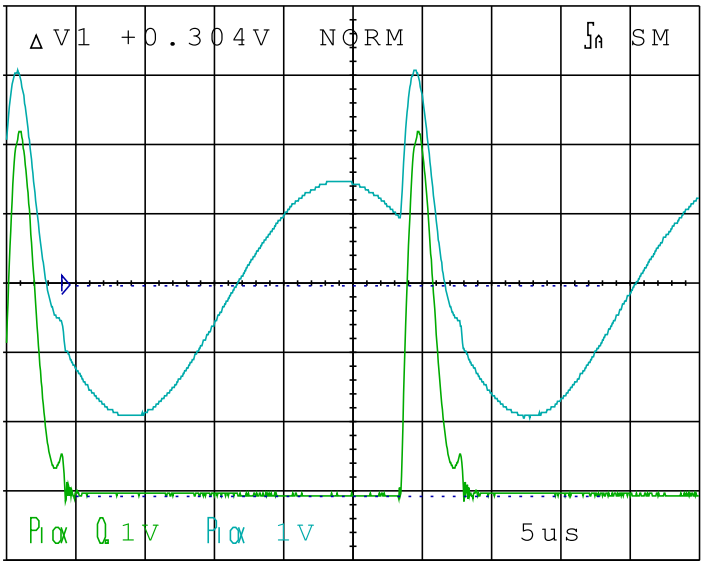

Figure 7.9: Plot of the primary current illustrating zero current at switch off instant. The upper trace shows lamp current (measured across 50 mΩ). The lower trace shows primary current (measured across 50 mΩ).

Figure 7.9 illustrates that it is possible to tune both the pulse width and frequency to enable the switching device to turn off under near zero current conditions with a fluorescent lamp

load. The basic frequency in this case is 34.7 kHz. Power conversion efficiency could only be improved in this mode of operation if the increase in total I^2R losses does not swamp the reduction in FET switching losses.

7.4 Conformance to Requirements

The new ballast conforms to the requirements listed in Chapter 4. The individual requirements and the level of conformance is detailed below:

7.4.1 Manufacturing Cost

The component and assembly cost compares well with the cost of the single transistor inverter. The components used are easily obtainable and, other than the inclusion of an insulating layers between the near field, primary and secondary windings, there are complex winding procedures.

7.4.2 Reliability

Whilst the author acknowledges that reliability cannot be accurately assessed until the units are in active service, a test unit has been functioning reliably for the past six months. The unit has been subjected to repeated switching cycles and occasional no load tests. No problems have been experienced thus far.

7.4.3 Ballast Efficiency

A power conversion efficiency of 85% was measured with the prototype using a resistive load. This efficiency far exceeds any of the other ballasts tested and is close to the highest figure quoted in the literature, *viz.* 90%[5]. The temperature of the switching device rises a mere 16ºC above ambient and so it does not require a heat sink. The detailed account of circuit losses given indicates that higher efficiencies are possible.

7.4.4 Operating Temperature Range

Starting was reliable at -12ºC and also with restarting a hot lamp. During the worst case scenario, *i.e.* continuous starting attempts, the FET temperature rises to 35ºC above ambient. If the ambient temperature is 60ºC then the FET temperature would be 95ºC. The junction temperature will then rise to approximately 98ºC, which is well below the maximum rated junction temperature of 175ºC. The bypass capacitor temperature would rise to approximately 80ºC under the same conditions, which is well below its maximum rating of 105ºC.

7.4.5 Lumen Efficacy

The average increase in lumen efficacy above 50 Hz operation is 16%. This figure is above that required in Chapter 4, *i.e.* 10%.

7.4.6 Current Crest Factor

The prototype circuit achieves a current crest factor of 2. This figure was measured for the combined load of the lamp plus starter components, the actual lamp crest factor is lower. Also, the current aberration responsible for increasing the crest factor has a duration of only 3 μs.

7.4.7 Lamp Current Frequency

The lamp current frequency of 34 kHz is a good compromise between excessive electrode heating due to suppression capacitor currents, and reduced lumen efficacy.

7.4.8 Starting Scenario

The starting scenario ensures low ion bombardment through a low starting voltage of 250 V and minimal near field current of 8 mA. Rated electrode preheating current of 180→200 mA is provided.

7.4.9 Lamp Power

The ballast provides the lamp with approximately 90% of rated power. The total luminous flux is similar to that obtained at rated mains power.

7.4.10 Open Circuit Voltage

The peak output voltage is only 800 V with no lamp present. The ballast can sustain this mode of operation indefinitely, without overheating.

7.4.11 Mains Insulation

A changeover relay is used to switch between mains and emergency lighting for maintained emergency applications and so there is no direct mains connection.

7.4.12 Safety

The luminaire chassis is earthed and the lamp is elevated above the chassis by the near field voltage. No high voltages are applied to the chassis with respect to earth.

8 Conclusions

8.1 General

The inverter meets all the requirements listed in Chapter 4. Its low cost, high efficiency and reliability makes it commercially attractive for use in both domestic and industrial lighting applications. The inverter compares well on price with the cheapest inverters in the market and also offers the industry a design which provides:

- A power conversion efficiency of over 85%, a high priority with battery powered equipment.
- A 16% increase in lumen efficacy above normal mains (50 Hz) operation,
- Reliable starting with compact fluorescent lamps having internal starters.
- A good starting scenario.
- Near sinusoidal lamp current.
- A design that is easily adaptable to other lamp types.

The author's main objectives have therefore been accomplished. Industry interest in the lamp performance data (Chapter 3) is reflected in the author being invited to publish this year (1995) at the South African National Council for Illumination (SANCI)[36].

The inverter performance has already aroused considerable interest from the industry. Samples have been requested by ESCOM for evaluation and an order has already been placed by a local company for over 200 units. The concept of using secondary capacitance, including the lamp suppression capacitor, to both facilitate rapid energy conversion and a natural primary current minimum is now subject to a provisional patent.

8.2 Other Lamp Types Tested

The prototype inverter was used without any modification to power an 18 W compact fluorescent lamp. Starting was reliable without the near field voltage due to the higher dynamic resistance of the glow starter. The dc input power was 13 W and so the lamp power was approximately 11 W. The FET dissipation rose to 300 mW resulting in an 18°C temperature rise above ambient. The supply bypass capacitor temperature rose by 15°C above ambient.

The output power could be increased by simply increasing the number secondary turns. The starting voltage increases linearly with increasing secondary voltage whilst the output power increases by the square of secondary voltage. Output power can therefore be increased without substantially increasing the starting voltage.

8.3 Further Development

The author is presently running a continuous test on the prototype inverter with a Philips lamp and so far, after 6 months, no problems have been experienced with ballast reliability. Also, there is no significant blackening of the lamp tube ends or substantial decrease in total luminous flux thus indicating that both the starting and arc discharge conditions are sound. Escom will soon be conducting tests which include lamp life expectancy. As the life expectancy of the lamp using mains is 8000 hours, the results of these tests will probably not be available within the next 12 months.

The inverter should not be permanently connected to the lamp in maintained emergency applications; a changeover relay must be used. The secondary circuit forms a high Q series resonant circuit across the lamp and, during mains ignition, voltages of approximately

40 V_{p-p} are generated across the primary of the ferrite transformer without the FET connected. Although the resulting reverse drain current does not exceed the specified value of 200 A, more tests are required to ensure reliable operation when used in this configuration.

Further investigation into the shift in chromacity co-ordinates using pulsed lamp current techniques and the resulting improvements in efficiency will be investigated. Coupled to this research will be an investigation into efficiency versus sinusoidal lamp current frequency. To investigate these phenomena a high bandwidth power amplifier (> 1 Mhz) must be constructed.

Research will be conducted to further improve efficiency and reduce costs. It is encouraging to note that the FET dissipation only accounted for approximately 25% of the total circuit losses, and less than 4% of the total converted power, in the prototype ballast. The theory and measurements presented in this document therefore indicate that a power conversion efficiency of 90% is possible.

Further electronic development will include a discrete transistor oscillator to replace the 555 and thereby further reduce manufacturing costs. The cost of a small signal transistor is approximately a tenth of the cost of a high current switching transistor, so the drive circuit complexity can be increased substantially before the total design cost equals that of a push-pull inverter. An improved gate drive circuit will also improve efficiency.

References

1 W. Elenbaas, "Fluorescent Lamps". Macmillan, 1971.

2 Chr. Meyer and H. Nienhuis, "Discharge Lamps". Philips Technical Library, 1988.

3 A. Bouwknegt, H. Nienhuis *et al*, "Electrodes In Discharge Lamps". *Philips Technical Review* No. 35 of 1975, pages 356 to 359.

4 S.T. Henderson and A.M. Marsden, "Lamps and Lighting". Edward Arnold, 1983.

5 M.A. Cayless and A.M. Marsden, "Lamps and Lighting" (Third Edition). Edward Arnold, 1983.

6 R. Bleekrode, M. Koedam and L. Rehder, "Discharge Lamps". *Philips Technical Review* No. 35 of 1975, pages 308 to 315.

7 J. Polman, H. van Tongeren and T.G. Verbeek, "Low Pressure Gas Discharges". *Philips Technical Review* No. 35 of 1975, pages 321 to 330.

8 A.G. Jack and Q.H.F. Vrehen, "Progress in Fluorescent Lamps". *Philips Technical Review* no. 10/11/12 of 1986, pages 342 to 351.

9 "OSRAM - Facts and Figures", OSRAM Technical Bulletin, September 1989.

10 "Philips - PL* LAMPS", Technical publication. Lighting Division 4-'82.

11 M.N. Hirsch and H.J. Oskam, "Gaseous Electronics". Academic Press, 1978.

12 B.N. Chapman, "Glow Discharge Processes". Wiley Interscience, 1980.

13 D.A Frank-Kamenetskii, "Plasma: The Fourth State of Matter". Macmillan, 1972.

14 M.L. Gayford, "Modern Relay Techniques". Newnes-Butterworth, 1969.

15 E.E. Hammer, "Starting Voltage Characteristics of 40W Biaxial Fluorescent Lamps". *IEEE Transactions on Industry Applications*. Vol 26, No 3, May/June 1990.

16 E. Gluskin, "High Harmonic Currents in Fluorescent Lamp Circuits". *IEEE Transactions on Industry Applications*. Vol. 26, March/April 1990.

17 J.M. Davenport and M.E. Duffy, "Current Interrupt System". *Journal of the Illuminating Engineering Society*, Winter 1989.

18 D.M. Vasiljevic, "The Design of a Battery Operated Fluorescent Lamp". *IEEE Transactions on Industrial Electronics*. Vol 36, No. 4, November 1989.

19 W.R. Alling, "The Integration of Microcomputers and Controllable Output Ballasts". *IEEE Industry Applications Society Meeting*, 1983.

20 W.R. Alling, "Important Design Parameters For Solid State Ballasts". *IEEE - Industry Applications Society Meeting*. Vol 2, 1987.

21 E.E. Hammer, "Characteristics of Various F40 Fluorescent Systems at 60 Hz and Higher Frequencies". *IEEE Transactions on Industry Applications*. Vol IA-21 No. 1 Jan/Feb 1985.

22 K.H. Jee *et al*, "High Frequency Resonant Inverter for Group Dimming Control of Fluorescent Lamp Lighting Systems". *IEEE International Conference on Industrial Electronics*. Vol. 1 1989.

23 E.L. Laskowsky, "A Model of a Mercury Arc Lamp's Terminal V-I Characteristic". *IEEE Transactions on Industry Applications*. Vol IA_17 No. 4 July/August 1981.

24 R.R. Verderber, "Effect of Filament Power Removal on a Fluorescent Lamp System". *IEEE Industry Applications Society Meeting*, 1985.

25 S.A. Kalinowsky, "Electrical and Illumination Characteristics of Energy Savings". *IEEE Industry Applications Society Meeting*, 1987.

26 E.E. Hammer, "Effects of Ambient Temperature on the Performance of Bent Tube Fluorescent Lamps". *IEEE Industry Applications Society Meeting*, 1987.

27 K. Kit Sum, "Switch Mode Power Conversion: Basic Theory and Design". Marcel Dekker, 1984.

28 R.P. Severns and G. Bloom, "Modern dc-dc Switch Mode Power Converter Circuits". Van Nostrand Reinold, 1985.

29 M.J. Fisher, "Power Electronics". Thomson Information/Publishing Group, 1991.

30 B.W. Williams, "Power Electronics". McGraw-Hill, 1992.

31 South African National Committee on Illumination (SANCI), "Code of Practice for Emergency Lighting in Buildings".

32 P. Richman and N. Walker, "A New Fast Computing RMS-to-DC Conversion".

IEEE Transactions on Instrumentation and Measurement. Vol. IM-20, No. 4, November 1971.

33 *Electronics World and Wireless World*, June 1990, page 527.

34 *Electronics World and Wireless World*, June 1992, page 517.

35 L. Bedocs, "Lighting Electronics". *South African National Committee on Illumination*, pages 29-32, 1990.

36 S.V. Marais, "Compact Fluorescent Lamps: An Electronic Ballast's Perspective". *South African National Committee on Illumination*. 1995.

37 A.A. Middlecote, "The Present Situation Regarding International Rules for Electrical Installations". *South African National Committee on Illumination*. 1980.

38 C.L. Alley and K.W. Atwood, "Electronic Engineering". John Wiley and Sons, 1973.

39 W.E. Barrows, "Light Photometry and Illuminating Engineering". McGraw-Hill, 1951.

40 J.G. Holmes, "Essays on Lighting". Adam Hilger, 1975.